Nitrogen transformation processes in the coastal zones of the Baltic Sea

-

On the turnover, regulation and role of coastal nitrification

Dissertation

zur Erlangung des akademischen Grades
doctor rerum naturalium
(Dr. rer. nat.)

vorgelegt der
Mathematisch-Naturwissenschaftlichen Fakultät
der Universität Rostock

von
Ines Bartl
geb. am 15.08.1988 in Dessau

Rostock, 2017

urn:nbn:de:gbv:28-diss2017-0103-3

Gutachter:

1. Gutachterin:

   Prof. Dr. Maren Voss,

   Leibniz Institut für Ostseeforschung Warnemünde

2. Gutachterin:

   Prof. Dr. Jane Caffrey

   Center for Environmental Diagnostics and Bioremediation

   University of West Florida

Datum der Einreichung: 28. Juni 2017

Datum der Verteidigung: 20. Oktober 2017

Contents

Summary

The overall aim of this thesis was the quantification of nitrification and the investigation of its role in the coastal nitrogen turnover. Therefore, two estuaries in the Baltic Sea, the Vistula estuary, located in the Bay of Gdansk, and the Öre estuary were chosen. It was checked whether hotspots of nitrification exist in the specific coastal environments river plume and bottom boundary layer and how nitrification was regulated. Also, the influence of sediment properties and processes on nitrification in the sediment overlying BBL were studied. Finally, nitrification rates from the Vistula estuary and Öre estuary were compared with the focus on the role of nitrification in the respective coastal zones. This study was based on the measurement of nitrification rates by using the stable nitrogen isotope ^{15}N in $^{15}N\text{-}NH_4^+$ tracer incubations. In the framework of the EU Bonus project COCOA, in which this thesis is integrated, three cruises and two field campaigns were conducted to the Bay of Gdansk and in Öre estuary, respectively. Information on environmental variables like salinity, temperature, and concentrations of oxygen, nutrients, organic matter and chlorophyll *a* were collected at both sites. A great focus lied in the sampling of water from the BBL close to the sediment surface and the river plume. Through the contribution and access to extensive data sets on environmental variables and processes from both water column and sediment, several intriguing results arose in this thesis.

Specific coastal environments and nitrification regulation were investigated in the Vistula estuary, the coastal estuarine part of the Bay of Gdansk. Only the distinct BBL in summer could be characterized as hotspot for nitrification due to enhanced nitrification rates under conditions of stable thermal stratification and strong coupling to organic matter degradation, as indicated by the positive relationship of nitrification to PON and POC concentrations. The river plume and BBL in winter and spring were surprisingly no nitrification hotspots. The river plume was a transition zone with a shift in magnitude and regulation of nitrification rates suggesting a shift in the nitrifier community. The BBL was indifferent to the overlying water column and a lack of correlations between nitrification rates and measured environmental variables suggests other potential regulation mechanisms. The influence of the hydrodynamic regime and physiological adaptations were discussed and partly supported by results from a storm event.

Nitrification rates in the sediment overlying BBL of the Vistula estuary are not related to sediment types. Also, the sedimentary NH_4^+ fluxes did not reflect different sediment

properties (e.g. permeability). Unexpectedly, also no direct correlation was found between BBL-nitrification rates and NH_4^+ fluxes. However, in winter and spring sedimentary NH_4^+ release is linked to BBL nitrification by refilling the ambient NH_4^+ pool at a slightly higher rate than NH_4^+ is consumed. Since NO_3^- produced by BBL-nitrification is hardly used by sedimentary denitrification, it remains in the BBL being subject to either resuspension and subsequent uptake by primary producers, or to transport by lateral bottom water currents. Due to the former process, NO_3^- might re-enter the coastal nitrogen cycle and by the latter process, NO_3^- could be exported from the Vistula estuary.

Compared to the eutrophied Vistula estuary in the southern Baltic Sea, which receives high DIN loads from the Vistula River, the Öre River discharges less nitrogen, dominated by DON, into the pristine Öre estuary in the northern Baltic Sea. Albeit these differences, nitrification rates surprisingly covered the same range in both estuaries. Similar environmental conditions during the sampling periods, not only physically (e.g. temperature) but also in similar concentrations of DIN, DON and PON, as well as the similar composition of the nitrifying community might be reflected in the indifferent nitrification rates. The difference between the two Baltic estuaries regarding nitrification evolved when the role of nitrification in the coastal N-turnover was studied. Nitrification rates in the BBL of the Öre estuary produce a significant amount of NO_3^- (DIN) compared to the low riverine DIN load in summer. Thus, nitrification is a significant DIN source in the Öre estuary, compared to the Vistula estuary.

The results of this thesis further show that coastal nitrification in the water column and especially in the BBL is recycling at least as much nitrogen as there is removed via sedimentary denitrification. Budgets derived from nitrification and NH_4^+ assimilation rates suggest a high contribution of N-recycling to N-retention. Benefits and risks of coastal N-retention dominated by N-recycling are discussed and suggestions for future research on coastal nitrogen cycling are given.

1. Introduction

This chapter includes passages from the "Introduction" of a submitted manuscript entitled: "River plume and bottom boundary layer – hotspots for nitrification in a coastal bay?" submitted to "Estuarine Coastal and Shelf Sciences" on January 12, 2017. Co-authors are Kirstin Schulz, Iris Liskow, Lars Umlauf and Maren Voss. The "Introduction" of the submission was entirely written by me.

This PhD-thesis was integrated in the EU Bonus project "COCOA" (Nutrient cocktails in the coastal zones of the Baltic Sea), which studies the coastal filter function and biogeochemical processes in coastal zones around the Baltic Sea. The work done by the IOW was located mainly at two different sites, the Bay of Gdansk and the Öre estuary. The introduction of this thesis is intended to firstly provide information on the impact of rivers to coastal zones and the coastal N-cycle. Secondly, the nitrogen transformation process nitrification and its regulation as well as specific coastal environments like the river plume and bottom boundary layer are introduced. The potential influence of sediment properties and riverine N-loads on coastal nitrification is also addressed. At last, the two distinct Baltic coastal zones, Bay of Gdansk and Öre estuary, are described.

1.1 The coastal zone: anthropogenic impacts and the role of rivers

The population growth and increase in food demand strongly perturbs the biogeochemical cycles of carbon, nitrogen and phosphorus (Rockström, 2009; Seitzinger, 2008; Vitousek et al., 1997). Nitrogen is introduced through fossil fuel combustion, fertilizer use, and waste water discharge by industries and husbandries (Gruber and Galloway, 2008). Nowadays, the global production of reactive nitrogen is more than twice as the amount generated through natural sources (Seitzinger, 2008; Galloway et al., 2008). Rivers are primary and rapid exporters of land derived material to the coastal sea (Sharples et al., 2017; Smith et al., 1999). Thereby, they connect terrestrial catchments with the coastal zone and the adjacent open sea. The oceans receive essential nutrients and trace metals to sustain ocean productivity this way, e.g. the oceans silica supply mainly comes from the rivers (Conley, 1997). The anthropogenic impact led to an increase in nutrient and organic matter concentrations in the rivers and hence in the loads draining into coastal zones (Seitzinger et al., 2010). Only recently, Sharples et al. (2017) estimated from a global model that 75 % of the riverine and estuarine dissolved inorganic nitrogen (DIN) entering the shelf sea could

be further exported to the open ocean. A process severely affecting coastal zones due to high riverine discharge of nutrients and organic matter is eutrophication (Nixon, 1995; Richardson and Jørgensen, 2013). It primarily leads to an increase in primary production followed by an enhanced secondary production leading to increased oxygen consumption and a change in species composition. This is followed by severe secondary implications like increased turbidity, harmful alga blooms and hypoxia (Diaz and Rosenberg, 2008), as well as to a loss of biodiversity and an increased mortality of species (Richardson and Jørgensen, 2013). Thereby, eutrophication also has a strong impact on biogeochemical processes in coastal and estuarine systems (Kemp et al., 2009; Middelburg and Levin, 2009). Nitrogen is known to be the main driver regarding coastal eutrophication (Howarth and Marino, 2006) and there are numerous studies dealing with nitrogen loading and nitrogen turnover in coastal zones (e.g. Almroth-Rosell et al., 2016; Brion et al., 2008; Dähnke et al., 2008 and 2010; Middelburg and Nieuwenhuize 2001). In the last centuries, nitrogen loads remained constantly high, whereas anthropogenic phosphorus loads were successfully reduced (Pearl, 2009; Soetaert et al., 2006). This alters the ratio of bioavailable nitrogen and phosphorus to primary producers and could lead to a loss of the coastal retention capacity regarding nitrogen (Howarth et al., 2011).

Coastal zones are defined as the interface of land and sea which experiences both terrestrial and marine influences (Alongi, 1998). Several types of coastal zones are categorized due to geographical and hydrological conditions: e.g. lagoons, archipelago, bays, embayments, and estuaries (e.g. Jickells, 2014; Mann and Lazier 1991; Wolanski 2007). The latter gains high attention in the coastal research, since they are primarily and directly affected by riverine nutrient and organic matter load. A classical estuary as a part of the coastal zone is a semi-enclosed body of water with a free connection to the open ocean and a measurable salinity gradient from freshwater to saltwater (Pritchard, 1967). Modern definitions refer to estuaries as variably enclosed structures with part time closing, disturbed freshwater inflow and negligible tidal influence as influencing factors (Wolanski, 2007). The basic pattern of river estuaries is influenced by the depth and by the occurrence of tides (Mann and Lazier, 1991). One type of river estuaries is the salt wedge estuary. Missing tidal currents and a greater depth are main characteristics of such estuaries. Since riverine fresh water is lower in density than the salt water of the coastal zone, a river plume develops and vertical stratification is enhanced. The point of changing salinity in the bottom water layer is the so-called salt wedge. At this position, the changing salinity leads to flocculation and sinking of

particles and a turbidity maximum can develop. Since this salt wedge moves along the land-sea-continuum depending on the strength of the freshwater outflow and saltwater inflow, particles and organic matter will be distributed widely. The direction of the river outflow at the surface depends on the geostrophic balance and wind driven surface currents. Thus, changes in wind direction for example can change the direction of the river plume leading to a wide distribution of nutrients which are transported by the river outflow. Simpson (1997) describes an estuarine mixing zone which extends beyond the conventional estuary definition to a highly variable, stratified "Region of Freshwater Influence" (RoFI) in coastal zones and shelf seas. Such region can be visually described by the river plume, where intense biological, physical and chemical processing occurs (Statham, 2012). Estuaries are generally regarded as "coastal filters" since nutrient and organic matter concentrations are retained during the passage of the water along the land-sea continuum (Cloern 2001). This nutrient retention in the coastal system can be achieved for example by along shore coastal currents, which physically separate the coastal system from the open sea (Voss et al., 2005a). Biogeochemically, nutrients and organic matter can be retained through continuous recycling, by e.g. nitrification within or removal from the coastal system by e.g. denitrification or burial (Joye and Anderson, 2008). However, eutrophication induced changes in nutrient and organic matter cycling in a coastal system can severely and partially irreversibly alter the system functioning (Richardson and Jørgensen, 2013).

1.2 The coastal nitrogen cycle

The complex nature of the nitrogen cycle lies in the great number of oxidation states and various reduction- and oxidation processes, which are all microbially mediated (figure 1). Figure 2 illustrates main processes in the coastal N-cycle which are described in the following. Dissolved inorganic nitrogen (DIN) as the sum of nitrate (NO_3^-), nitrite (NO_2^-) and ammonium (NH_4^+), particulate organic nitrogen (PON) and dissolved organic substances (DON) are imported into the coastal zone by rivers and will be assimilated or degraded by phytoplankton and heterotrophic bacteria (Brion et al., 2008; Ward et al., 1984). Via primary production biomass will be built up and secondary production follows. Thereby generated PON eventually sinks to the coastal seafloor through close benthic-pelagic coupling. Also, riverine particles (including PON) sink to the seafloor when confronted with coastal saltwater (Mann and Lazier, 1991). When settled onto the sediment, PON from both sources, primary production

and river load, will be consumed, degraded or buried by the benthic community (micro- and macroorganisms). Through resuspension PON can be mixed back into the bottom water, where it is not only subject to degradation (Floderus et al., 1999) but also to transport (Emeis et al., 2002). Via ammonification, NH_4^+ is produced during the degradation of organic matter. Under oxic conditions, NH_4^+ undergoes nitrification both in the bottom water and in oxic sediment layers. Via nitrification NH_4^+ is first oxidized to NO_2^- (ammonium oxidation) followed by nitrite oxidation to NO_3^- (see chapter 1.3). Under anoxic conditions NO_3^- is reduced to dinitrogen (N_2) which is not bioavailable and may escape to the atmosphere. This process, called denitrification, is the most important N-removal process in coastal zones. It is mediated by facultative heterotrophic, anaerobic denitrifiers which use NO_3^- as electron acceptor for POC degradation (Devol et al., 2015). There are two other N-transformation processes occurring under anoxic conditions which are not further considered in this study: anaerobic ammonium oxidation (anammox) and dissimilatory nitrate reduction to ammonium (DNRA, Figure 1). Via anammox, NH_4^+ is used together with NO_2^- to produce N_2, thereby being also a N-removal pathway (Dalsgaard et al., 2005). The reduction from NH_4^+ to NO_3^- occurs via DNRA which has only recently been recognized to be of significance in estuarine and coastal sediments especially under occurrence of free hydrogen sulfide (Bonaglia et al. 2014 and 2017; Jäntti et al., 2012). The regenerated NO_3^-, NO_2^- and NH_4^+ are transported back from the sediment and the bottom water into the water column by resuspension events through physical mixing. In the euphotic zone, they are again bioavailable to primary producers and thus enter a new N cycle.

The cycle of uptake, particle formation, sedimentation and remineralization or removal of nitrogen is influenced by several factors such as 1) eutrophication/oxygen concentration, 2) coastal morphology and 3) benthic macrofauna. High riverine N-loads to coastal systems promote eutrophication (Pearl and Piehler, 2008), which in turn impacts internal coastal N-cycling. The only N-removal process known to offset N-input in rivers and coastal zones is benthic denitrification. However, a study in freshwater streams revealed that increased NO_3^- concentrations can lead to a decrease in the denitrification efficiency (Mulholland et al., 2008). Furthermore, Lunau et al. (2012) showed that nitrification rates are increasing with higher N:P ratios in growth experiments. Similar effects could evolve in coastal zones: increasing riverine NO_3^-

loads, especially relative to PO_4^{3+}, reduce the N-removal efficiency while N-recycling by nitrification could increase resulting in a positive feedback in eutrophication.

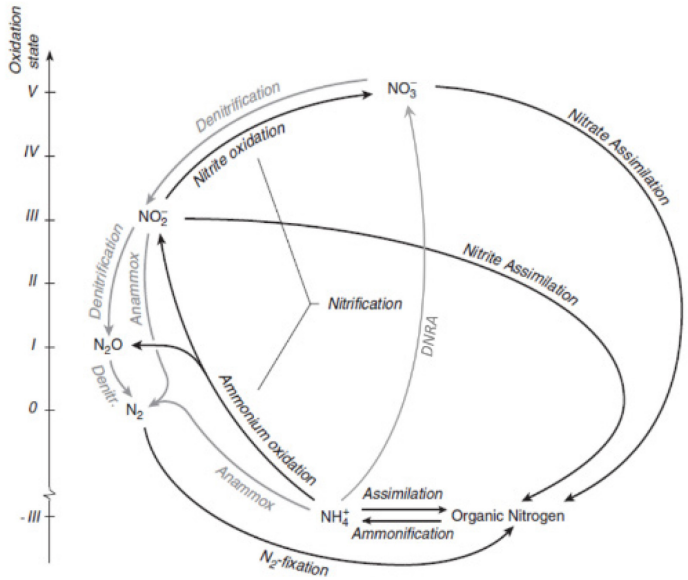

Figure 1: The marine nitrogen cycle. The different N-species and assigned N-transformation processes are plotted against their oxidation state. Nitrate is the most oxidized N-species while ammonium and organic nitrogen display the most reduced N-species in the cycle. Processes shown in grey occur under anoxic conditions (modified from Gruber, 2008).

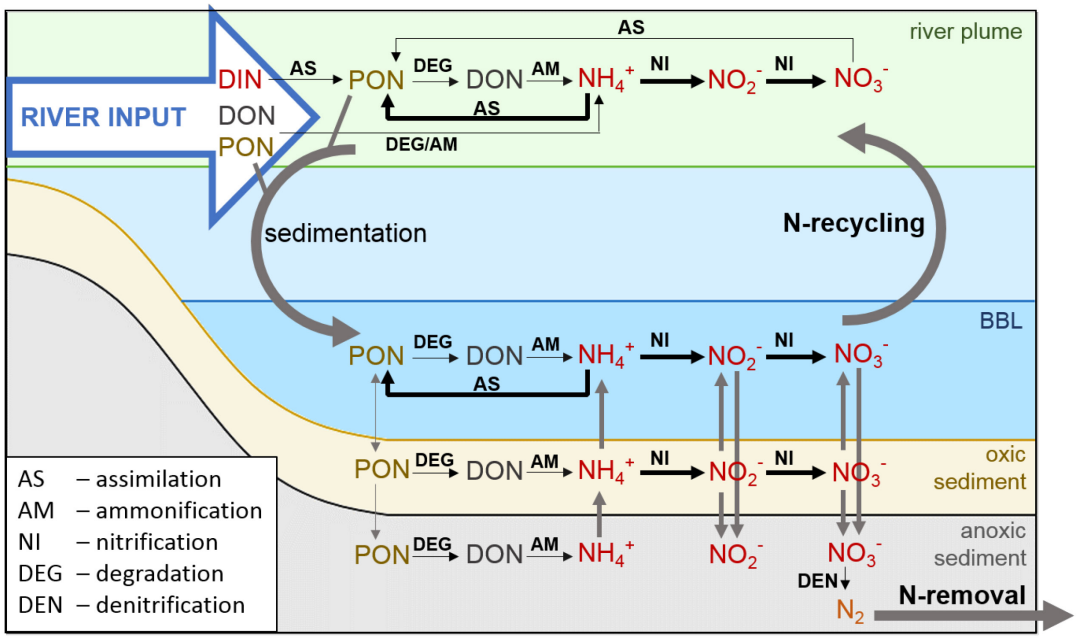

Figure 2: Key nitrogen transformation processes in a coastal zone. Black arrows represent N transformation processes, whereby processes highlighted by bold arrows were measured in this study. Grey arrows represent transport pathways of the N-species.

In eutrophied systems the oxygen consumption (respiration and oxidation processes) increases as a result of high organic matter loads reaching the bottom water layers. When oxygen consumption exceeds oxygen supply, hypoxia is the consequence. Under hypoxic and anoxic conditions ammonium effluxes out of the sediment increase and reduction processes start to dominate (Jäntti and Hietanen, 2012). Especially denitrification is enhanced as long as there is supply of NO_3^-. If the NO_3^- supply from oxic water zones cannot compensate the NO_3^- demand of denitrification in anoxic zones, denitrification will be mitigated (Middelburg and Levin, 2009). Hence, not only the increase in NO_3^- concentrations (Mulholland et al., 2008) but also prolonged hypoxic to anoxic conditions potentially mitigate N-removal and support N-recycling (Jäntii, 2012; Middelburg and Levin, 2009). Geographical and hydrological characteristics of coastal zones can also have an impact on nitrogen cycling. Especially, the residence time was found to be a main driver for nitrogen removal (Jickells et al., 2014; Nixon et al., 1996). Calculations by Jickells et al. (2014) indicate, for example, that the area of an estuary and the flushing rate of the rivers are key controls on benthic denitrification. Furthermore, Voss et al. (2010) revealed that with duration of the residence time (average time a water molecule or particle stays in a system) more nitrogen is removed out of the system by denitrification. Due to the low depth of coastal zones, organic matter which sinks to the seafloor remains “fresh”, meaning it has not been degraded much during sedimentation. In this context, the lagoons (Voss et al., 2010) are more efficient sites of removal processes than estuaries and open bays. Macrofauna is directly influencing organic matter processing at the seafloor by the initial uptake and reworking (Josefson et al. 2012). Other effects on N-cycling by fauna are burial, bioturbation and deposition of POM, oxygenation of sediment and generating microhabitats for microorganisms (Hunter et al. 2012; Norkko et al. 2001). It has been shown that macrofauna enhances the coupling of nitrification and denitrification in the sediment, thus increasing N-removal (Devol, 2015; Stief, 2013). Through the ventilation of their burrows via bioirrigation, benthic macrofauna increase the surface area of the oxic-anoxic interface in the sediments where coupled nitrification-denitrification occurs (Stief, 2013). Furthermore, macrofauna is known to increase the sedimentary nutrient release by several orders of magnitude compared to diffusive transport (Stief, 2013), which can enhance biogeochemical processes in the sediment overlying water.

1.3 Nitrification

A key process in the coastal nitrogen cycle is nitrification, that is, the microbially mediated 2-step oxidation of ammonium (NH_4^+) to nitrite (NO_2^-) and subsequently to nitrate (NO_3^-). Together with ammonification, nitrification is an important remineralisation pathway. Furthermore, it connects the ammonification with nitrogen removal processes (anammox, denitrification) and other nitrogen recycling processes (DNRA, or assimilation, Figure 1). Nitrification does not change the amount of nitrogen in a system but rather composition, distribution and fate of DIN (Carini et al., 2010). Especially the coupling of nitrification to sedimentary denitrification is an important component of the coastal filter function (Jäntti and Hietanen, 2012).

The first step of nitrification is realized by ammonia oxidizing bacteria (AOB) and archaea (AOA), respectively, and produces NO_2^-. The oxidation of NO_2^- to NO_3^-, the closely coupled second step of nitrification, is realized by nitrite oxidizing bacteria (NOB). Ammonium oxidation is considered to be the rate limiting process (Ward, 2008). Recent studies found a nitrifying bacteria species which was capable of complete nitrification from NH_4^+ directly to NO_3^-, but its ecological relevance is not yet known (Daims et al., 2015; van Kessel et al., 2015). Nitrifiers (AOA, AOB and NOB) are mainly chemolithoautotrophic and gain energy via aerobic oxidation of NH_4^+ or NO_2^- while incorporating dissolved inorganic carbon. However, it has been found that many AOB and NOB as well as some AOA species are also able to use organic nitrogen, like urea, instead of ammonium (Alonso-Sàez et al., 2012; Koops and Pommerening-Röser, 2001). Furthermore, Qin et al. (2014) showed, that there exist mixotroph AOA which also grew with organic carbon instead of CO_2 as carbon source. In general, nitrifiers are slow growing microorganisms (Koops et al., 2006; Mosier et al., 2012), and their affinity to the substrate NH_4^+ is highly variable. AOB are generally less sensitive to NH_4^+ than AOA (Horak et al., 2013; Martens-Habbena et al., 2009). Because of their high NH_4^+ affinity and their high abundance AOA are considered to be the main driver for nitrification in the oligotrophic ocean (Bemann et al., 2008; Francis et al., 2005; Wuchter et al., 2006). In coastal zones, however, contradicting results were found regarding the dominance of AOA (Caffrey et al., 2007; Lipsewers et al., 2014; Mosier and Francis, 2008; Tolar et al., 2013) or AOB (Li et al., 2015; Magelhaes et al., 2009) in the nitrifier community.

Additional to the physiological variability of nitrifiers, coastal zones are highly dynamic and variable systems regarding environmental variables that influence the nitrification activity, i.e. nitrification rates. The high variability in nitrification rates caused by

numerous environmental factors have not yet led to a consistent explanation of the rates encountered in coastal zones (Damashek et al. 2016). The main environmental variables influencing coastal nitrification are salinity, temperature, oxygen, NH_4^+, and particulate suspended matter (SPM) which includes PON. Nitrification rates are usually highest at low salinities because riverine freshwater contains high concentrations of NH_4^+ (Bianchi et al., 1999; Brion et al., 2008) and may be limited at higher salinities due to the slow growth rate and thus slow adaptation of nitrifiers (Damashek et al., 2016; Santoro and Casciotti, 2011). Regarding temperature some studies found positive relationships with nitrification rates (e.g. Bianchi et al. 1999; Dai et al. 2008; Iriarte et al. 1998). However, correlations are often weak and cannot be converted into a seasonal pattern (Damashek et al. 2016). In some estuaries or coastal zones nitrification rates are highest during summer or spring, in others highest nitrification rates are found in autumn or winter. Ward (2008) ascribes temperature to be of minor importance on the regulation of nitrification, since nitrifying populations are generally adapted to the ambient temperature of their environment. This is underlined by Horak et al. (2013) and Baer et al. (2014) who found no influence of temperature on nitrification rates in manipulation experiments. Nitrifiers need oxygen to gain energy via nitrification, but they are assumed to be microaerophilic, which means they are most active at lower oxygen concentrations (Park et al., 2010; Ward, 2008). Therefore, they could react sensitively to the oxic-anoxic interfaces typical of coastal waters (Ward, 2008). Indeed, some coastal studies have reported negative relationships between nitrification rates and oxygen concentrations (e.g. Bristow et al., 2015; Jäntti and Hietanen, 2012). While there is convincing evidence that NH_4^+ concentrations enhance nitrification rates, suggesting a regulation by substrate availability (Bianchi et al., 1999; Damashek et al., 2016; Hsiao et al., 2014), such a correlation has not been consistently demonstrated (Grundle and Juniper, 2011; Heiss and Fulweiler, 2016). Instead, their relationship is attributed to an adaptation of nitrifiers to ambient NH_4^+ concentrations (Peng et al., 2016) or to the tight coupling between ammonium production and oxidation (Bronk et al., 2014; Horrigan et al., 1990). Moreover, in a variety of coastal zones nitrification positively correlates with SPM (Damashek et al., 2016; Feliatra and Bianchi, 1993) or PON (Hsiao et al., 2014). The association or attachment of nitrifiers to particles suggest that rapidly generated supplies of NH_4^+ are growth promoting (Karl et al., 1984; Koops and Pommerening-Röser, 2001; Phillips et al., 1999; Stehr et al., 1995).

1.4 Nitrification in specific coastal environments

Coastal zones comprise specific environments, such as river plumes and bottom waters. Yet, nitrification, its regulation and its ecological role in these different water bodies have rarely been compared, despite the inherent differences in their environmental conditions. For example, Heiss and Fulweiler (2016) found that the regulation of nitrification differed in surface and deep waters. In bottom water, concentrations of nutrients and particles may be higher than in surface water such that nitrification will be enhanced. In their study of the Scheldt estuary, Brion et al. (2008) modelled N-budgets and identified a missing NH_4^+ sink that was presumably balanced by nitrification in the particle-rich bottom water of the estuary. Korth et al. (2013) pointed out the important role of bottom water nitrification and its coupling with sedimentary denitrification in the outflow region of Szczecin lagoon (Baltic Sea) and recognized the need to distinguish between surface and bottom water processes in investigations of coastal N-cycling.

In estuarine coastal zones, a river plume can develop in the surface water layer. This riverine fresh water in the plume transports the loads of DIN, DON and PON. Stratification due to the less dense river plume on top of the coastal water together with the riverine DIN fuels primary production. Riverine NH_4^+ and NH_4^+ remineralized from DON and PON could also be used for nitrification in the river plume (Figure 3). But in the photic surface water layer, nitrifiers have to compete for NH_4^+ with phytoplankton (Smith et al., 2014) or might be light limited (Ward, 2008). On the other hand, high turbidity of the river plume water might support nitrification in the competition for the substrate, because primary production could be attenuated. Lunau et al. (2012) suggested that in eutrophied waters, where the N:P ratio is above 32:1, DON production by phytoplankton is enhanced which could fuel ammonification and nitrification. Indeed, Bianchi et al. (1999) found higher nitrification within the Rhône river plume than at the sea and linked it to higher NH_4^+ concentrations found in the plume. Pakulski et al. (2000) suggest high nitrification activity also in the Mississippi river plume. But they also found indications of less nitrification activity in the Atchafalaya river plume and concluded, that different hydrology or different nutrient loading lead to different biogeochemical processes in river plumes (Pakulski et al., 2000). Hence, the specific coastal environment “river plume” has the potential for high nitrification rates, mainly due to high riverine NH_4^+ loads.

In shallow coastal waters a tight benthic-pelagic coupling exists connecting the euphotic zone where nutrients are consumed and particulate organic matter (POM) is produced with the bottom water layer where POM is consumed and nutrients are produced (remineralisation). The bottom water layer includes the bottom boundary layer (BBL, also referred to as the benthic boundary layer or benthic mixed layer). The BBL is defined as a near-bottom region of very few to tens of meters thickness, characterized by turbulent boundary layer flow (Dade, et al., 2001), and by enhanced turbulence levels and reduced vertical density gradients compared to the overlying water column (Richards, 1990; Figure 3). Turbulence and mixing in this energetic region are typically fuelled by bottom friction and the interaction of internal waves with the sloping topography (Grant and Madsen, 1986; Thorpe, 2005). The vertical extent of the BBL is determined by the complex interplay of numerous factors, including near-bottom shear and density stratification, that account for the large spatial and temporal variability (Lappe and Umlauf, 2016; Umlauf et al., 2011). Furthermore, the BBL not only modulates the exchange of particles and dissolved constituents between the sea bed and the overlying water, it also provides an energetic environment for biogeochemical processes (Floderus et al., 1999; Holtappels et al., 2011; Turnewitsch and Graf, 2003). Studies of aggregate formation and its variability over time in the BBL (Jähmlich et al., 1999; Turnewitsch and Graf, 2003) as well as microbial activity and organic matter utilization in this layer have demonstrated its prominent role in microbial nutrient cycling (Ritzrau, 1996; Ritzrau et al., 1997). Similarly, nitrification in the BBL may be of major importance because the high substrate availability, the absence of light limitation and reduced competition for NH_4^+ provide favourable conditions for the nitrifying community (Figure 3).

Since the BBL is the interface between sediment and overlying water, biogeochemical processes like nitrification might also depend on biogeochemical processing and transport of nutrients and organic matter in the sediment. Coastal sediments can be a source of NH_4^+ to the overlying BBL depending on the sediment type (e.g. Ehrenhauss et al., 2014; van Raaphorst et al.,1992) and could thus be a substrate source for BBL-nitrification. Likewise, the benthic macrofauna community and their bioturbation activity influence the sedimentary NH_4^+ release (Stief et al., 2013) and thus BBL-nitrification. The produced NO_3^- from BBL-nitrification could be a source for sedimentary denitrification. Especially when NO_3^- concentrations are higher in the BBL than in the sediment, NO_3^- will be transported into the sediment where it is denitrified

(Rysgaard, 1994). In permeable sediments, NO_3^- from the BBL can be advectively transported into the sediment to be denitrified (Huettel et al., 2014) and is therefore considered by some authors to be the main source for denitrification in permeable sediments (e.g. Kessler et al., 2013; Rao et al., 2008). Furthermore, Huettel et al. (1998) showed, that sedimentary NH_4^+ release in permeable sediments can be enhanced through advective porewater flow by the formation of "anoxic chimneys" directly connected to the overlying water. Such a direct input of NH_4^+ into the BBL could also be a positive effect for nitrification. In contrast, coupled nitrification-denitrification and non-advective NH_4^+ transport are dominating processes in muddy sediments. Hence, when investigating nitrification and the fate of the produced NO_3^- in the BBL, sediment properties and processes, as well as the benthic macrofauna community have to be considered.

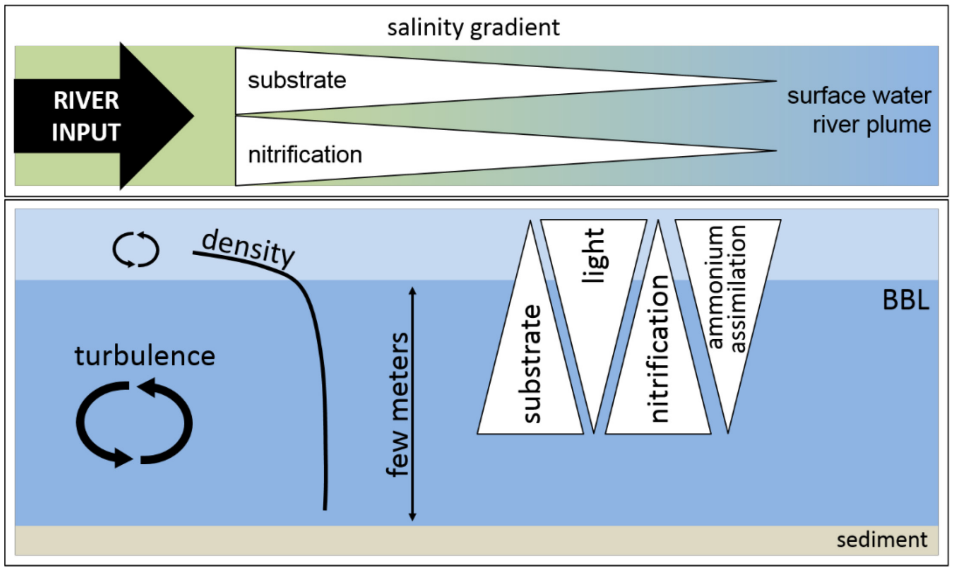

Figure 3: The upper panel shows nitrification along a salinity gradient in the river plume with high nitrification rates at low salinities where the substrate concentration is high. The lower panel describes the BBL and nitrification in the BBL. The BBL is characterized by higher turbulence than in the overlying water and by a reduced density gradient. In the several meters thick BBL, the substrate NH_4^+ can accumulate and promote nitrification. Additionally, the absence of light and less competition for the substrate (ammonium assimilation) lead to favourable conditions for nitrification in the BBL.

1.5 The Baltic Sea and its coastal zone

The Baltic Sea is a semi-enclosed, brackish sea in northern Europe with a single connection to the North Sea in the south-west and without tidal influence. Due to its geographical settings, high riverine fresh water input and restricted exchange of saline water with the North Sea, a permanent salinity gradient exists. High salinities are found

in the south-western part of the Baltic Sea and decreasing salinities exist towards the east and the north. Along with the salinity gradient there exists a gradient in terrestrial agriculture and population. The catchment of the rivers entering the southern and eastern Baltic Sea are highly populated (Lääne et al., 2005) and mainly consists of arable land with intense agriculture (Figure 4). The catchments of rivers discharging into the northern Baltic Sea, are much less populated (Lääne et al., 2005) and consist of boreal forests not affected by agriculture (Figure 4). Furthermore, the northern coastal zones/estuaries are considered to be pristine, whereas southern coastal zones, like the Bay of Gdansk (Vistula River) or Szczechin lagoon (Oder River) are clearly eutrophic (Humborg et al., 2003; HELCOM 2009). The riverine discharge into the coastal zones are an important nutrient source and accounts for approximately 75 % of the total nitrogen input to the Baltic Sea. Thereby, coastal zones in the southern Baltic Sea are highly affected by riverine N-loads originating from the cultivated catchments. Indeed, some coastal sites in the Baltic Sea experience hypoxia, a severe eutrophication effect (Conley et al., 2011).

A closed circulation cell exists in the central Baltic Sea with little exchange with the coastal zone, and it had been suggested that there is limited transport of riverine nutrients to the Baltic proper (Voss et al., 2005a). Additionally, Voss et al. (2005b) described a transport parallel to the southern coast, which transports riverine nutrients alongshore, due to prevailing westerly and southerly winds, with little exchange with the open Baltic Sea. Furthermore, Voss et al. (2005a) suggests that the nitrogen is mainly processed and finally removed within the coastal rim of the Baltic Proper. However, still little is known about the internal nitrogen cycling in Baltic coastal zones and quantifications of N-recycling as well as N-removal processes are rare. Since the coastal zones are severely understudied compared to the basins, the selected study areas are the Bay of Gdansk in the southern Baltic Sea and the Öre Estuary in the northern Baltic Sea (Figure 4). At each site, a river, the Vistula River and the Öre River, respectively, enters the coastal system and is the main source of nutrients. The Bay of Gdansk is an open coastal bay which can be characterized as a "RoFI" (region of freshwater influence, see definitions in chapter 1.1) that receives high nutrient loads from the Vistula River, the largest single N-source entering the Baltic Sea (Witek et al., 2003). The coastal area of the bay ($<$ 50 m water depth) is directly affected by the riverine discharge (Thoms et al., unpublished) and has a saltwedge-like, estuarine character. Therefore, it will be named Vistula estuary (VE) in this thesis. The annual riverine N-load is ca. 98 kt yr^{-1}, of which 63% is dissolved inorganic nitrogen (calculated

from data of Pastuzak and Witek 2012). Roughly 23% of the total nitrogen and as much as 80% of the dissolved inorganic nitrogen from Vistula River loads are estimated to be retained the Bay of Gdansk (Witek et al., 2003) during the mainly eastward transport of riverine waters along the coast (Radtke et al., 2011; Voss et al., 2005). While, previous studies showed that this river plume fuels primary production by both phytoplankton and bacteria (Ameryk et al., 2005; Wielgat-Rychert et al., 2013), it might also allow a high level of nitrification (Voss et al., 2005b). The Öre estuary is a semi-enclosed estuary and much smaller than the Bay of Gdansk. As many estuaries in the northern Balic Sea, the Öre estuary is a saltwedge estuary (Humborg et al., 2003). The N-loads from the Öre River are only 0.44 kt yr-1 (Wikner and Andersson, 2012) and hence this coastal zone can still be regarded as pristine (Humborg et al., 2003). However, most of the riverine N-load consists of organic N (85 %), which turns the Öre estuary to a net-heterotrophic system (Sandberg et al., 2004). The different riverine N-input of these two coastal systems could affect the N-cycle and might lead to different N-processing.

Figure 4:
Map of the Baltic Sea in northern Europe with land-cover and catchment area (modified from Helcom, 2013). The Bay of Gdansk is located in the southern Baltic Sea and the Öre estuary in the northern Baltic Sea (squares) with the Vistula River and the Öre River, respectively, discharging into these coastal zones (blue arrows).

1.6 Aim of the study

Nitrification is a key process in the coastal N-cycle, since it 1) provides the substrate for N-removal by denitrification and 2) it is a feedback process regarding eutrophication, since it recycles N into a bioavailable form for primary production. Therefore, the overall aim of this PhD thesis is not only to quantify this process but also to expand our understanding of coastal water column nitrification and its role in the coastal nitrogen turnover. Specific coastal environments like the river plume and the BBL could play a crucial role for coastal nitrification providing favourable conditions for this process. To investigate whether nitrification is enhanced in the river plume or BBL, nitrification rates and their regulation were examined in the Bay of Gdansk. Since the BBL links sediments with the water column, favourable conditions for BBL-nitrification might originate from the sediment, e.g. in the form of sedimentary NH_4^+ release, which in turn depends on sediment properties and the macrofauna community. Hence the second aim was to investigate the influence of sediment properties and nutrient fluxes on BBL-nitrification. In the Baltic Sea both, eutrophied and oligotrophic coastal zones can be found which however differ in the composition of the N-compounds (DIN, DON, PON) entering the coastal zones via rivers. Nitrification might depend strongly on the magnitude and composition of the riverine nitrogen load. So, the third aim was to investigate the influence of magnitude and composition of riverine N-loads on coastal nitrification during time periods of high riverine outflow (winter/spring) and high coastal productivity (summer). In the following, the three main questions (Q) and hypotheses (H) are summarized:

1. Q: Are river plume and BBL hotspots for nitrification and how is this process regulated?
   H: River plume and BBL are hotspots for nitrification, because they provide favourable conditions for nitrification like oxic conditions, high NH_4^+ concentrations.
2. Q: Is nitrification in the BBL related to sediment properties and the sedimentary NH_4^+ release?
   H: BBL-nitrification rates from the Vistula estuary are high above sandy permeable sediment, which can have high remineralization activity as result of advective porewater flow and can provide a high amount of NH_4^+ to the

BBL. In turn NO_3^- from BBL-nitrification is a substrate in sediment denitrification (Dw: denitrification of water column nitrate).

3. Q: Does the magnitude and compositions of the riverine N-load from two distinct coastal zones lead to different nitrification rates?

   H: Nitrification rates are higher in the eutrophic Vistula estuary than in the oligotrophic Öre estuary.

2. Materials and Methods

This chapter contains parts of the "Materials and Methods" section of a submitted manuscript entitled: "River plume and bottom boundary layer – hotspots for nitrification in a coastal bay?". The manuscript was submitted to "Estuarine Coastal and Shelf Sciences" on January 12, 2017. Co-authors are Kirstin Schulz, Iris Liskow, Lars Umlauf and Maren Voss. The writing of the "Materials and Methods" section of the manuscript was done by myself. Only for subchapter "Definitions of water layers", Kirstin Schulz and Lars Umlauf participated in writing.

2.1 Study sites

2.1.1 The Bay of Gdansk

The Bay of Gdansk is located in the southern Baltic Sea and covers both Polish and Russian coastal waters (Figure 5). Our studies were carried out in the Polish region, where the Vistula River drains into the bay with a mean river discharge of 1080 $m^3 s^{-1}$. The Bay of Gdansk encompasses an area of 4940 km^2, with a corresponding volume of 291 km^3 and a maximum depth of 118 m in the Gdansk Deep (Cyberska and Krzyminski, 1988). The Vistula plume can extend 4 - 30 km into the bay, with a vertical extension of 0.5 - 12 m (Cyberska and Krzyminski, 1988). The outflow direction and the spread of the river plume depend on wind speed and direction (mostly from the southwest), the discharge rate, sea level, and the duration and interactions of these parameters.

Three cruises to the Bay of Gdansk took place on July 4 - 17, 2014, with the R/V Elisabeth Mann-Borgese, from January 31 until February 13, 2015, with the R/V Alkor and from February 27 until March 12, 2016, again with the R/V Elisabeth Mann-Borgese. During the second cruise, a storm event occurred on February 7 - 8, 2015, and station V02 was investigated before and after the storm (Figure 5). The three cruises cover the summer, winter (end phase) and spring (start phase) seasons, with the latter two coinciding with the main outflow period of the Vistula River. As in previous cruises (Voss et al., 2005), sampling stations were chosen from a highly-resolved station grid and were located close to the shore, separated from each other by a distance of 1 - 3 nautical miles. Additionally, the south-north transect from the river mouth (VE04-VE07) was elongated to include the Gdansk Deep (VE38-TF0233), with a distance of 5.4 - 8.1 nautical miles between stations. The sampled stations in the coastal area of the Bay of Gdansk differed among the three cruises, because the choice of stations to be

sampled depended on the location of the river plume and transects were then set accordingly.

2.1.2 The Öre estuary

The Öre Estuary is located in Swedish coastal waters in the northern Baltic Sea at the Kvarken between Bothnian Sea and Bothnian Bay (Figure 4, Figure 6). The Öre River drains into the Öre estuary with a mean discharge of 35 $m^3 s^{-1}$ (Malmgren and Brydsten, 1992; http://vattebwebb.smhi.se, monitoring data 2004 - 2016). The estuary comprises an area of 71.2 km^2, a volume of 0.74 km^3 and an average depth of 10 m (depth range of 3 - 38 m, Svenskt Vattenarkiv, SMHI, 2003). It is separated from the open Sea by an archipelago to the west and by a small sill at 30 m depth to the south. At this location, the origin of currents changes from wind-driven currents inside the estuary to the typical current field of the Bothnian Sea outside the estuary (Brydsten, 1992). At the surface, the connection to the open sea is broad whereas in greater depth ($>$ 20 m) the outlet becomes narrow (Malmgren and Brydsten, 1992). During peak discharge, the extension of the Öre River plume can be up to 10 km long and several km wide with a depth extension of 2 – 3 m (Forsgren and Jansson, 1992). As in the Bay of Gdansk, the spread of the river plume in the Öre Estuary depends on the discharge rate (Forsgren and Jansson, 1992) and the wind conditions, as all water movement and mixing is driven by wind induced waves and wind-driven currents (Brydsten and Jansson, 1989).

Two field campaigns took place in the Öre estuary in April, 20 - 24, 2015, and in August 3 - 8, 2015, covering the spring (start phase) and summer seasons. Samples were taken and partly processed during daily cruises to the estuary with the R/V Lotty from the Umea Marine Science Centre (UMF). The remaining processing of samples took place at the UMF after $\leq$ 3 hours. Sampling stations covered 1) a highly resolved transect from the river mouth to the estuary mouth with a distance between stations of 0.1 - 1 nautical miles and 2) stations chosen regarding the sediment type in order to compare muddy and sandy sediments in the Öre estuary.

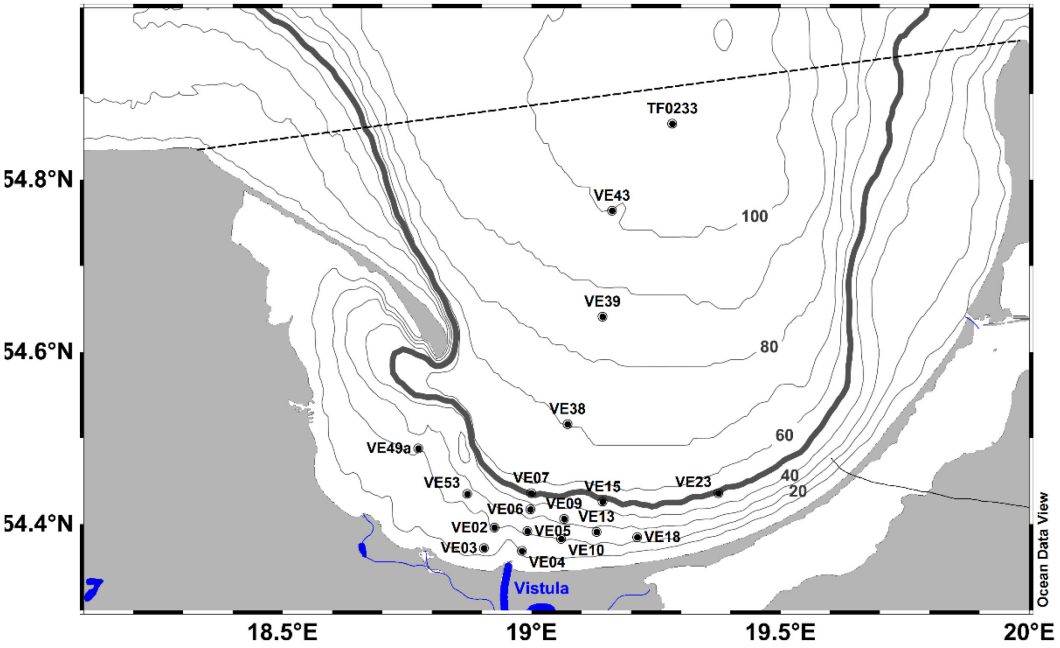

Figure 5: The Bay of Gdansk in the southern Baltic Sea. The Vistula River discharges into the bay. The Vistula estuary is marked by the 50-m isobath (bold line) whereas the deepest area is the Gdansk Deep, around station TF0233, at the border to the Baltic Proper (dashed line).

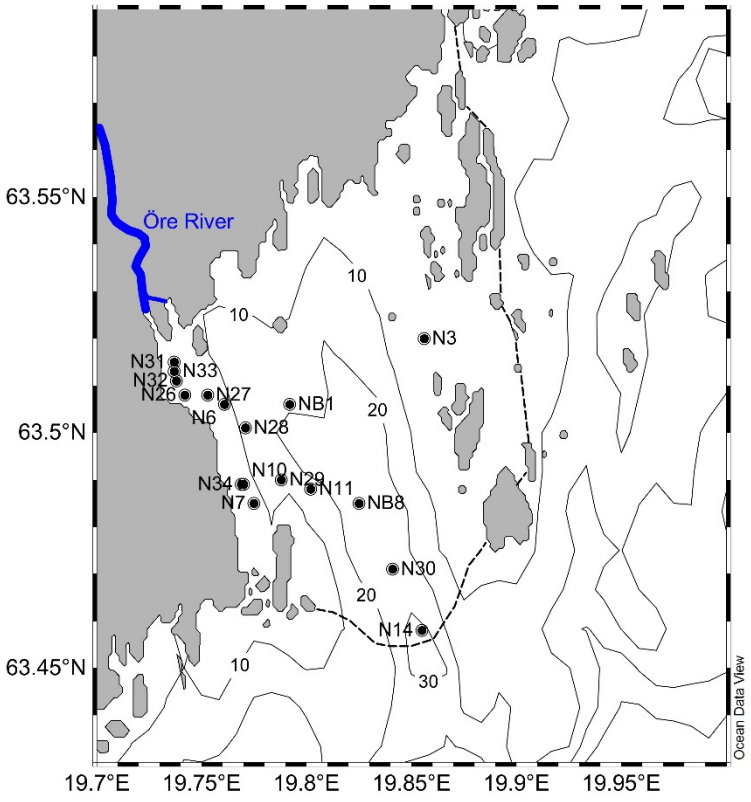

Figure 6: Station map of the Öre Estuary in the northern Baltic Sea. The Öre River discharges in to the semi-enclosed estuary, with a connection to the open Sea in the south. A small sill bounds the estuary (dashed line).

2.2 Environmental data in the water column

2.2.1 CTD and inorganic nutrients

In the Bay of Gdansk, water column measurements were performed with a Seabird CTD-system (Seabird 911plus) equipped with an oxygen sensor (SBE43), a fluorescence and turbidity sensor (Wetlab FLNTU), and a PAR sensor (Biospherical QCP 2300). The time resolution of these sensors was 24 Hz and the data were averaged into 25-cm bins. On the R/V Elisabeth Mann-Borgese, the CTD winch is equipped with a wave compensation system that allows CTD profiling, that is virtually unaffected by wave-induced ship motions, down to 0.5 m above the sea bed. Connected to the CTD was a rosette system containing 13 5-L water samplers. For measurements of environmental variables and the determination of nitrification rates, water samples were taken from the surface and the bottom water and occasionally at one or two water depths in between (mid water column). To examine the depth directly above the seafloor, we also collected water samples from the overlying water, 30 - 50 cm above an intact sediment core obtained with a Multi Corer (MUC). To ensure the integrity of the MUC samples, the measured concentrations of nutrients were compared to the values determined using a chamber lander system (30 cm above the sea floor, Thoms et al., unpublished data). Enhanced concentrations of nutrients, indicative of disturbed cores, were never detected. Concentration of the nutrients PO_4^{3-}, NO_2^-, NO_3^-, and NH_4^+ were measured on board. During the summer and first winter cruise, nutrient concentrations were measured with a continuous segmented flow analyser (QuAAtro, Seal Analytical). Colorimetric measurements were performed after Grasshoff et al. (1999) with minor modifications. The accuracy of the analyser was $\pm$ 5 %, except for NH_4^+ measurements, which were slightly less sensitive (accuracy: $\pm$ 5 – 10 %). During the second winter cruise, in 2016, nutrients were measured using standard colorimetric analyses (Grasshoff et al., 1999).

In the Öre Estuary, water column measurements were performed with seabird CTD systems (April: Seabird SBE19plus equipped with a PAR sensor, August: Seabird SBE 19plus V2) and a Seaguard CTD (Aanderaa) which was equipped with an oxygen optode (4430, Aanderaa) and sensors for PAR, turbidity, chlorophyll a and cDOM. The time resolution of the seabird CTDs was 4 Hz and the data were averaged into 15 cm bins. The sampling interval and thus the time resolution of the seaguard sensors was 0.5 Hz and the data were averaged into 45 cm bins. Water samples were taken with a 5

L or 10 L Niskin bottle which was not attached to the CTD. The water was sampled at two to three depths covering surface, mid, and bottom water. As in the Bay of Gdansk, samples from immediately above the seafloor (BBL) were taken from cores (20 to 40 cm above sediment). Those cores were taken either by a Gemini-corer or a HAPS-corer (KC Denmark). In April 2015, samples from the overlying core-water were collected for nutrients, DON, PON, and POC but not for nitrification rates. In August 2015, samples for determining nitrification rates were additionally collected. During the cruise, samples were stored in the dark at in situ temperature, and were processed at the UMF two to four hours after sampling. Nutrient concentrations were measured at the UMF by Henrik Larsson. Inorganic nutrients (NH_4^+, NO_3^-, NO_2^- and PO_4^{3-}) were measured in whole water samples using a continuous segmented flow analyser (QuAAtro, Seal Analytical), following methods outlined in Grasshoff (1999) and HELCOM guidelines. Background subtraction of the colorimetric signals was also adapted to account for the color of the water caused be a relatively high DOM content.

2.2.2 Chlorophyll *a*, DON, PON and POC

For chlorophyll *a* (Chl.*a*) analyses of samples from the Bay of Gdansk, 0.25 - 1.5 L water was filtered onto GF/F filters (Whatman) and the filters were then frozen at -20 °C. For the determination of the Chl.*a* concentration (µg L^{-1}) at the IOW, filters were transferred into 10 ml 96% ethanol for extraction (3 h). Measurements were then carried out with a Turner Fluorometer (10-AU-005) (Wasmund et al., 2006). Chl.*a* concentrations from the Öre Estuary were measured and kindly provided by Lumi Haraguchi (Aarhus University, Denmark, collaboration within COCOA).

For particulate organic nitrogen (PON) and carbon (POC) determinations of samples from both study sites, up to 2 L of water was filtered through precombusted GF/F filters (Whatman, 3 h at 450 °C). All filters were frozen immediately at -20 °C. Concentrations of PON and POC were measured at the Leibniz Institute for Baltic Sea Research Warnemünde (IOW). The filters were dried at 60 °C overnight and packed into tin caps. Pellets were measured with an element analyser (Thermo Flash 2000). Calibration for the PON and POC content was done with acetanilid (Merck; 10.36 % N; 71.09 % C).

Also at both study sites, 40 ml of the filtrate was frozen in acid washed (10% HCl) and precombusted (3h at 450°C) 50-ml-glass vials for analysis of total dissolved nitrogen (TDN). TDN is needed to determine the concentrations of DON as the difference between TDN and DIN concentrations. TDN concentrations were measured at the IOW

with the persulfate oxidation method (Koroleff, 1983). The oxidation to nitrate was performed in a microwave (MarsXpress, CEM) at 180 °C for 50 min. EDTA standards were used to check for complete conversion to nitrate. Nitrate concentrations were determined with the spongy cadmium method (Jones, 1984). The oxidation efficiency ranged from 90 % to 110 %. The blank was always lower than 2.5 µmol L^{-1} and subtracted from the TDN concentration in the sample. When samples contained high NO_3^- concentrations (e.g. river plume water), we found that they bias the DON-determination. Therefore, such samples were diluted prior to the oxidation in the microwave. The accuracy of the spongy cadmium method was ± 2.9 % (0.32 µmol L^{-1}). For the complete method of TDN-determination had an accuracy of ± 4.7 % (1.44 µmol L^{-1}), showing that the digestion of the samples with potassium persulfate introduces only slightly higher uncertainty. Nitrogen loss from the sample would increase the uncertainty in the measurement. In particular, NH_4^+ could be lost from the water sample via filtration, freezing, thawing of the water sample. However, NH_4^+ concentrations measured at the IOW from frozen filtrate after storage, were similar to the concentrations measured on board during the cruises. Therefore, we are certain that significant nitrogen loss was not a concern and was not introducing additional error into the TDN measurements. Since the DON concentration is determined by the difference of TDN and the inorganic N-compounds, not only the accuracy of the TDN measurement introduces uncertainty to the DON concentration, but also the accuracy of the measurements of NO_3^- (± 5 %), NO_2^- (± 5 %) and NH_4^+ (up to ± 10 %). In turn, the uncertainty of the DON determination is larger with an error of ± 13 %.

2.2.3 Definitions of water layers

In the Bay of Gdansk and in the Öre estuary, the surface water layer was defined as the topmost water layer, where the river plume water occurred. It covered a depth range from 0 – 5 m in the Bay of Gdansk and 0 - 3 m in the Öre estuary, as derived from vertical profiles of density and dissolved silicate concentrations (proxy for river plume water). Environmental variables from these thin layers were obtained from samples of the first CTD-depth or by sampling with a clean bucket. The bottom boundary layer at the two sites was derived from vertical density stratification, based on CTD measurements (Figure 7). Measured temperature (T) and salinity (S) were used to calculate vertical profiles of the buoyancy frequency $N^2(z)$

$$N^2(z) = -\frac{g}{\rho}\frac{\partial \rho}{\partial z} \quad (1)$$

with g = 9.81 m s^{-2}, ρ is the density and the other quotient is the partial derivative of the density over depth. The thickness of the BBL was defined as the distance from the seafloor to the first local maximum of N^2 above the bottom. To confirm the integrity of this method of estimation, BBL thickness was also estimated from the beginning of the invariable distribution of T, S and density in vertical profiles (Figure 7, Turnewitsch and Graf, 2003). Additionally, an increase in turbidity that coincided with the beginning of the BBL was frequently observed. In the winter of 2015 at four stations and the winter of 2016 at one station in the Bay of Gdansk the BBL thickness could not be determined because the CTD could not be lowered close enough to the seafloor. Thus, identification of the peak of N^2 or the invariable distribution of T, S, or density was not possible. However, the MUC water samples taken at these stations were assumed to lie well within the BBL, as the extent of the BBL at all other stations exceeded this sampling depth. The deep water layer (DWL) at offshore stations of the Bay of Gdansk with a permanent halocline (stations VE38 to TF0233, Figure 11A) was defined as the water layer between the halocline (also a peak in N^2) and the seafloor and thus included BBL samples (figure II in appendix).

At the Öre estuary the BBL thickness was only determined for the stations where nitrification rates were measured and water samples from the overlying water of sediment cores were taken (figure I in appendix). This includes 4 stations along the transect in April 2015 and 8 stations in August 2015. The BBL was successfully sampled with the Niskin bottle at only two stations (both in April 2015). Otherwise only the samples from the overlying core water can be assigned to the BBL in the Öre estuary.

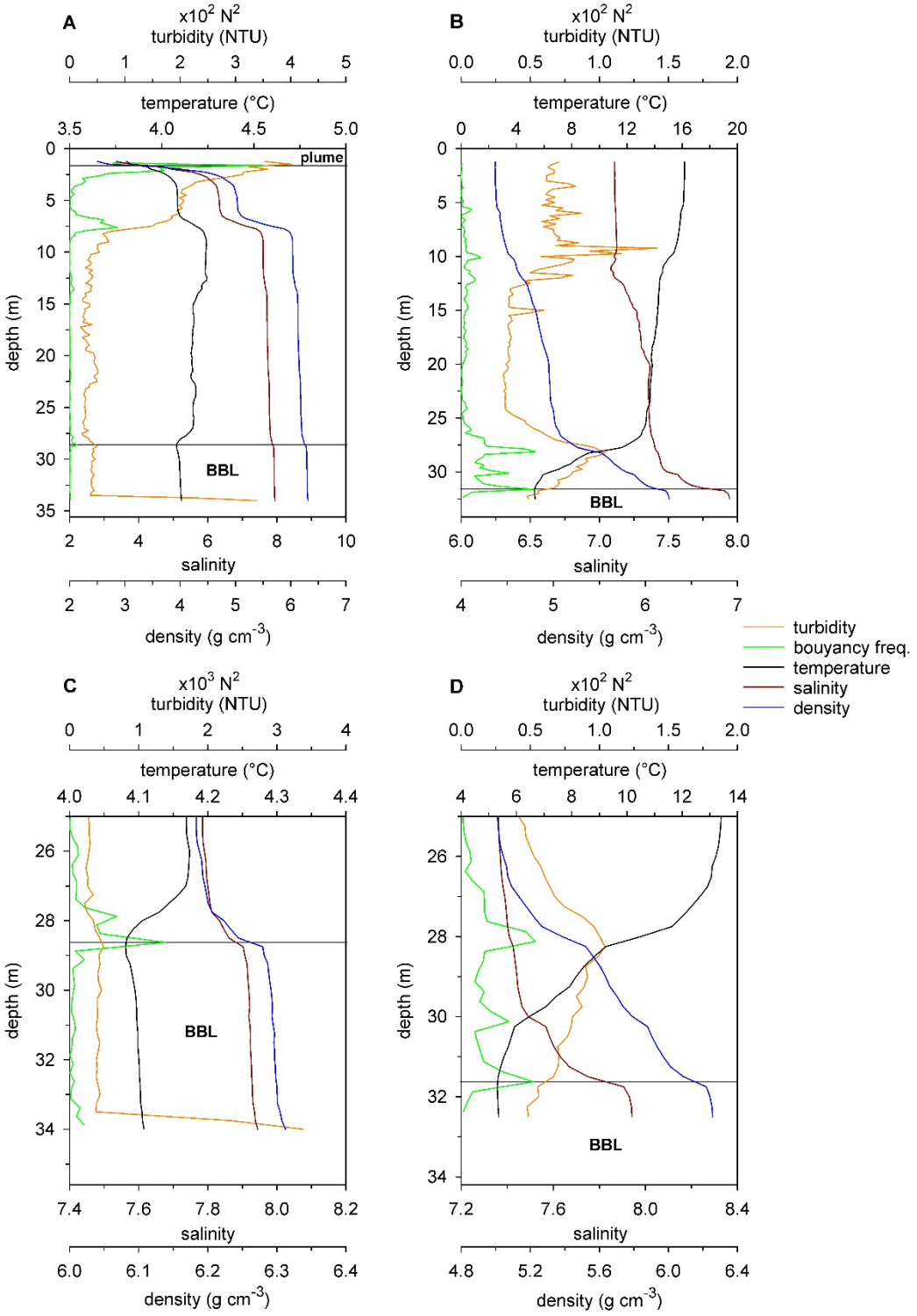

Figure 7: Depth profiles of temperature (black), salinity (red), density (blue), buoyancy frequency N^2 (green) and turbidity (orange) in the Bay of Gdansk: A and B) profiles of the coastal stations VE06 (spring 2016) and VE09 (summer2014), respectively, to identify a river plume layer, the surface mixed layer (SML) and the bottom boundary layer (BBL); B and C) the same coastal stations in higher resolution. The upper boundary of the BBL was identified by the peak in N^2 and the beginning of invariable distribution of temperature, salinity and density. Please note the different scaling of the variables. Distinct water layers are marked by the horizontal black line.

2.2.4 BBL profiles

On the cruise EMB123 in March 2016, it was possible to sample water from the BBL on a more highly resolved profile. Therefore, the Automated Mini Chamber Lander System (Unisense) was modified to sample water within the BBL from several heights above the sediment after deployment (Figure 8). The silicon tubes that are attached to the syringe sampler were mounted on a rod at several heights. For each height two silicon tubes and thus two syringes were used in order to sample 100 ml water in total from each depth. The rod itself is mounted onto the frame of the lander. The heights were tubes were attached at the rod were 5, 15, 30 and 45 cm from lander base i.e. above the sediment. Additionally, tubes were mounted at the lander frame at 60 cm and at 80 cm height, respectively. The lander was programmed to sample water from bottom to top after a delay-time of ≥ 30 minutes to allow disturbed sediment to resettle and to sample under in situ conditions. After retrieving the device, the water samples were filtered through GF/F filters (Whatman) and nutrient concentrations were analysed as described above (see section 2.2.1.).

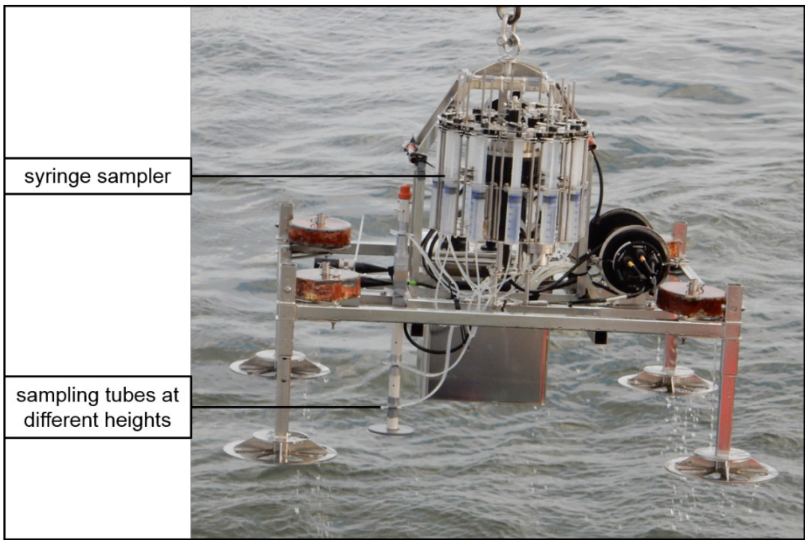

Figure 8: The Automated Mini Chamber Lander System (Unisense) modified to a bottom water sampler. By mounting the sampling tubes at different heights above the lander base, a profile within the BBL could be sampled from 5 to 80 cm above the seafloor after deploying the system.

2.3 Environmental data in the sediment

The sediment data shown in this thesis are from the Bay of Gdansk only. From the cruise EMB077 in summer 2014, the surface sediment characteristics water content and loss on ignition (LOI) are kindly provided from Urszula Janas from the University of Gdansk (collaboration in the EU Bonus project COCOA). Sediment samples from the other two

cruises were processed at the IOW and kindly provided by Franziska Thoms (framework of COCOA, Franziska Thoms, PhD-thesis). A short description of methods can be found in the appendix.

2.4 Nitrification rates and ammonium assimilation rates

Nitrification and NH_4^+ assimilation rates were determined at both study sites using the ^{15}N-NH_4^+ tracer method as described in previous studies (Damashek et al., 2016; Veuger et al., 2013; Ward, 2005). Six polycarbonate (PC) bottles were filled with the water samples via the overflow technique to avoid air in the sample. The bottles were sealed with a butyl septum and a drilled lid used to inject the label directly into the bottle. The water samples were amended with 50 – 200 nmol L^{-1} ^{15}N-NH_4Cl (99 atom% ^{15}N) to yield an enrichment of < 30 %. The contents of three of the six PC bottles were filtered immediately to serve as the t_0 and as control. The remaining triplicates were incubated for 3 - 7 h in a dark temperature-controlled room at the in situ temperature. The incubation was stopped by filtration (200 mbar) through precombusted GF/F filters (Whatman, 3 h at 450 °C). The filtrates (start and end of the incubation) were frozen at -20 °C for later use in the analysis of nutrient concentrations and the ^{15}N content of NO_2^- and NO_3^- (in the following referred to as NO_x^-) in order to calculate nitrification rates. Filters frozen at -20 °C were used to determine the PON concentration and in the isotopic analysis of $\delta^{15}N$-PON to calculate NH_4^+ assimilation rates. The ^{15}N content of NO_2^- and NO_3^- was measured at the IOW using the denitrifier method after Sigman et al. (2001) and Casciotti et al. (2002). The bacterium *Pseudomonas chlororaphis* (ATTC 13985), lacking N_2O reductase activity, quantitatively converts NO_2^- and NO_3^- to nitrous oxide. The N_2O was automatically extracted (PAL autosampler), purified in a Finnigan GasBench II, and analysed in a Delta V advantage (Thermo). Every 12th sample, two to three NO_3^- isotope references (IAEA-N3 and USGS 34) were analysed. After each set of labelled triplicates, one IAEA-N3 standard was used as buffer to avoid the dragging of extremely high ^{15}N signals from the previous to the next triplicate sample, although dragging rarely occurred. The accuracy of the isotope measurements was $\pm$ 0.14 ‰. Only in samples with a NO_x^- concentration of ≥ 1 µmol L^{-1} could the isotopic composition of N be detected. Samples ($n = 7$) collected in the middle of the water column during the summer cruise had NO_x^- concentrations < 1 µmol L^{-1}. These were spiked before the measurements with the IAEA-N3 standard, which has a known concentration and a known isotopic signal (4.69

$\pm$ 0.14 ‰). From the known NO_x^- concentrations of the sample and IAEA-standard, and the known isotopic signal of IAEA-N3, the ^{15}N content of the samples could be calculated. Tests with samples of known ^{15}N-content resulted in recoveries of 97 $\pm$ 19 % when measured by the spiking method.

Considering the accuracies of the concentration and isotopic measurements as well as variations in sample and standard injections (leading to dilution errors), the uncertainty of the spiking method was $\pm$ 20 %. Since the ^{15}N-content of the nitrate-depleted t_0-samples was not detectable, the nitrification rates of those summer samples were calculated based on a mean of all measurable ^{15}N-contents of the t_0-samples from the summer cruise (0.370 $\pm$ 0.002 atom%). Since the error was high and the true t_0-value of the summer samples with nitrate concentrations at the detection limit were unknown, the nitrification rates were rough estimates and therefore excluded from the statistical analysis.

PON concentrations were measured as described above. For additional measurement of the ^{15}N content of PON, the element analyser (Thermo Flash 2000) was coupled to the CF-IRMS (Thermo Delta V advantage) via the interface Conflo IV. The reference gas was ultra-pure N_2 from gas bottles and was calibrated by means of IAEA-N1, N2, and N3. The analytical precision was < 0.2 ‰. The calibration material for N analysis was acetanilide (Merck). Peptone (Merck Chemicals) served as the internal standard, which was run after every fifth sample. Nitrification rates (NR) were calculated after Veuger et al. (2013):

$$NR = \frac{[^{15}N\text{-}NO_x^-] \times \frac{[NH_4^+]_{tot}}{[^{15}N\text{-}NH_4^+]_{add}}}{\Delta t} \qquad (2)$$

where $[^{15}N\text{-}NO_x^-]$ is the excess concentration of ^{15}N in NO_x^-, $[NH_4^+]_{tot}$ is the sum of the ambient and added NH_4^+-concentrations, $[^{15}N\text{-}NH_4^+]_{add}$ is the added $^{15}N\text{-}NH_4^+$ concentration, and Δt is the incubation time. The excess concentration of ^{15}N in NO_x^-, was calculated as the difference in ^{15}N-content (in atom%) of the t_{end} and t_0 sample:

$$[^{15}N\text{-}NO_x^-] = \frac{(^{15}N\text{-}NO_x^-start - {}^{15}N\text{-}NO_x^-end)}{100} \times [NOx^-] \qquad (3)$$

whereby $^{15}N\text{-}NO_x^-{}_{start}$ is the ^{15}N content of the t_0 sample and $^{15}N\text{-}NO_x^-{}_{end}$ is the ^{15}N content at the end of the incubation, and $[NO_x^-]$ is the mean concentration of triplicate NO_x^- measurements from t_0 and t_{end}. The concentration average of all six samples (t_0 and t_{end}) was used for NH_4^+ and NO_x^-, because concentration differences were minor. NH_4^+-assimilation rates (AAR) were calculated after Dugdale and Wilkerson (1986):

$$AAR = V_m \times [PON_m] \quad (4)$$

where V_m is the mean specific ^{15}N uptake rate and $[PON_m]$ the mean of the beginning and final PON concentrations. The calculation of V_m also includes both the ^{15}N-PON content of the t_0 and the t_{end} sample.

Instead of a NH_4^+ concentration ratio as used in the calculation above, Damashek et al. (2016) calculated the nitrification rate based on the estimated atomic ratio of $^{15}N\text{-}NH_4^+$. However, an estimated $\delta^{15}N\text{-}NH_4^+$ value could lead to overestimations, if the ambient natural $\delta^{15}N\text{-}NH_4^+$ content is high. In recalculations using high natural $\delta^{15}N\text{-}NH_4^+$ values (up to 50 ‰) Damashek et al. (2016) showed only a marginal change in nitrification rates (second and third decimal places). Since this change is negligible and the rates calculated using the two formulas are the same, we used the equation of Veuger et al. (2013). Mean nitrification rates were averaged from the triplicates and used in the statistical analyses.

2.5 Statistical analyses and calculations

2.5.1 Statistical analyses

Due to variation in samples size and not meeting the prerequisites for parametric tests (normal distribution and homogeneity of variances), non-parametric tests were used to explore significant differences among the data. To check for significant differences between samples the Mann-Whitney-U-test (U-test) and the Kruskal-Wallis-test (1-way ANOVA) were performed with SPSS (version 22). Only datasets with a sample size of $n \geq 4$ were used for comparison analyses. Relationships between nitrification rates and environmental variables were identified in correlation analyses (Pearson correlation coefficient, R) using SAS (version 9.4). Only datasets with a sample size of $n \geq 5$ were included in the correlation analyses.

2.5.2 Calculation of riverine N-loads

River samples, from the Vistula River and the Öre River, were taken during all cruises, except for the EMB077 in the Bay of Gdansk in summer 2014. All Environmental variables were determined as described above. Based on the dates of river sampling the river discharge could be extracted from monitoring data (Bay of Gdansk: Polish national monitoring by Institute of Meteorology and Water Management National Research Institute, Öre estuary: http://vattenwebb.smhi.se). With these data, I calculated the riverine nitrogen loads by multiplying the concentration of the N-compound and the river discharge. The sampling stations were further upstream at both rivers (Table 1), so the calculated N-loads are not the exact loads at the river mouth. However, they are still valuable to see differences in the magnitude of loads and the riverine composition of the nitrogen species between seasons and sites.

Table 1: Sampling and monitoring sites at the Vistula River and Öre River and their distance from the river mouth.

	station water sampling	distance (km)	station river discharge	distance (km)
Öre River	63.5625N, 19.6979E	5.6	63.7044N, 19.5982E (Torrböle 2)	25
Vistula River	54.2568N, 18.9470E (Kiezmark)	12	54.0927N, 18.0861E (Tczew)	35

3. Results and Discussion

3.1 Measurement and calculation of nitrification rates

There are several methods for the quantification of nitrification which are well summarized by Ward (2011) or Damashek (2016). A widely applied method uses the stable nitrogen isotope by adding a ^{15}N-labelled nitrogen compound and tracing its enrichment or dilution in another nitrogen compound via mass spectrometry. The stable nitrogen isotope techniques have the advantage of short incubation times, small amendments of ^{15}N and high sensibility of mass spectrometry to measure ^{15}N concentrations. Most important, the signal of transfer from ^{15}N in the substrate to ^{15}N in the product can be detected irrespective of other biogeochemical processes. To quantify nitrification, there are two stable N isotope techniques currently applied. The heavy isotope ^{15}N can either be used in the substrate NH_4^+ (tracer method; Ward, 2011) or in the product NO_3^- (dilution method; Carini et al., 2010). In the dilution method, ^{15}N-NO_3^- is added to the water sample prior to incubation in a higher concentration than natural NO_3^- concentrations. Thereby, the product of nitrification is enriched in ^{15}N and dilution by the production of ^{14}N due to nitrification will be measured. This rate of dilution equals the rate of nitrification (Carini et al., 2010). With this dilution method, the substrate pool will not be influenced, however the product pool is enriched in nitrate which could stimulate other biogeochemical processes and indirectly influence nitrification. Furthermore, the detection limit in the HPLC-method described by Carini et al. (2010) is rather high resulting in a lowest measurable nitrification rate of 192 nmol L^{-1} d^{-1}, but rates can be lower in the Baltic Sea (Enoksson, 1986; Hietanen et al., 2012). In the tracer method, small concentrations of ^{15}N-NH_4^+ are added to water samples (as much as 10 % of the ambient NH_4^+-concentrations) prior to incubation. In the end, the ^{15}N in the product NO_3^- can be detected by different techniques, e.g. denitrifier method (Ward, 2011). The advantage of the tracer method is the addition of the substrate in very low concentrations which should not influence in situ nitrification rates. However, the process of ammonification can dilute the substrate pool biasing rate calculations. Therefore, short incubation times (1 – 3 hours; Ward, 2011) are to be preferred to avoid this dilution effect. An additional advantage of using the tracer technique is the simultaneous possibility to measure NH_4^+-assimilation by measuring the ^{15}N concentrations in the particles which are caught on the filter, after terminating

the incubation experiments by filtration (Ward, 2011). Therefore, in this PhD-thesis, the tracer method was applied to measure in situ nitrification and NH_4^+ assimilation rates (see section 2.4). I did not differentiate between ammonium oxidation and nitrite oxidation, but determined the bulk nitrification rate from NH_4^+ to NO_2^- and NO_3^- (in the following referred to as NO_x^-). However, in spring 2016, I removed NO_2^- from samples at the end of the incubation (Granger et al., 2009) and results showed, that most of the ^{15}N was recovered in NO_2^- (82%, n=6) and not in NO_3^- when NO_2^- was removed (table II in the appendix). So it is likely, that nitrification rates from this study mainly reflect NH_4^+ oxidation rates.

Due to unknown ambient NH_4^+ concentrations in the Bay of Gdansk and the Öre estuary, a low amount of tracer was added (0.05 – 0.2 µmol L^{-1} d^{-1}). However, some samples experienced strong enrichment in NH_4^+ when the ambient NH_4^+ concentration was very low. When the ^{15}N-NH_4^+ enrichment exceeded 40 % of the ambient NH_4^+ concentration, measured nitrification rates were considered potential and excluded from the data set. The method applied here (after Veuger et al., 2013) only uses a start and end point of the incubation for the calculation of the nitrification rate. This method presumes a linear increase in the ^{15}N content of the product NO_x^- and is applied in several studies (e.g. Heiss and Fulweiler, 2016; Peng et al., 2016, Small et al., 2013, Ward et al., 2005). This "start/end" method could potentially over- or underestimate nitrification when nitrate (preferentially ^{14}N-NO_3^-) is consumed or NH_4^+ is produced during the time of incubation, respectively. To prevent a strong influence of these effects, my samples were incubated 1) under dark conditions to prevent NO_3^- uptake by primary producers and 2) during short time scales of 2 -7 hours to prevent dilution of the NH_4^+ pool. Nevertheless, I cannot completely rule out any effect of substrate dilution which could have occurred at the same rate as nitrification. Especially during summer, nitrification rates in the Bay of Gdansk and in the Öre estuary might be underestimated due to degradation of organic nitrogen to NH_4^+, leading to dilution of the substrate pool during incubation. However, incubation times in summer were not longer than 3 hours. If I assume NH_4^+ production twice as high as the calculated nitrification rates, e.g. 227 nmol L^{-1} d^{-1} nitrification and 454 nmol L^{-1} d^{-1} NH_4^+ production, this would lead to 0.4 µmol L^{-1} additional NH_4^+ after two hours of incubation. Correction of the rate calculation by this additional NH_4^+ source would result in a nitrification rate of 230 nmol L^{-1} d^{-1}, only 1 % higher than the actual measured nitrification rate. Only, when

increasing the NH_4^+ production by a factor of 10 or 100, this would have a strong effect on the calculation of nitrification rates. It is, however more likely, that nitrification and ammonification occur at similar rates in coastal zones, as it was shown by Brion et al. (2008). Another possibility to determine nitrification rates is to obtain a time series and calculate the rate via the linear increase of ^{15}N in the product NO_x^- (e.g. Bristow et al., 2015; Hsiao et al., 2014). However, time series are not applicable on short cruises, when 1 – 2 stations were sampled in triplicates at several water depths as it was the case in this study. As discussed above, I am confident that the use of the ^{15}N-tracer method , with a calculation using start and end values, quantifies nitrification as they are naturally present in coastal waters of the Baltic Sea.

3.2 River plume and bottom boundary layer – Hotspots for nitrification in an open coastal bay?

This chapter is closely related to the results and discussion of a submitted manuscript entitled: "River plume and bottom boundary layer – hotspots for nitrification in a coastal bay?" submitted to "Estuarine Coastal and Shelf Sciences" on January 12, 2017. Co-authors are Kirstin Schulz, Iris Liskow, Lars Umlauf and Maren Voss. My contribution to these chapters of the manuscript were 90 % and included all data analyses and most of the writing.

River plume and BBL, can provide favourable conditions for nitrification and thus be hotspots for nitrification in a coastal zone (see section 1.4.). A hotspot is defined in this thesis as a location or time point of enhanced nitrogen turnover rates, in this case nitrification rates. To investigate whether river plume or BBL are nitrification hotspots, nitrification rates and its regulation were examined in the Vistula estuary of the Bay of Gdansk (southern Baltic Sea).

3.2.1 Environmental variables and nitrification rates in the Bay of Gdansk

The environmental data from the Bay of Gdansk showed both seasonal and spatial differences (Table 2, Figure 9), with the latter detected not only between Vistula estuary and offshore sites but also between different coastal water layers. The Vistula estuary and the offshore area of the Bay of Gdansk are separated at 50 m depth (Figure 5) and could be distinguished 1) by the existence of a permanent halocline at the offshore sites, 2) by higher δ^{15}N-PON values in the coastal sediment (Thoms et al., unpublished), and 3) via EOF-analyses of the BBL water showing a significant change in environmental variables at 50 m depth (Voss et al. EGU Geophys. Res. abstracts 2017). These results suggest a close sediment – water coupling to a depth of approximately 50 m.

From the halocline to the seafloor, a 10 to 36 m thick deep water layer (DWL) extended, and there was no light penetration at these depths. In the Vistula estuary, no permanent halocline was observed, but a stable thermal stratification was found at all coastal stations during the summer cruise (Figure 11A). Instead, in winter and spring, the water column was well mixed and only the fresh water from the river plume created stratification in the surface water (Figure 7). However, the BBL formed a distinct water layer with a mean thickness of 3.2 $\pm$ 1.5 m in summer 2014 and 5.7 $\pm$ 1.2 m and 4.7 $\pm$

1.3 m in winter 2015 and spring 2016, respectively. The BBL was significantly thicker in winter 2015 and spring 2016 compared to summer 2014 (Kruskall-Wallis Test, $p = 0.02$). During all cruises at all stations, ≤ 0.1 % of the surface radiation reached the seafloor in the Vistula estuary.

Offshore, no clear seasonal differences in the DWL were measured, except for minor differences in DIN concentrations (Table 2). High salinity, low temperature and low oxygen concentrations were characteristic for the DWL compared to the Vistula estuary. However, concentrations ranges of the N-species were similar (Figure 9, Table 2). Within the Vistula estuary, there was a general increase in salinity and a decrease in oxygen concentration from the surface water to the BBL (Figure 9A and C) and PON concentrations were highly variable (Figure 9F). Seasonal differences in the Vistula estuary were reflected in the distribution of temperature and DIN concentrations (c). In summer, temperatures were overall higher than in winter and spring, and they decreased from the surface to the BBL (Figure 9). Highest concentrations of NO_x^- and NH_4^+ were measured in the BBL in summer and in the river plume in winter and spring. Distinct physical and biogeochemical BBL-characteristics could only be detected in summer, while environmental variables of the BBL in winter and spring were similar to the mid water column (Figure 9). High riverine discharge in winter and spring led to a strong river plume signal which was reflected in low salinity and high nutrient concentrations in the surface water (Figure 9, Table 2). Thus, in these seasons, the river plume displayed distinct physical and biogeochemical characteristics.

Table 2: Environmental variables, and nitrification and NH_4^+ assimilation rates from the Bay of Gdansk separated spatially into coastal water and offshore deep water layer (DWL), and seasonally according to cruises conducted in summer, winter and spring. Data are shown as median (m, in bold) and standard deviation (s).

		salinity		**temp.** (°C)		**oxygen** (ml L^{-1})		**$NO_{3/2}^-$** (µmol L^{-1})		**NH_4^+** (µmol L^{-1})		**DON** (µmol L^{-1})		**PON** (µmol L^{-1})		**POC** (µmol L^{-1})		**Chl.*a*** (µg L^{-1})		**NR** (nmol L^{-1} d^{-1})		**AAR** (nmol L^{-1} d^{-1})	
		m	*s*	*m*	*s*	*m*	*s*	*m*	*s*	*m*	*s*	*m*	*s*	*m*	*s*	*m*	*s*	*m*	*s*	*m*	*s*	*m*	*s*
coastal area	summer 2014	**7.3**	0.4	**14.6**	4.0	**6.3**	1.0	**0.6**	0.8	**1.3**	1.7	**15.9**	23.2	**4.9**	7.6	**36.1**	73.6	**2.7**	8.6	**52**	165	**277**	289
	winter 2015	**7.4**	1.0	**3.9**	0.7	**8.6**	0.6	**5.8**	26.2	**0.4**	1.6	**10.9**	5.2	**1.2**	1.8	**10.5**	17.7	**0.5**	0.8	**52**	58	**65**	34
	spring 2016	**7.6**	1.3	**4.2**	0.2	**8.4**	0.5	**6.0**	55.0	**0.4**	1.4	**16.8**	3.1	**3.1**	2.3	**16.4**	13.0	**3.5**	2.5	**40**	37	**44**	450
offshore DWL	summer 2014	**10.3**	1.6	**5.3**	3.0	**3.4**	1.4	**3.8**	2.5	**0.4**	1.2	**11.9**	3.1	**2.1**	2.8	**19.7**	20.9	**0.1**	0.0	**93**	56	**155**	269
	winter 2015	**11.3**	1.8	**7.1**	1.5	**1.9**	2.9	**7.5**	1.5	**1.4**	0.8	**12.7**	1.7	**1.1**	3.9	**9.2**	32.1	**0.1**	0.3	**284**	588	**101**	71
	spring 2016	**11.9**	1.0	**6.7**	0.7	**2.3**	1.5	**9.1**	0.5	**1.2**	0.4	**18.3**	3.7	**0.9**	1.5	**10.0**	2.2	**0.1**	0.2	**117**			

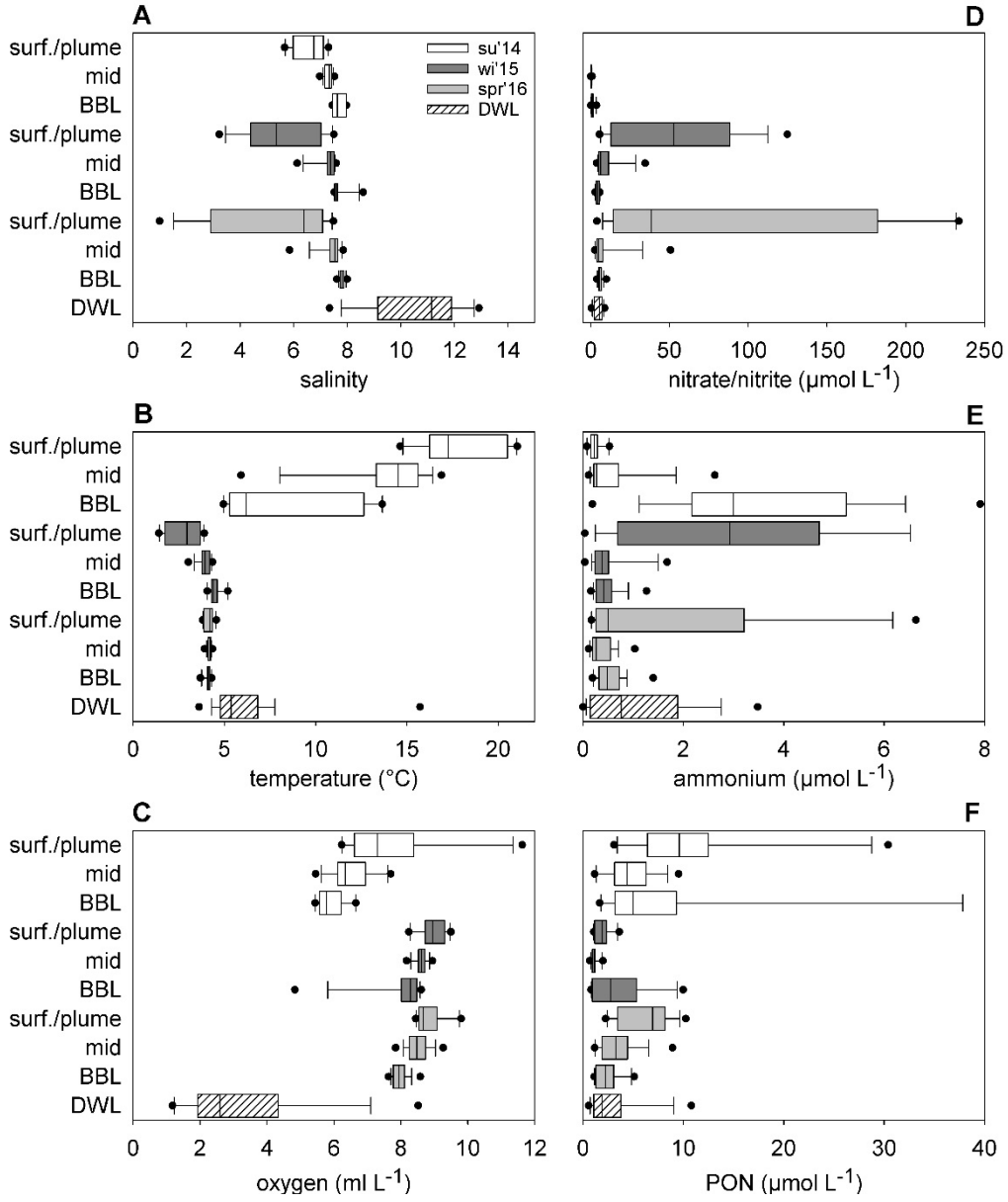

Figure 9: Distribution of environmental variables in the surface water (surf./plume), mid water column (mid) and the bottom boundary layer (BBL) of the Vistula estuary as well as the deep water layer (DWL) of the offshore area in the Bay of Gdansk during cruises in summer 2014 (su'14), winter 2015 (wi'15) and spring 2016 (spr'16). The DWL covers data from all cruises. The error bars cover the 10th and 90th percentiles, the black points show 5th and 95th percentiles.

High discharge of the Vistula River occurred with 1100 $m^3 s^{-1}$ and 1500 $m^3 s^{-1}$ in winter 2015 and spring 2016, respectively, creating a strong river plume signal in the surface water. Silicate concentrations (winter 2015) and turbidity (spring 2016) clearly distinguished the river plume from coastal surface water. I found significantly higher silicate concentrations (winter 2015, U-test, $p < 0.001$) and turbidity values (spring 2016, U-test, $p = 0.006$) in surface waters with a salinity lower than 6 (Figure 10). Those surface waters were defined as river plume water. The typical surface salinity in the Bay of Gdansk without river influence was around 7. During both cruises, the river plume was directed to the east, but it spread further into the bay in spring 2016 (Figure 10). We observed significantly higher NO_x^-, NH_4^+, and PON concentrations in the river plume water compared to the non-influenced surface water, except for PON in spring 2016 (U-test, $p < 0.05$, Table 3).

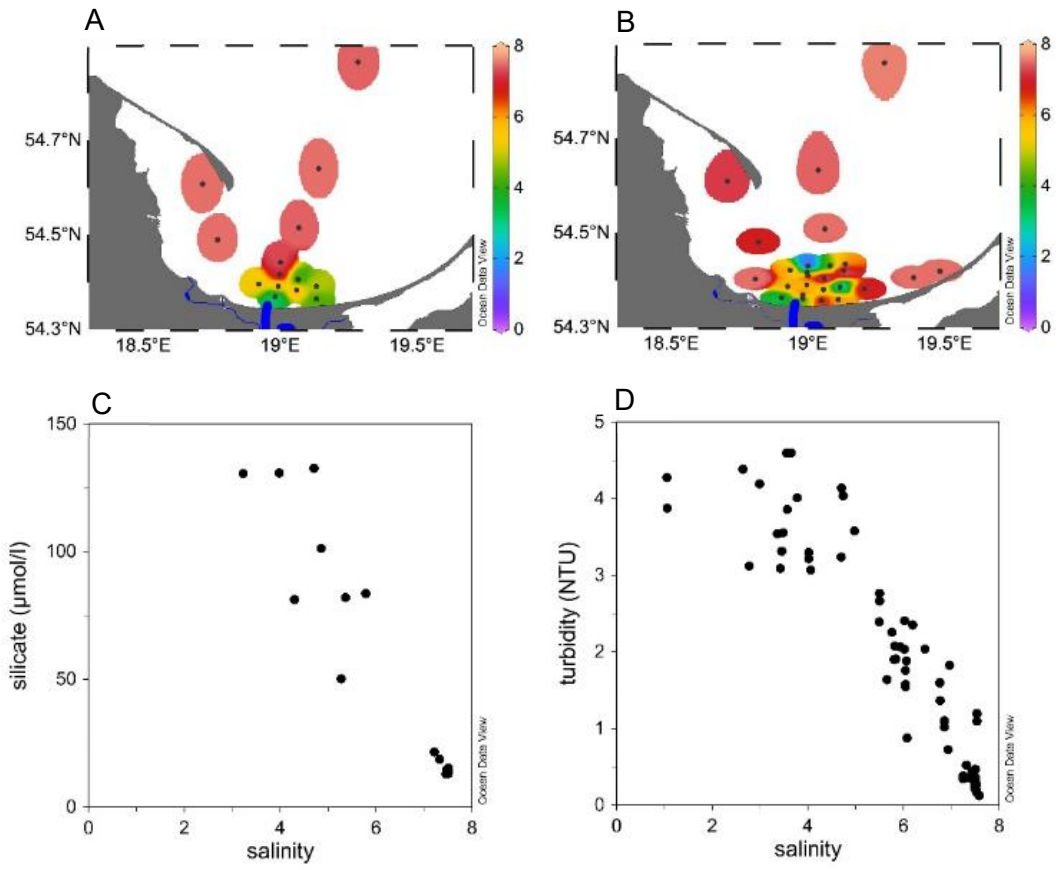

Figure 10: The distribution of salinity in the Bay of Gdansk in winter 2015 (A) and spring 2016 (B). Salinities < 6 indicate the river plume which is directed eastward during both seasons, but is more widely spread in spring 2016. Significant higher concentrations of silicate in winter 2015 (C) and turbidity values in spring 2016 (D) reveal a riverine fresh water influence up to a salinity of 6.

Table 3: Comparison of the concentration of N-species between river plume water (salinity < 6) and coastal surface water (salinity > 6). The river plume water contains significantly higher concentrations than the coastal surface water, except for PON concentrations in spring 2016. Mean concentrations (m) and standard deviation (s) are given.

		NO_x^- µmol L^{-1}		NH_4^+ µmol L^{-1}		PON µmol L^{-1}	
		m	s	m	s	m	s
winter 2015	river plume (S < 6)	**78.34****	27.97	**3.84****	1.89	**2.33***	1.30
	coastal surface (S > 6)	**5.25**	1.99	**0.38**	0.16	**1.17**	0.20
spring 2016	river plume (S < 6)	**182.10***	78.70	**2.90***	2.24	**6.94**	2.15
	coastal surface (S > 6)	**13.24**	20.70	**0.37**	0.17	**4.56**	2.24

siginificant differences: *p<0.05; **p<0.001

During a storm event on February 7 – 8, 2015, wind speeds peaked at 21 m s^{-1} and the wind direction shifted from 270° west to 0° north (www.wunderground.com). The profiles of salinity, temperature, and nutrient and PON concentrations perfectly mirrored the complete loss of stratification during the storm event (Figure 11B). PON concentrations were significantly higher throughout the water column after the storm.

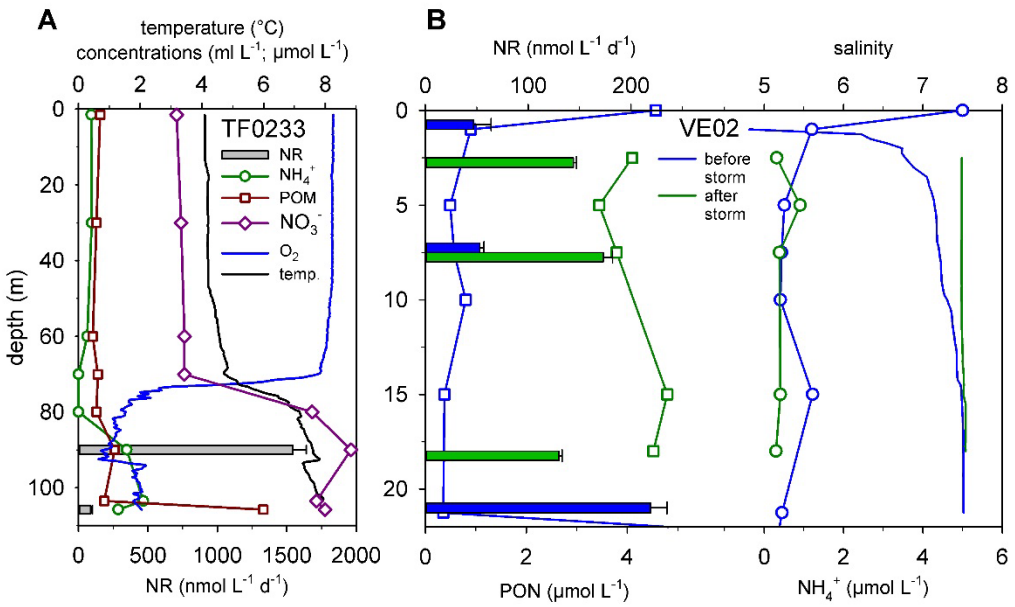

Figure 11: A) Profiles of temperature, oxygen, NH_4^+, PON and NO_3^- (upper x-axis) as well as the nitrification rates (NR, bars) at the Gdansk Deep (station TF0233) in winter 2015. Below 90 m depth the oxygen concentration increases slightly due to a Major Baltic Inflow. B) Profiles of salinity (line), NH_4^+ (circles), POM (squares) and nitrification rates (bars) at station VE02 before and after the storm event in the Bay of Gdansk in winter 2015.

Overall, nitrification rates did not differ between seasons, neither in the coastal nor in the offshore area. Large ranges of 3 – 525 nmol L^{-1} d^{-1} (mean: 73 nmol L^{-1} d^{-1}) in the coastal area and 18 – 1544 nmol L^{-1} d^{-1} (mean: 282 nmol L^{-1} d^{-1}) in the offshore area were determined (Figure 12A). Nitrification rates also did not differ between the offshore DWL and the coastal BBL, both "dark" water layers. Although the nitrification rates in the mid water column in summer were estimated via spiking (see section 2.4.), they seemed generally lower than the nitrification rates in the BBL (Figure 12A). In winter 2015, nitrification rates in the BBL were slightly but significantly higher than in the surface water (U-test, $p < 0.001$), while nitrification rates covered the same ranges in all water layers in spring 2016 (Figure 12A). The highest rates among the coastal sites were measured in the BBL in summer 2014 (VE53, 525 nmol L^{-1} d^{-1}), after a storm event in winter 2015 (130 – 173 nmol L^{-1} d^{-1}), and in the Vistula River in spring 2016 (River: 397 nmol L^{-1} d^{-1}). In the DWL, highest rates of 1544 nmol L^{-1} d^{-1} at TF0233 and 420 nmol L^{-1} d^{-1} at VE39 in winter 2015 were measured at depths characterized by the lowest oxygen concentrations (1.19 ml L^{-1} and 1.92 ml L^{-1}) and high temperatures (7.6°C and 6.8°C), accompanied by elevated POM and NH_4^+ concentrations (Figure 11A). The storm event in winter 2015 induced a significant increase in the nitrification rates of the surface water and mid water column (t-test, $p = 0.003$; Figure 11B). The depth integrated nitrification rate increased by a factor of 1.7, from 104 ± 31 nmol L^{-1} d^{-1} before the storm to 173 ± 34 nmol L^{-1} d^{-1} after the storm. The relative contribution of nitrification to the total NH_4^+ consumption (sum of nitrification rates and NH_4^+ assimilation rates) in the coastal area of the Bay of Gdansk is shown in Figure 12B. Compared to the overlying, water nitrification in the BBL contributed more to the total NH_4^+ consumption in summer, but NH_4^+ assimilation was the dominating process. In winter and spring, the contributions of nitrification in these water layers were comparable while surface water NH_4^+ assimilation consumed more NH_4^+ than nitrification. Nitrification consumed a significant amount of NH_4^+ in winter and spring in the mid water and BBL. Although the sample size of nitrification rates in the coastal surface water was too small to perform a statistical test, Figure 13 shows that there is no difference in nitrification rates of the two water types.

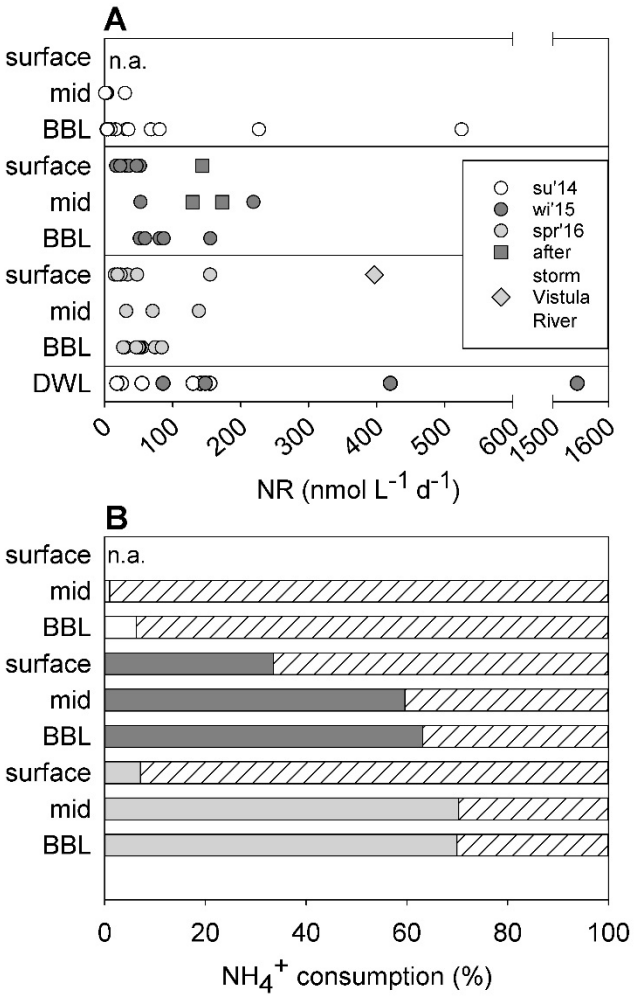

Figure 12:
A) Mean nitrification rates (NR) in the surface water (surface), the mid water column (mid) and the bottom boundary layer (BBL) of the Vistula estuary as well as in the deep water layer (DWL) in the offshore Bay of Gdansk in summer 2014 (su'14), winter 2015 (wi'15) and spring 2016 (spr'16). Nitrification rates in the surface water in summer 2014 were not measured (n.a.). Standard deviations from triplicate samples are not shown here. B) Relative contribution of nitrification rates (see colour coding in panel A) to the total NH_4^+ consumption, which is the sum of nitrification rates and NH_4^+ assimilation rates (shaded bars).

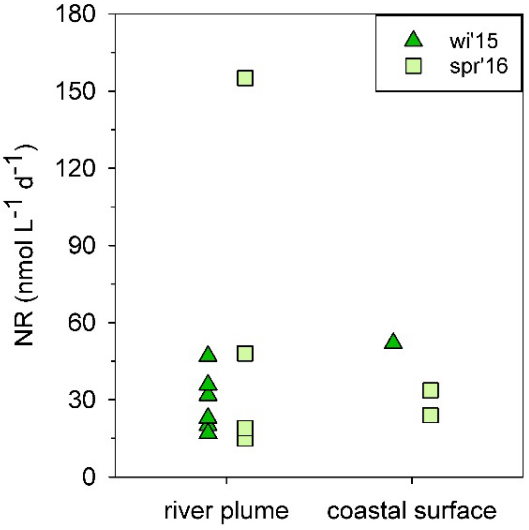

Figure 13:
Comparison of nitrification rates in river plume water (salinity < 6) and coastal surface water (salinity > 6). Data were collected during cruises in winter 2015 (wi'15) and spring 2016 (spr'16), respectively).

Correlations between nitrification rates and environmental variables could not be established for the coastal area (all cruises merged), or from single seasons/cruises. However, within the surface water and the BBL significant correlations were identified (Table 4). Relationships between environmental variables and nitrification rates in the surface waters from winter and spring showed different patterns. In winter 2015, the river plume was smaller than in spring 2016 and nitrification rates increased with increasing salinity and decreased with increasing NH_4^+, PON, POC, and Chl.a concentrations as well as NH_4^+ assimilation rates (Table 4). In spring 2016, when the river plume was widely spread, correlations of nitrification rates with NH_4^+ and NH_4^+ assimilation rates were positive, while no relationships were found with the remaining environmental variables (Table 4). Yet, when plotting nitrification rates along the salinity gradient including the Vistula River as fresh water endmember, a more consistent picture of nitrification regulation evolved (Figure 14). Nitrification rates first decreased with increasing salinity up to a salinity of 3 followed by a subtle but significant increase of nitrification rates at higher salinities (Figure 14A). The exact converse pattern was found between nitrification rates and PON concentrations, with a positive relationship for the low salinity nitrification rates and a significant negative correlation, i.e. increasing nitrification rates with decreasing PON concentrations for the nitrification rates at higher salinities (Figure14C). NH_4^+ concentrations led to increasing nitrification rates at low salinity (0-3), whereas no relationship was found at higher salinities (Figure 14B). NH_4^+ assimilation rates co-occurred with the highest nitrification rates, but otherwise no correlation was found (Figure 14D). In the BBL, no relationship between nitrification rates and the environmental variables salinity, temperature, oxygen, and NH_4^+ and Chl.a concentrations was found, neither for the complete data set (all seasons merged, data not shown) nor for the single seasons (Table 4, Figure 15A and B). In summer, nitrification rates were significantly positively correlated to PON concentrations (Figure 15C, Table 4), whereas in winter and spring no relationship was found. NH_4^+ assimilation rates were positively correlated with nitrification rates in the BBL in summer 2014 and winter 2015 (Figure 15D). In the offshore DWL, nitrification rates were positively *correlated* to temperature while a negative trend with oxygen concentration was found (Table 4).

Table 4: Correlation analyses (Pearson correlation coefficient, R) between nitrification rates and environmental variables. Significant correlations ($p < 0.05$) are highlighted in bold. Strong but not significant correlations ($R > 0.5$) are also shown, results of no correlations are denoted as 'n.c.'. The results are structured as Pearson correlation coefficient R in the first line, the significance value p in the second line, and the sample number n in the third line for each location and environmental variable. The Vistula River was excluded in the analysis of the surface water layer in spring 2016.

cruise/ season	**water layer**	**temp.** (°C)	**sal.**	**O_2** (ml L^{-1})	**NH_4^+** (µmol L^{-1})	**PON** (µmol L^{-1})	**POC** (µmol L^{-1})	**Chl.*a*** (µg L^{-1})	**AAR**
all cruises	*DWL*	**0.89**	*n.c.*	-0.57	*n.c.*	*n.c.*	*n.c.*	*n.c.*	*n.c.*
		0.02	*n.c.*	0.14	*n.c.*	*n.c.*	*n.c.*	*n.c.*	*n.c.*
		6	9	9	11	11	11	7	10
winter 2015	*surface water*	0.78	0.83	*n.c.*	**-0.94**	**-0.75**	-0.72	**-0.96**	*-0.71*
		0.11	0.09	*n.c.*	**0.001**	**0.05**	0.07	**0.01**	*0.08*
		5	5	5	**7**	**7**	7	**5**	7
spring 2016	*surface water*	*n.c.*	*n.c.*	*n.c.*	**0.71**	*n.c.*	*n.c.*	*n.c.*	**0.89**
		n.c.	*n.c.*	*n.c.*	**0.05**	*n.c.*	*n.c.*	*n.c.*	**0.003**
		8	8	8	**8**	8	8	8	**8**
summer 2014	*coastal BBL*	*n.c.*	*n.c.*	*n.c.*	*n.c.*	**0.78**	**0.79**	*n.c.*	0.74
		n.c.	*n.c.*	*n.c.*	*n.c.*	**0.02**	**0.02**	*n.c.*	0.06
		8	8	8	8	**8**	**8**	8	7
winter 2015	*coastal BBL*	*n.c.*	*n.c.*	*n.c.*	*n.c.*	-0.54	-0.62	n.c.	0.60
		n.c.	*n.c.*	*n.c.*	*n.c.*	0.21	0.13	n.c.	0.16
		7	7	7	7	7	7	7	7
spring 2016	*coastal BBL*	*n.c.*	*n.c.*	*n.c.*	*n.c.*	-0.52	-0.56	*n.c.*	n.c.
		n.c.	*n.c.*	*n.c.*	*n.c.*	0.09	0.06	*n.c.*	n.c.
		12	12	11	11	12	12	12	12
all cruises	*DWL*	**0.89**	*n.c.*	-0.57	*n.c.*	*n.c.*	*n.c.*	*n.c.*	*n.c.*
		0.02	*n.c.*	0.14	*n.c.*	*n.c.*	*n.c.*	*n.c.*	*n.c.*
		6	9	9	11	11	11	7	10

DWL-deep water layer, BBL-bottom boundary layer; AAR - ammonium assimilation rate in nmol L^{-1} d^{-1}

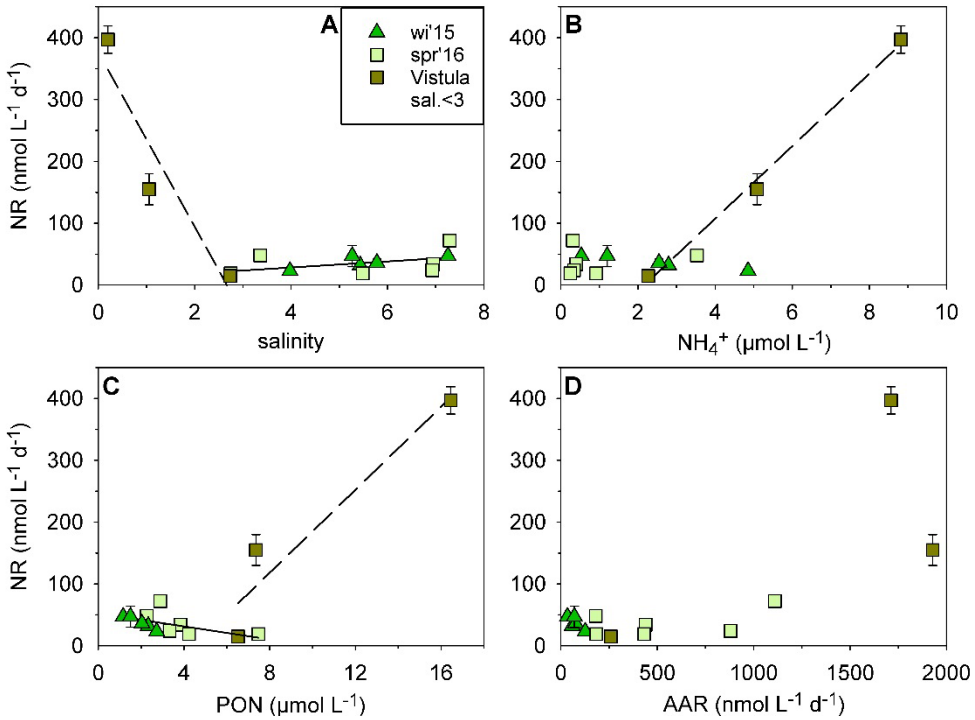

Figure 14: Relationships between nitrification rates (NR) and the environmental variables salinity (A), NH_4^+ concentration (B), PON concentration (C), and NH_4^+ assimilation rate (AAR, panel D) in the surface water/river plume in winter 2015 and spring 2016 in the Bay of Gdansk.

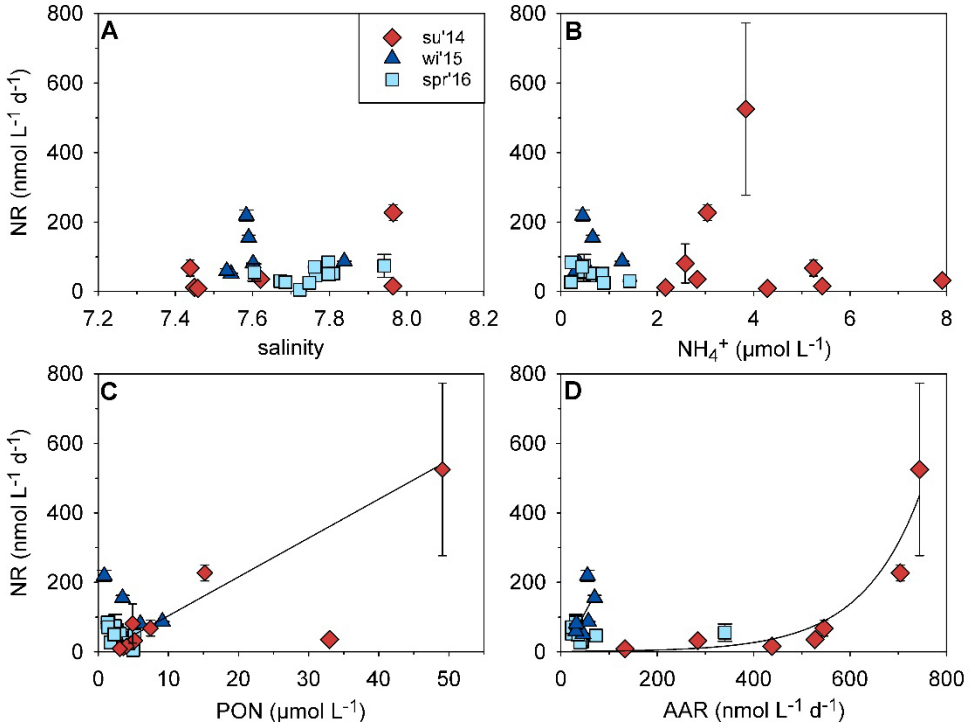

Figure 15: Relationships between nitrification rates (NR) and the environmental variables salinity (A), NH_4^+ concentration (B), PON concentration (C), and NH_4^+ assimilation rate (AAR, panel D) in the BBL in summer 2014, winter 2015, and spring 2016 in the Bay of Gdansk. Significant correlations (Pearson, $p < 0.05$) are indicated by a regression line.

3.2.2 Nitrification rates in the Bay of Gdansk

Nitrification rates in coastal zones range widely, between rates as low as in the open ocean (e.g. Heiss and Fulweiler, 2016; Newell et al., 2011; Peng et al., 2016) and rates extremely high in eutrophied estuaries (e.g. Brion et al., 2008). The nitrification rates that characterize the Bay of Gdansk are in the lower range of those measured in other coastal areas, but similar to San Francisco Bay, the coastal Gulf of Mexico and the open Baltic Sea (see references in Table 5).

The first surprising result of nitrification rates in the Bay of Gdansk was the lack of a seasonal difference (Figure 12A). I expected much higher rates in summer, when temperature and NH_4^+ availability was high in the BBL. However, there seems to be no general seasonal pattern of nitrification rates in temperate coastal zones as for example found by Andersson et al. in the Scheldt estuary (2006). Other studies measured highest nitrification rates either in winter (Veuger et al., 2013), in summer (Bianchi et al., 1999) or in spring and autumn (Brion et al., 2008). Furthermore, nitrification rates from the shallow Vistula estuary were not correlated to temperature (Table 4), a finding supported by temperature manipulation experiments, in which nitrification rates were not higher at higher temperatures (Baer et al., 2014). The lack of seasonality and influence of temperature, suggests other factors, like NH_4^+ availability, concentrations of particles or oxygen concentrations, to affect nitrification.

A second surprising result is the same range of nitrification rates in the Vistula estuary and the offshore DWL (Figure 12A). This indicates that nitrification is not enhanced in the shallow coastal zone, which is fuelled with nitrogen by the Vistula River. Furthermore, the highest nitrification rates measured during the three cruises were found in the DWL at lowest oxygen concentrations and elevated temperatures (Table 4). The usually anoxic deep water in the area of the Gdansk deep received oxygenated North Sea water during a Major Baltic Inflow in 2014 and 2015 (Mohrholz et al., 2015). Thus, hypoxic conditions were present during the cruises in 2014 and 2015 (Figure 11A), which must have enhanced nitrification. Similar results are shown by Hietanen et al. (2012), who studied nitrification rates at the oxic-anoxic interface in the Baltic Proper and found the same relationship with oxygen. Together these findings suggest that nitrifiers are very active under low oxygen conditions supporting the assumption of nitrifiers being microaerophilic (Ward, 2008). Hypoxic conditions were not present in the Vistula estuary and nitrification was not correlated with ambient oxygen

concentrations. Thus, oxygen is not regulating nitrification in the shallow Vistula estuary.

Table 5: Coastal nitrification rates as reported in the primary literature with a focus on open coastal zones as well as surface and bottom water layers.

location	classification	water layer	water depth (m)	nitrification rate (nmol L^{-1} d^{-1})	NH_4^+ (µmol L^{-1})	reference
Baltic Proper (Baltic Sea)	coastal sea	mixed layer	ca. 0 - 60	**ca. 2 - 45**	ca. 0.2–1.4	Enokson, 1986
		halocline to bottom	ca. 60-105	**ca. 35 - 280**	ca. 0.2-4.5	
Baltic Proper (Baltic Sea)	coastal sea	oxic anoxic interface	80-117	**0 - 83.6**	0.7–17.0	Hietanen et al., 2012
Bay of Gdansk/ Vistula river plume	open coastal zone	SML/river	0-2.5	**13 - 400**	0.25-8	This study
		BBL	15-50	**5 - 525**	0.2-8	
		DWL	63-107	**18 - 1544**	0.6-4	
Chang Jiang river plume	open coastal zone	surface	0-5	**ca. 0 - 3000**	ca. 0.0-2.0	Hsiao et al., 2014
		bottom	5-55	**ca. 32 - 4600**	ca. 0.2-1.2	
Qiantang river mouth		surface	0-5	**ca. 210 - 500**	ca. 0-1	
		bottom	5-25	**ca. 800 - 1000**		
Rhône river plume	open coastal zone	surface	1.5	**ca. 500 - 4300**	ca. 0.5 - 11	Bianchi et al., 1999
		bottom	50-200	**ca. 120 - 1200**	ca. 0.5 - 4	
coastal Gulf of Mexico	open coastal zone	surface	7-20	**ca. 9 - 50**	-	Bristow et al., 2015
		bottom	15-63	**ca. 150 - 494**	ca. 0.37-0.72	
Narragansett Bay + offshore	open coastal zone	surface	<20m	**0 - 0.2**	0-1.5	Heiss and Fulweiler, 2016
		bottom	>20m	**0 - 20**	0.1-3.0	
Scheldt estuary	estuary	surface	2	**0 - 14400**	0–150	Brion et al., 2008
San Francisco Bay	estuary	surface	2	**ca. 7 - 150**	ca. 0.4-18.2	Damashek et al., 2016
		bottom	10-46	**ca. 10-310**	ca. 3.4-18.9	

3.2.3 Is the Vistula river plume a hotspot for nitrification?

As described for a number of other coastal zones, I expected increased nitrification rates in the river-impacted, low-salinity waters of the Bay of Gdansk (Damashek et al., 2016, see Table 2 therein). But contrary to our expectations, nitrification rates did not differ between river plume water and the coastal surface water (Figure 13), although substrate availability was higher in the river plume (Table 3). Hence, the river plume in the Bay of Gdansk is no hotspot for nitrification. This is underlined by the results of the correlation analyses between nitrification rates and environmental variables. The magnitude and the relationships of nitrification rates to salinity, NH_4^+ and PON concentrations shifted already at a salinity of 3, while riverine influence was found up to a salinity of 6 (Figure 14A). Nitrification activity was high only in the freshwater of the Vistula River and in very fresh river plume water (stations VE07, salinity of 1). The positive trend of nitrification rates with NH_4^+ and PON concentration (Figure 14D, E) suggests that nitrification in freshwater and river plume water of very low salinity is substrate driven and that nitrifiers are attached to the organic particles transported by the river (Hsiao et al., 2014; Karl et al., 1984; Stehr et al., 1995). However, this was not the case in the surface water of the remaining sites, where the rates, while lower in magnitude, increased with increasing salinity and decreasing PON concentrations (Figure 14). So, the river plume seems to be a transition zone where not only the magnitude of nitrification rates, but also its regulation changes. To our knowledge, this is the first report of such a shift in magnitude and regulation of nitrification along a river plume salinity gradient. Reasons for the transition of nitrification rates in the river plume could be 1) the sedimentation of riverine particles, 2) a change in the nitrifier community, and 3) competition for the substrate with phytoplankton or NH_4^+ assimilating bacteria.

Nitrifiers form strong associations with particles (Phillips et al., 1999; Stehr et al., 1995) which were most abundant in the Vistula River. When mixing with saline water, the riverine particles (PON and POC) can flocculate and sink to the seafloor (Mann and Lazier, 1991) and thus particle-associated nitrifiers may become entrained. In our study, this may explain the very low nitrification rates at intermediate PON concentrations (Figure 14E), a finding supported by the strong non-linear decline of Nitrifiers form strong associations with particles (Phillips et al., 1999; Stehr et al., 1995) which were most abundant in the Vistula River. When mixing with saline water, the riverine particles (PON and POC) can flocculate and sink to the seafloor (Mann and

Lazier, 1991) and thus particle-associated nitrifiers may become entrained. In our study, this may explain the very low nitrification rates at intermediate PON concentrations (Figure 14E), a finding supported by the strong non-linear decline of PON with increasing salinity. The steepest slope until a salinity of 3 coincides with the lowest nitrification rate (Figure 16). With further decreasing PON concentration, nitrification rates increased again (Figure 14E), possibly reflecting a community composition containing other nitrifying organisms, either free-living (Hsaio et al., 2014) or associated with planktonic particles (Phillips et al., 1999). Such a change in the nitrifying community may have occurred along the Vistula river plume salinity gradient. Stehr et al. (1995) reported a decline in the number of ammonium-oxidizing bacteria (AOB) from freshwater to brackish water in the Elbe estuary. Niche separation between AOB and AOA has also been described, with AOB dominating at lower and AOA at higher salinities (Bouskill et al., 2012; Mosier and Francis, 2008; Tolar et al., 2013). Unfortunately, none of these studies measured nitrification rates at the same time. In the Vistula river plume, a decline in the abundance of freshwater nitrifying species with increasing salinity may have led to the decrease in nitrification rates at the transition zone (salinity of 3), where freshwater and brackish water mix. The subsequent increase in nitrification rates with increasing salinity suggests a shift to nitrifying species which are adapted to brackish conditions.

Phytoplankton and NH_4^+ assimilating bacteria are known to successfully compete with nitrifiers for the substrate NH_4^+ (Santoro and Casciotti, 2011; Smith et al., 2014). Ameryk et al. (2005) and Wielgat-Rychert et al., (2013) showed that the Vistula River plume fuels primary production by both phytoplankton and bacteria in the Vistula estuary. Indeed, in spring2016, the highest Chl.a concentrations as well as the highest phytoplankton abundance (Figure III in appendix) were measured at the salinity of 3, where the nitrification rates were lowest (Figure 14). This clearly indicates that phytoplankton was competing for NH_4^+ and nitrifiers came short.

In summary, the river plume is not a hotspot but a transition zone for nitrification in the Vistula estuary. Along the salinity gradient, nitrifiers may experience a combination of regulation mechanisms which are entrainment with sinking particles, the competition for the substrate NH_4^+, and increasing salinity leading to a change in the abundance, composition, and activity of the nitrifiying community.

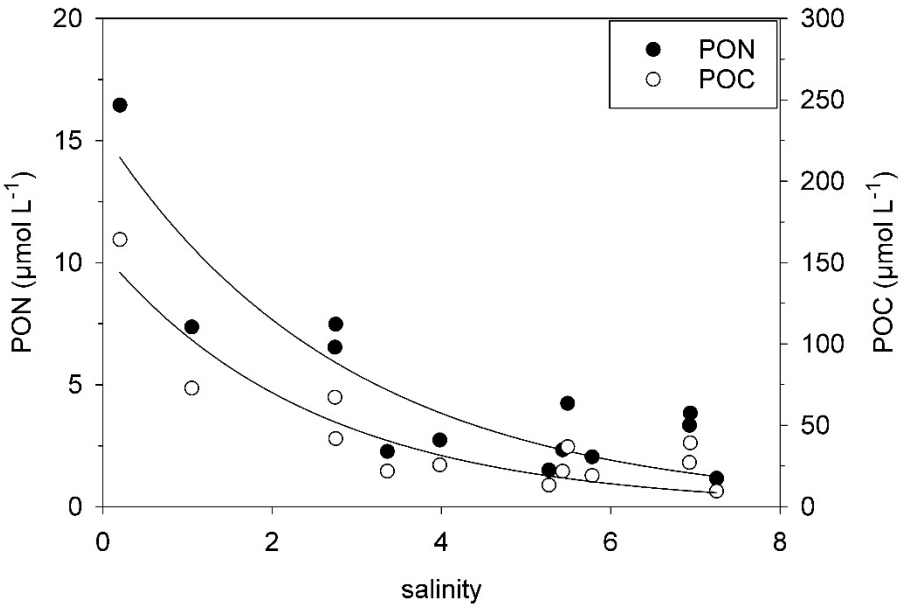

Figure 16: Salinity mixing plot with concentrations of PON and POC. The exponential decline indicates sedimentation of organic particle.

3.2.4 Is the BBL a hotspot for nitrification and what are the regulating mechanisms?

I expected that favourable environmental conditions such as high NH_4^+ and POM concentrations, the lack of light limitation and reduced competition for the substrate would result in high nitrification rates in the coastal BBL of the Bay of Gdansk. But the similarity of coastal BBL-nitrification rates with rates from the offshore DWL indicate that the coastal BBL is not a general hotspot for nitrification. However, within the Vistula estuary, the BBL in summer was clearly a hotspot for nitrification with higher rates than in the overlying water. Due to stable thermal stratification, the BBL displayed distinct physical and biogeochemical characteristics, like low oxygen concentration, and high PON and nutrient concentrations which suggest intense remineralization and accumulation of the latter (Figure 7, Figure 9). Ritzrau et al. (1997) denoted the BBL to be a layer of high bacterial activity and rapid organic matter modification. Especially in the warm summer, the degradation of organic matter is enhanced in coastal zones (Davis and Benner, 2005; Lonborg et al., 2009) and the supply of NH_4^+ from organic matter degradation (ammonification) to nitrification could be high. Indeed, the positive correlation of nitrification rates and PON not only suggests particle association of the nitrifiers (see above) but also a strong coupling of nitrification to ammonification (Bronk et al., 2014; Pakulski et al., 2000). This is further supported by the missing

positive correlation between nitrification rates and the high ambient NH_4^+ concentrations in the BBL in summer, indicating that nitrifiers are either well adapted to ambient concentrations or other sources than dissolved NH_4^+ are important. In a recent study, NH_4^+ fluxes out of sinking diatom aggregates were detected, even under oxic conditions (Ploug and Bergkvist, 2015), which underline the importance of particulate organic matter as a NH_4^+ source for associated microorganisms, like nitrifiers. Positive relationships of nitrification rates with suspended particulate matter (Feliatra and Bianchi, 1993) or PON (Hsaio et al., 2014) were found in several coastal zones (summarized in Damashek et al., 2016) suggesting that particles play a key role as substrate supplier for coastal nitrification.

In winter and spring, the BBL was not a hotspot for nitrification, since rates from the overlying mid water and even partly from the surface water (spring) cover the same range (Figure 12A). Interestingly, rates from the winter and spring season are as high as in the BBL in summer, which I declared as nitrification hotspot. Concluding, all water layers, BBL as well as mid water and surface water (only in spring) are nitrification hotspots in winter and spring. Furthermore, there is a lack of correlations between nitrification rates and environmental variables in the BBL (Table 4) or other combinations of water layers (e.g. in mid + BBL). For example, particulate organic matter concentrations (PON and POC) which drove nitrification in summer, were lower and did not correlate with nitrification rates in winter and spring (Table 4). Organic matter degradation is usually lower in winter (Davis and Benner, 2005; Lonborg et al., 2009) and the organic material in the Vistula estuary was in a degraded state with C/N ratios of 11.4 in and 10.6 in spring, compared to 8.8 in summer. Thus, ammonification might be reduced and may not be a significant NH_4^+ source for nitrifiers. This leads to the conclusion, that other factors than the measured environmental variables must drive nitrification. So, what causes to equally high rates of nitrification in winter and spring compared to the BBL in summer?

In contrast to summer, when the water column was warmer and strongly stratified, in winter and spring the water column was colder and well-mixed indicating stronger currents and more turbulence which continuously mix the water. A turbulent hydrodynamic regime can improve the accessibility of particle associated microorganisms to their substrates, if the particle host is large enough (Ritzrau et al., 1997 and cites therein). Ritzrau (1996) calculated an increased diffusive flux of dissolved amino acids to particles of 40 to 400 µm due to increased shear in the

turbulent hydrodynamic regime (current velocities of 0.05 to 0.3 m s^{-1}) in an Antarctic BBL. He used this mechanism as an explanation for the increased bacterial activity in the BBL, since this bacterial activity was not correlated to organic matter concentrations. Unfortunately, there is no data about the size of particles in the Vistula estuary, but particles with the size of 505 – 605 µm and 211 – 523 µm were found in the Mecklenburg Bight and the Pomeranian Bight (southern coastal Baltic Sea), respectively (Jähmlich et al. 1999 and 2003). It is very likely, that a similar range of particle size exists in the Vistula estuary, which is also located in the coastal southern Baltic Sea, only a few 100 nautical miles to the east. Current velocities in the Vistula estuary were measured with an ADCP and were 0.05 – 0.2 m s^{-1}. Hence, the situation described by Ritzrau (1996) can be well compared to the situation in the Vistula estuary in winter and spring. Nitrifiers in aquatic systems are generally living associated to particles and AOB are able to attach to particles within 30 min after introduction (Hagopian and Riley, 1998 and cites therein). So, it is likely that in a turbulent hydrodynamic regime like in winter and spring in the Vistula estuary leads to increased diffusive fluxes of NH_4^+ to particles. The thereby increased accessibility of NH_4^+ to the particle associated nitrifiers might be a factor which sustains the high nitrification rates in winter and spring, when organic matter degradation is low and ammonification is decoupled from nitrification.

Another possibility of the high nitrification rates in winter and spring, is the reduced competition for the substrate NH_4^+ with NH_4^+ assimilating microorganisms. Smith et al. (2014) showed that nitrification in the surface water is driven more by the competition for NH_4^+ than by light inhibition, which highlights the importance to also check NH_4^+ assimilation rates as an influencing factor for nitrification. NH_4^+ assimilation rates measured in the Vistula estuary are derived from dark incubation and exclude NH_4^+ uptake by primary producers. Nevertheless, NH_4^+ is taken up by a vast number of microorganisms (e.g. heterotroph bacteria), who compete for the substrate with nitrifiers. The relative contribution of NH_4^+ assimilation to total NH_4^+ consumption was much lower in winter and spring than in summer (Figure 12B) indicating less activity of NH_4^+ assimilating microorganisms which leaves relatively more substrate in the water column for the nitrifiers.

Also, a physiological adaptation could sustain nitrification rates in Vistula estuary at the same level in winter and spring. Schmidt et al. (2004) showed that cultured *Nitrosomas eutropha* and other AOB are able to accumulate NH_4^+ and hydroxylamine, both

compounds in the NH_4^+ oxidation pathway, to yield energy. The accumulation of these compounds is suggested to be mediated by active transport of NH_4^+ and hydroxylamine. Indeed, molecular and genetic studies state the existence of NH_4^+ or NH_3 transporters in both AOB and AOA (Offre et al., 2014; Weidinger et al., 2007) and NH_4^+ accumulation has also recently been suggested for an acidophilic AOA species (Lehtovirta-Morley et al., 2016). Furthermore, the existence of such transporters might be important at low ambient substrate concentrations and may explain the high affinity of AOA to NH_4^+ (Offre et al., 2014). In the Vistula estuary in winter and spring, low ambient NH_4^+ concentrations of 0.4 µmol L^{-1} (Table 2), might stimulate the active accumulation of NH_4^+ by ammonium oxidiziers, to sustain their energy supply via NH_4^+ oxidation. Thereby higher accessibility of NH_4^+ due to the hydrodynamic regime (Ritzrau, 1996; see above) and less competition for NH_4^+ could support NH_4^+ accumulation and the combination of the three mechanisms may finally lead to nitrification rates as high as in summer.

In summary, the BBL is a hotspot for nitrification in the Vistula estuary in summer and nitrification rates are most likely driven by the strong coupling of POM degradation to NH_4^+ via ammonification and particle associated nitrification. In winter and spring, however, the BBL is not a single hotspot and equally high nitrification rates were measured in the whole water column. Furthermore, correlation analyses indicate that nitrification is differently regulated than in summer and by other factors than the environmental variables measured. The turbulent hydrodynamic regime in winter and spring, could lead to a higher accessibility of particle associated nitrifiers to their substrate NH_4^+, which they may accumulate via active transport. These two mechanisms can be supported by overall less competition for NH_4^+ as indicated by low NH_4^+ assimilation rates in winter and spring.

3.2.5 A storm event as example for the influence of the hydrodynamic regime on nitrification

The storm that passed over the entire southern and central Baltic Sea on February 7 – 8, 2015 allowed us to obtain samples before and after the storm, from a station close to the river mouth (VE02). The complete loss of stratification and the significant higher PON concentrations after the storm clearly reflect intense mixing of the water column and resuspension from the sediment. The water depth affected by the storm was at least that of station VE02 (22 m), such that a large area of the coastal Bay of Gdansk was certainly affected by a significant increase of nitrification activity by a factor of 1.7 (Figure 11B). A similar result was found by Horrigan et al. (1990) after a storm event in the Chesapeake Bay, with NH_4^+ oxidation rates even increasing by an order of magnitude. The increased nitrification rates after a storm event are likely due to the resuspension of active sediment nitrifiers into the water column (Horrigan et al., 1990). This can be underlined by results of the nitrifier community composition in the Vistula estuary. The community composition of AOA and AOB which was found only in the BBL before the storm was distributed over the whole water column after the storm (Münster-Happel et al., unpublished). NH_4^+ was also released from the sediment during the storm (Thoms et al., unpublished) and may have triggered nitrification, although an increase in the NH_4^+ concentration in the water column was no longer detectable 24 h after the storm (Figure 11B). More importantly, turbulences in the water column during and after the storm most likely have improved the accessibility of NH_4^+ to particle associated nitrifiers (Ritzrau, 1996). Two days after the storm, re-sampling of the BBL at station VE02 showed that the nitrification rate was similar to that measured in the BBL prior to the storm (43 ± 1 nmol $L^{-1} d^{-1}$ and 59 ± 6 nmol $L^{-1} d^{-1}$, respectively). These results well demonstrate how significant storm events can rapidly but transiently change environmental conditions, leading to enhanced nitrification over short time-scales (Horrigan et al., 1990). Finally, the storm event perfectly illustrated enhancement of nitrification due to the hydrodynamic regime by 1) resuspending active particle associated nitrifiers from the BBL and the sediment and 2) better accessibility of NH_4^+ to these nitrifiers due to increased turbulences in the water column.

3.2.6 Summary and Conclusion

The results revealed by the extensive amount of data acquired in this study included the following:

1) Surprisingly, there was no seasonal difference in the magnitude of the nitrification rates. However, the relative contribution of nitrification to total NH_4^+ consumption was much higher in winter than in summer, suggesting that N-recycling is dominated by NH_4^+ uptake into biomass in summer and by NO_x^- production in winter.

2) The Vistula river plume is not a hotspot but a transition zone with a significant shift magnitude and regulation of nitrification due to particle sedimentation and/or a change in the nitrifier community composition and activity.

3) The role of the BBL in determining nitrification rates has seldom been addressed and, unexpectedly, this layer was not an overall hotspot for coastal nitrification. Only in summer, when the stratification of the water column was pronounced and remineralization activity was high, nitrification rates were increased and most likely driven by a close coupling of ammonification and nitrification.

4) In winter and spring, high nitrification rates were found in the whole water column, where nitrification rates may be driven by the hydrodynamic regime, less competition for the substrate and physiological adaptation of the nitrifiers.

5) The effect of the hydrodynamic regime on nitrification rates were nicely reflected in a storm event in winter 2015 which briefly increased nitrification rates in the Vistula estuary.

The absence of nitrification hotspots in river plume and BBL of the Vistula estuary in winter and spring as well as the lack of relationships to environmental variables could be related to a complex hydrodynamic regime in this open coastal bay which should be included in further biogeochemical studies in open coastal zones like the Vistula estuary in the Bay of Gdansk.

3.3. Is BBL-nitrification related to sediment properties?

Since the BBL links sediments with the water column, favourable conditions for BBL-nitrification might originate from the sediment, e.g. in the form of sedimentary NH_4^+ release, which in turn depends on sediment properties and the macrofauna community. In this chapter, results on the influence of sediment properties and nutrient fluxes on BBL-nitrification will be presented and discussed.

3.3.1 Sediment types and their relationship to BBL-nitrification rates

Results on basic sediment properties (Thoms et al., unpublished) are shortly described in the appendix. A categorization of the sediments in the Bay of Gdansk according to grain size alone would not be sufficient to investigate the connection between the sediment and the overlying water (BBL). Also, sediment permeability and the presence of macrofauna play a crucial role for biogeochemical processes in the sediment (Huettel et al., 2003, Stief, 2013). Hence, I grouped the sediment according to permeability (Forster et al., 2003; Huettel et al., 2003) and the presence of macrofauna (Thoms et al., unpublished; pers comm. Halina Kendzierska, Table 6). Permeability data were provided by Dana Hellemann (University of Helsinki) for those sediments that were visually determined on board as fine, medium or coarse sands. Muddy sediments (silts) were defined as non-permeable, and low grain size, high water content and high porosity underline the decisions. At a permeability threshold of $K_m \geq 2.5\ 10^{-12}\ m^2$ sediments were assumed permeable enough for advective porewater flow with significant effects on sediment biogeochemistry (Forster et al., 2003). Macrofauna was present in all estuarine sediments, while in the offshore sediments, only very few or no macrofauna was found. Differences among the stations regarding species composition and abundances existed, but will not be further considered in this study. I distinguished three types of sediments according to permeability and macrofauna: non-permeable sediment without macrofauna (N-M), non-permeable sediment inhabited by macrofauna (N+M), and permeable sediment inhabited by macrofauna (P+M) (Table 6).

When basic sediment properties, ammonium fluxes and BBL nitrification rates are plotted over the sediment types some intriguing patterns emerge (sample sizes of the variables are shown in table III in the appendix). Significant differences in grain size, water content, LOI and PON content (only winter and spring cruise) existed between the sediment types (Kruskal-Wallis ANOVA on ranks, $p < 0.05$). The sedimentary NH_4^+

pool in the upper 3 cm also differed (Kruskal-Wallis ANOVA on ranks, $p < 0.05$), while the deep NH_4^+ pool was similar in N+M and P+M (U-test, $p = 0.056$). This shows, that also below the permeable surface sediment in P+M, a relatively large NH_4^+ pool is providing substrate for mineralization processes. The lowest grain size, and accordingly highest water, organic matter contents (LOI and PON), and highest NH_4^+ contents were found in N-M (Figure 18). The opposite was the case in P+M, whereas N+M had a high variability of sediment properties consisting of both, silty sediments and non-permeable fine sands (Figure 18). The NH_4^+ fluxes could only be compared between the N-M and P+M sediment types, since for N+M only one value exists. Fluxes from the N-M sediment type were diffusive fluxes calculated from pore water profiles. Fluxes from the P+M sediment type were total fluxes derived from in situ incubations with a chamber lander system. The total fluxes were kindly provided by Franziska Thoms (Thoms et al., unpublished). The diffusive fluxes of N-M were in the same range as the total fluxes of P+M (U-test, $p = 0.286$). BBL-nitrification rates covered the same range above the two non-permeable sediment types with mean rates of 106 nmol L^{-1} d^{-1} and 104 nmol $L^{-1}d^{-1}$ above N-M and N+M, respectively (Figure 18).

In contrast, rates above P+M with a mean of 42 nmol L^{-1} d^{-1} were significantly lower compared to the two non-permeable sediment types (N-M: U-test, $p = 0.019$, N+M: U-test, $p = 0.037$). The highest variability regarding nitrification rates was found at N+M (Figure 18) and although, there is a statistical significant difference, 4 of the 6 nitrification rates in N+M covered the same range as rates in P+M. The N-M sediment type solely consisted of samples from the deep offshore stations, where conditions in the BBL strongly differed to the BBL in the Vistula estuary, i.e. above N+M and P+M (see chapter 3.2.2.). Correlation analyses to check for relationships between BBL-nitrification rates and the properties of the different sediment types, were conducted for the complete data set, as well as for three the sediment categories, and for the three seasons. No significant correlations were found between nitrification rates and the basic sediment properties (PEARSON, $p > 0.05$). Furthermore, no positive correlation existed between BBL-nitrification rates or BBL-NH_4^+ concentrations and NH_4^+ fluxes, irrespective of the sediment type (PEARSON, $R = 0.10$). This means that at sites with high NH_4^+ fluxes, I did not simultaneously measure high nitrification rates or high NH_4^+ concentrations in the BBL (Figure 17).

In summary, although sediment types based on permeability and presence/absence of macrofauna differed significantly in basic sediment properties, the sedimentary NH_4^+

fluxes in organic-poor, permeable sediments (P+M) were as high as diffusive fluxes in organic-rich, non-permeable sediment (N-M). BBL-nitrification rates above the permeable sediment type were not enhanced.

Table 6: Sediment types based on their permeability, presence/absence of benthic macrofauna, and their main transport mechanisms according to Huettel et al. (2003). Ranges of measured permeabilities from the Bay of Gdansk are shown (provided by Dana Hellemann, University of Helsinki).

sediment type	main transport mechanism	measured permeability (m^2)
non-permeable, no macrofauna (N-M)	diffusion	-
non-permeable, macrofauna (N+M)	bioturbation	$8.4\ 10^{-13}$ - $2.4\ 10^{-12}$
permeable, macrofauna (P+M)	bioturbation + advection	$2.5\ \ 10^{-12}$ - $2.0\ 10^{-11}$

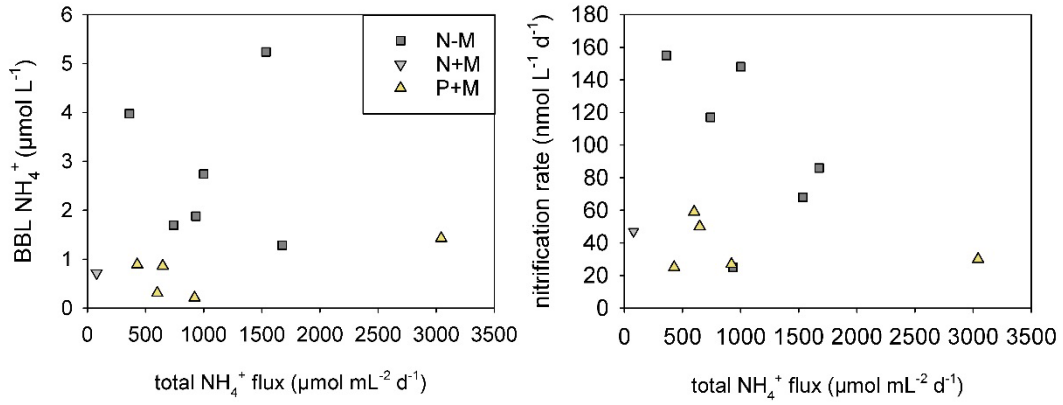

Figure 17: NH_4^+ concentrations (left) and nitrification rates (right) plotted over NH_4^+ fluxes of all sediment types. Total NH_4^+ fluxes were kindly provided by Franziska Thoms (IOW; Thoms et al., unpublished).

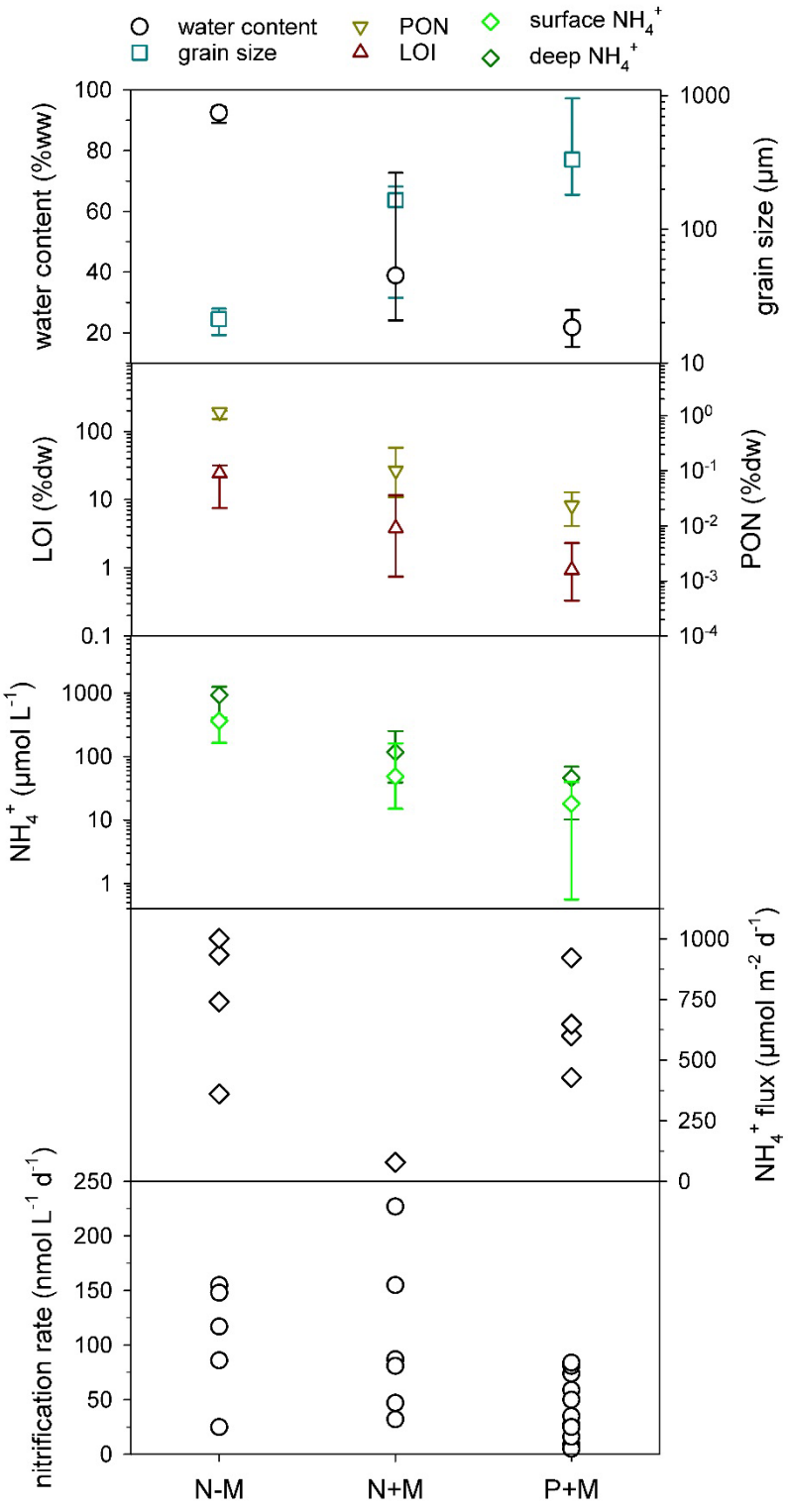

Figure 18: Basic sediment properties (grain size, water content, LOI, PON, NH_4^+ pools), NH_4^+ fluxes out of the sediment, and BBL-nitrification rates plotted for the three sediment types: non-permeable sediment without macrofauna (N-M), non-permeable sediment with macrofauna (N+M), permeable sediments with macrofauna (P+M). The NH_4^+ pools are separated into surface NH_4^+ from 0-3 cm and deep NH_4^+ from 3-11 cm sediment depth. NH_4^+ fluxes from N-M are diffusive fluxes derived from pore water profiles, while NH_4^+ fluxes from N+M and P+M are total fluxes determined via in situ incubations with a chamber lander (total flux data kindly provided by Franziska Thoms, IOW; Thoms et al., unpublished).

3.3.2 NO_3^- and NH_4^+ concentrations in the BBL and in the pore water

Nutrient concentration profiles in the BBL could be measured during the spring cruise in 2016, using the modified chamber lander system (see section 2.2.4., discussion in the appendix). NO_3^- and NH_4^+ profiles from the BBL (P+M: station VE13 and VE10, N+M: station VE07) did not show any gradient towards the sediment surface (Figure 19). Only at station VE07 (water depth: 50 m) the NH_4^+ concentrations were slightly elevated in the last 30 cm above the sediment, compared to the BBL water above. NO_3^- concentrations were slightly higher in the last meter above the sediment, but do not show a clear gradient of increasing concentrations towards the sediment surface. At station VE13, NO_3^- concentrations increased down to 30 cm above the sediment but decreased again further towards the seafloor. NO_3^- concentrations at station VE07 indicated an increase of NO_3^- towards 30 cm above the sediment.

At station VE05, there was no increase in NH_4^+ concentration within the BBL neither in spring nor in winter (Figure 20). In summer however, the NH_4^+ concentrations increased within the last 50 cm above the sediment from 0.19 to 7.48 µmol L^{-1} (Figure 20). Similarly, the NO_3^- concentration increased in summer from 0.16 µmol L^{-1} at 55 cm above the sediment to 1.49 µmol L^{-1} at 1 cm above the sediment. In contrast, winter concentrations in the BBL remained the same and concentrations in spring were slightly increased within the last meter above the seafloor (Figure 20). So, the sediment overlying BBL water differed seasonally by 1) overall higher NH_4^+ concentrations in summer than in winter and spring, and 2) by an increase in nutrient concentrations towards the sediment in summer. slightly increased within the last meter above the seafloor (Figure 20). So, the sediment overlying BBL water differs seasonally by 1) overall higher NH_4^+ concentrations in summer than in winter and spring, and 2) by an increase in nutrient concentrations towards the sediment in summer. There was a clear increase of NH_4^+ concentrations within the first centimeters of the pore waters in the sediments in all seasons (Figure 20). Overall, pore water NH_4^+ concentrations were several orders of magnitudes higher in the surface sediment than in the BBL (Table 7).

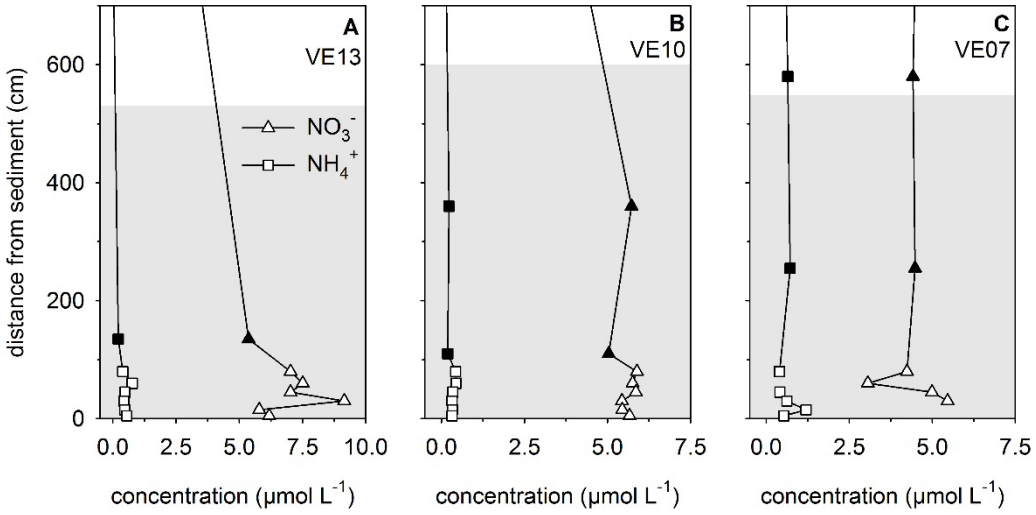

Figure 19: Profiles of NH_4^+ and NO_3^- in the BBL at three estuarine stations in the Bay of Gdansk. BBL-samples (white symbols) were taken within 1 m above the sediment during the spring cruise in 2016 with a modified chamber lander system. Black symbols represent concentrations from the deepest CTD-samples. The thickness of the BBL is marked in grey.

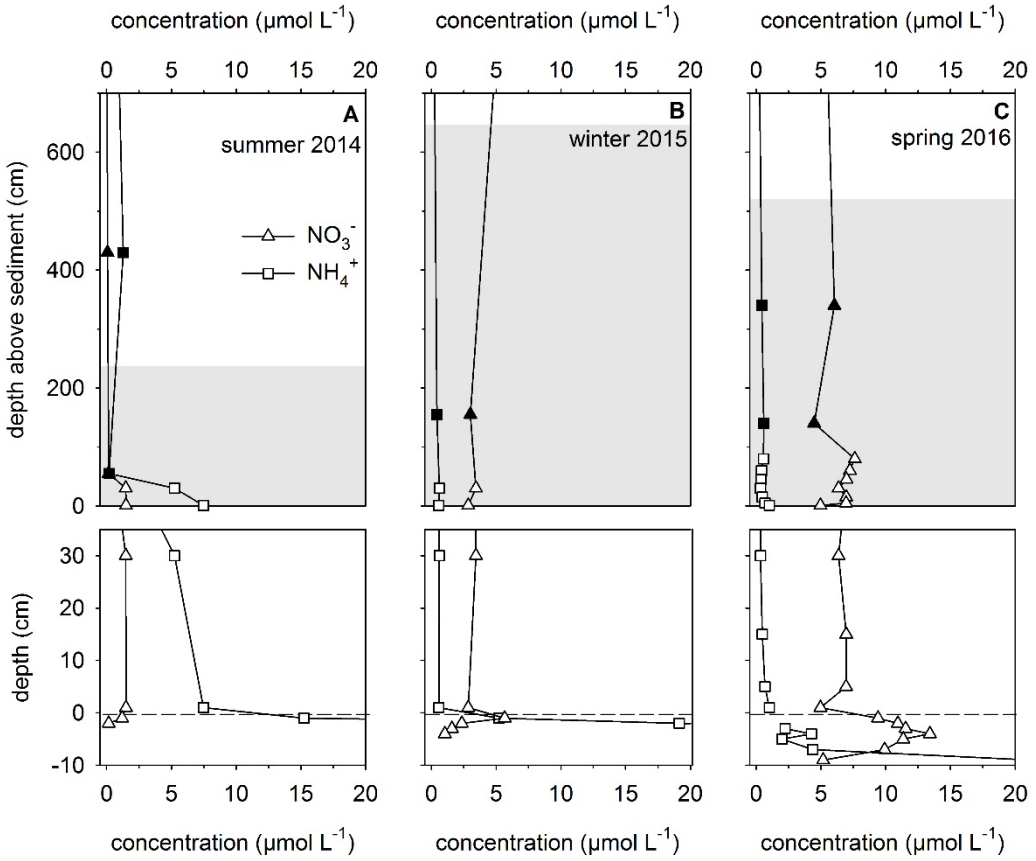

Figure 20: BBL and pore water concentrations of NH_4^+ and NO_3^- at station VE05 in summer (A), winter (B) and spring (C). Black symbols are concentrations derived from CTD-samples. In summer and winter, BBL samples are derived from the CTD sampling rosette at lowest sampling depth, the overlying core water and water 1 cm above the sediment from the pore water sampling. In spring, BBL profiles were taken with the modified chamber lander.

Yet, the three seasons differed from each other in sedimentary NH_4^+ and NO_3^- concentrations (Figure 20, Table 7). Comparing the pore water NH_4^+ concentration integrated over the first 3 cm of the sediment, I found much lower NH_4^+ concentrations in winter and spring compared to the summer season (Table 7). In summer, the NO_3^- concentration at station VE05 in the first cm of sediment showed no peak and decreased to 0.16 µmol L^{-1} at a sediment depth of 2 cm. Nevertheless, mean NO_3^- concentrations in the permeable surface sediment were higher than in the BBL in summer (Table 7). A nitrate peak of 5 µmol L^{-1} in winter and 13 µmol L^{-1} in spring was detected in the sediment at station VE05 and the mean NO_3^- concentrations were also overall higher in the surface sediment than in the BBL (Table 7,). Furthermore, the higher sedimentary NO_3^- concentrations reached a greater sediment depth which coincided with lower NH_4^+ concentrations (Figure 20).

Station VE05 was chosen as an example to illustrate seasonal differences in a P+M sediment type. In both impermeable sediment types (N+M and N-M), NH_4^+ concentrations were much higher in the surface sediment compared to the BBL, whereby the difference was greatest in N-M. In the N+M sediment type, higher surface sediment NO_3^- concentrations compared to the BBL were measured in summer, while NO_3^- concentrations in winter and spring were higher in the BBL (Table 7).

Table 7: Comparison of mean NO_3^- and NH_4^+ concentrations from the BBL with concentrations from the surface sediment. Data are separated according to sediment type and season and shown as mean (m) and standard deviation (s).

sed.-type	**season**	**NO_3^- (µmol L^{-1})**				**NH_4^+ (µmol L^{-1})**			
		BBL		sediment		BBL		sediment	
		m	*s*	*m*	*s*	*m*	*s*	*m*	*s*
P+M	summer 2014	**1.7**	1.1	**4.0**	1.2	**4.6**	1.2	**31.9**	8.5
	winter 2015	**4.7**	0.4	**7.8**	1.0	**0.3**	0.04	**14.0**	8.1
	spring 2016	**5.3**	1.0	**7.4**	2.4	**0.6**	0.3	**10.8**	8.0
N+M	summer 2014	**0.9**	0.1	**1.2**	1.1	**4.5**	2.4	**78.3**	60.3
	winter 2015	**5.6**	0.0	**3.0**	0.7	**1.0**	0.3	**42.0**	27.1
	spring 2016	**9.7**	-	**3.1**	-	**0.7**	-	**46.0**	-
N-M	summer 2014	**4.2**	-	**6.4**	-	**2.9**	1.0	**265.8**	101.7
	winter 2015	**7.9**	-	**1.9**	-	**2.0**	0.7	**280.5**	87.5
	spring 2016	**7.6**	-	**5.0**	-	**1.7**	-	**411.9**	-

3.3.3 BBL nitrification rates above different sediment types

We hypothesized that nitrification rates are highest above sandy sediments, due to the permeable character that enables advective porewater outflow of NH_4^+. Sedimentary NH_4^+ release from permeable sediments was found for example in the North Sea (Ehrenhauss et al., 2004, van Raphorst et al., 1992) and is most likely transported via advection through anoxic channels which can form in sediment mounds or ripples (Huettel et al., 1998). Furthermore, permeable sandy sediments are effective biocatalytic filters with a high turnover of organic matter, which is trapped and degraded to NH_4^+ in the interstices of the sand (Huettel et a., 1996; Huettel and Rusch, 2000). Macrofauna is known to increase the sedimentary NH_4^+ release by several orders of magnitude compared to diffusive transport (Stief, 2013). Thus, not only permeability of the sediment, but also the presence of macrofauna enhances NH_4^+ release into the BBL, which in turn potentially enhances BBL-nitrification. The Vistula estuary in the Bay of Gdansk is dominated by fine to medium sands which are mainly permeable. Macrofauna species, like *Hediste diversicolo*r, *Peringia ulvae*, *Corophium volutator*, and *Marenzellereia* spp., are present over the entire Vistula estuary (Thoms et al., unpublished, Kendierska, unpublished data) and affecting nutrient fluxes through bioturbation (Thoms et al., unpublished). However, NH_4^+ fluxes covered the same range in permeable and non-permeable sediments (Figure 18). This result was surprising since we expected higher NH_4^+ fluxes from the permeable sediments. The total NH_4^+ fluxes determined via in situ incubation with a chamber lander include both, diffusive transport and macrofauna induced transport, but not advective transport. Assuming that bottom water currents were high enough to enable advective transport, the NH_4^+ fluxes above the permeable sediments (P+M) could be even higher. So, the sedimentary NH_4^+ release out of organic poor sandy sediments is at least as high as in the organic rich silty sediments (Figure 18). This result clearly reflects the effective biocatalytic function of permeable sediments as described by Huettel and Rusch (2000). Thus, permeable sediments in the Vistula estuary can effectively process organic matter and are a source of NH_4^+ to the BBL. Also, nitrification rates in the overlying BBL of permeable sediments were not enhanced, as expected (Figure 18). Surprisingly, they were even slightly lower than nitrification rates above non-permeable sediments. The slightly higher nitrification rates above the N-M sediment type is not related to the organic- and NH_4^+-rich sediment but to the different conditions in the overlying BBL.

Compared to the sites in the Vistula estuary (N+M and P+M), oxygen concentrations were low at the offshore sites (N-M, mean = 2.5 ml L^{-1}). Such suboxic conditions can enhance nitrification rates (Ward, 2008) when NH_4^+ is available (mean: 2.3 µmol L^{-1}). Nevertheless, both the sedimentary NH_4^+ release and BBL-nitrification rates, are independent from the sediment type in the Vistula estuary, and BBL-nitrification is also not directly related to sedimentary NH_4^+ release. Reasons of the missing links could be the turbulent character of the BBL and the lack of NH_4^+ limitation for BBL-nitrification in the Vistula estuary.

The BBL is known to be a dynamic water layer compared to the sediments. By deflection of the bottom water current at the sediment surface, turbulences develop turning the BBL into a layer of turbulent flow compared to laminar free flow in the overlying water. This turbulent character can lead to the invariable distribution of salinity, temperature and density in the BBL (Turnewitsch and Graf, 2003). Similarly, dissolved constituents like NH_4^+ released from the sediment, can be strongly mixed due to turbulences in the BBL leading to the invariant distribution in the BBL profiles in winter and spring (Figure 19, Figure 20). This can be underlined by the lack of a positive correlation between NH_4^+ fluxes and BBL-NH_4^+ concentrations (Figure 17). Also in previous studies, profiles of organic matter or dissolved amino acids showed no increase in concentration within an Antarctic BBL (Ritzrau, 1996; Ritzrau et al., 1997). However, there is a seasonal difference, with a physical distinct BBL in summer but not in winter (see section 3.2.). In summer, turbulences in the less thick BBL (3.2 $\pm$ 1.5 m thick) must have been lower than in winter and spring (BBL 5.4 $\pm$ 1.4 m thick) since there is an increase of NH_4^+ towards the seafloor. Increasing concentrations of nutrients towards the sediment have also been measured by Holtappelts et al. (2011) in a summer season in the Pomeranian Bight (southern Baltic Sea) which he attributed to high NH_4^+ fluxes. However, not only high sedimentary NH_4^+ release but also intense organic matter degradation to NH_4^+ can lead to these high concentrations in the BBL in summer. Also, higher NH_4^+ concentrations in the surface sediment were a sign of high NH_4^+ production via organic matter degradation in summer. Indeed, BBL-nitrification rates in the Vistula estuary (N+M and P+M) are associated to organic particles in summer and are most likely coupled to intense organic matter degradation and ammonification (see section 3.2.). Hence, the sedimentary NH_4^+ release may not be an important substrate source for nitrification in summer.

Organic matter degradation can be low in the winter and spring season, due to low temperatures (Lonborg et al., 2009; Davis and Benner, 2005). This might also be the case in the Vistula estuary, indicated by low NH_4^+ concentrations in the surface sediment layer and BBL (Table 7). The organic material in the BBL in winter and spring was refractory, as the high C:N ratios of the particulate organic matter with 11.4 and 10.6, respectively, show. Hence, organic matter degradation to NH_4^+ is probably not a significant NH_4^+ source at that time of the year. The NH_4^+ input from the Vistula River with 475 and 496 t $month^{-1}$ in winter and spring, respectively, might be an important NH_4^+ source for nitrification, if the river water reaches the BBL. However, riverine NH_4^+ conservatively dilutes within the surface water (data not shown) and might only reach the seafloor through strong mixing but is thereby also diluted over the whole water column. Hence, sedimentary NH_4^+ release must be an important substrate source for BBL nitrification. The invariant distribution of nutrient concentrations in the BBL-profiles (Figure 19, Figure 20) indicate high turbulences which could proscribe a direct relationship between nitrification rates and NH_4^+ fluxes. Nevertheless, sedimentary NH_4^+ release might be a principal factor maintaining nitrification rates in the BBL. Assumed is a BBL box of the dimensions of 1 m length, 1 m width and 5.4 m height (equals mean thickness of the turbulent BBL) above permeable sediment (P+M) where total NH_4^+ fluxes were measured. In the calculation, mean values from the BBL above the permeable sediment (P+M) in the Vistula estuary are used. In the BBL box (volume: 5400 L), the nitrification rate is 275 µmol d^{-1} and the ambient NH_4^+ pool is 2700 µmol. Nitrification consumes 10 % of the ambient BBL-NH_4^+ pool per day. Together with NH_4^+ assimilation (189 µmol d^{-1}), the consumption of NH_4^+ increases to 17 %. So, within approximately 6 days the NH_4^+ in the BBL box would be depleted. The sedimentary NH_4^+ release into the BBL box over 1 m^2 sediment measures 666 µmol d^{-1} which adds 21 % to the ambient NH_4^+ pool per day. With this NH_4^+ flux the concentration of the ambient NH_4^+ pool would be achieved in 4 days, 2 days less than the depletion via nitrification and NH_4^+ assimilation. Consequently, by adding NH_4^+ to the BBL-NH_4^+ pool, the sedimentary NH_4^+ release does assure the substrate supply to BBL-nitrification in the Vistula estuary in winter and spring. However, in those seasons the BBL was not a physically distinct layer compared to the overlying mid water (see chapter 3.2.), which suggest that NH_4^+ from the sediment might be mixed and thus diluted into a greater volume than the here assumed BBL box. On the other hand, the

mid water column could also receive NH_4^+ from the river plume water by wind induced mixing. At last, NH_4^+ from the sediment will firstly mix with the sediment overlying water before mixing with the upper water column. Hence, the calculation of the contribution of sedimentary NH_4^+ release to BBL nitrification considered to be representative for the Vistula estuary.

The lack of correlations between nitrification rates and both, NH_4^+ concentrations in the BBL (see chapter 3.2) and NH_4^+ fluxes from the sediment, could also indicate that BBL-nitrification is generally saturated with the substrate NH_4^+. Even in winter and spring, when NH_4^+ concentrations in the BBL were low (Table 7), nitrification consumed only 2 – 23 % (mean: 11%) of the available substrate per day. In summer, the portion was even smaller with an average of 2 % per day. It is known that nitrifiers, specifically AOA, are able to sustain high specific NH_4^+ oxidation rates with half saturation constants as low as 0.13 µmol NH_4^+ L^{-1} in the ocean (Martens-Habbena et al., 2009) or 0.01 µmol NH_4^+ L^{-1} in a coastal canal (Horak et a., 2013). Measured BBL-NH_4^+ concentrations in the Vistula estuary (P+M and N+M) were always higher than 0.2 µmol L^{-1} in all seasons. Hence, assuming high affinity of AOA in the Bay of Gdansk, the ambient NH_4^+ concentrations might be sufficient for the nitrifiying community.

Concluding, the sediment type does not influence BBL-nitrification rates during three seasons in the Bay of Gdansk. The turbulent character of the BBL leads to a fast dilution of the released sedimentary NH_4^+ which makes it difficult to resolve the linkage between sediment and overlying water with our in situ data. However, the sedimentary NH_4^+ release is an important substrate source for BBL-nitrification in winter and spring by refilling the ambient NH_4^+ pool in the BBL at a slightly higher rate than its consumption.

3.3.4 Is BBL-nitrification supplying substrate for sedimentary denitrification?

There are two possible biological pathways for the product of nitrification NO_3^-: 1) further recycling by re-assimilation into biomass (e.g. uptake by phytoplankton) or by DNRA, or 2) removal by sedimentary denitrification. Furthermore, as dissolved constituent, NO_3^- is subject to transport in lateral bottom water currents. To be removed by sedimentary denitrification NO_3^- from the BBL must be transported into the sedimentary oxic-anoxic interface, where denitrification occurs. Kessler et al., (2013) suggest, that in permeably sandy sediments, NO_3^- from the overlying water, is

preferentially used by denitrifiers compared to nitrate from sedimentary nitrification (coupled nitrification-denitrification). On the contrary in non-permeable silty sediments, coupled nitrification-denitrification is the dominant N-removal pathway (Devol, 2015). Regardless of the sediment types, environmental variables like oxygen and nitrate concentrations in the sediment overlying water, the existence of an oxic sediment layer, and NH_4^+ availability are influencing the coupling of nitrification and denitrification, i.e. which NO_3^- source is used (Rysgaard et a., 1994). In permeable surface sediment of the Vistula estuary, pore water NO_3^- concentrations are higher than in the BBL (Table 7), indicating high sedimentary nitrification activity in the oxic sediment layer. In particular, the high NO_3^- peaks reaching to a sediment depth of up to 9 cm suggest accumulation of NO_3^- in winter and spring (Figure 20). This is not only a sign of high nitrification activity, but also of low denitrification activity, which was also assumed by Dana Hellemann (unpublished data). Additionally, positive total nitrate fluxes from sediment to the BBL measured via in situ incubations (Thoms et al., in prep.) underline these assumptions. Comparable results have been found by Ehrenhauss et al., (2004) in permeable sands in the coastal North Sea. This shows that coastal permeable sediments can feature intense N-recycling by nitrification, even releasing the product NO_3^- into the BBL. Furthermore, Dana Hellemann (unpublished data) found, that only 4 % of the denitrification activity in permeable sediments of the Vistula estuary is coupled to NO_3^- from the BBL, while 96 % makes use of NO_3^- from sedimentary nitrification. This stands in contrast to the results of Kessler et al. (2013), who found a higher contribution of water nitrate to denitrification in flume experiments and concluded an indirect coupling of nitrification in the sediment overlying water and sedimentary denitrification. However, there are several reasons why BBL-NO_3^- is not necessarily the main substrate for denitrification in permeable sediments. The oxic-anoxic interface lies deeper in permeable than in non-permeable sediments due to flushing of the surface with oxic BBL water (Huettel et al., 1998). Deeper oxygen penetration depths in permeable sediments were indeed found in the Vistula estuary in winter/spring (Dana Hellemann, unpublished data). This leads to a longer distance for BBL-NO_3^- to travel to the zone of denitrification. Advective transport of NO_3^- could overcome this distance, but pore water flow velocities and pore water residence times are highly variable in permeable sediments (Reimers et al., 2003). Reimers et al. (2003) also found a decrease of pore water flow velocities with increasing sediment depth and there always exists a zone of diffusive transport close to the oxic-anoxic interface (pers.

comm. Dana Hellemann). This might limit the access of BBL-NO_3^- to the denitrification zone. Additionally, Huettel et al. (1998) found steep concentration gradients of oxygen and NH_4^+ in permeable sediments and suggested a tightly coupled oxic-anoxic interface, which would enhance coupled nitrification-denitrification. The large NH_4^+ pools in the deeper permeable sediments of the Vistula estuary suggests high substrate availability for sediment nitrification in the oxic sediment layer and supports the assumption of Huettel et al. (1998). In the non-permeable sediment of the Vistula estuary inhabited by macrofauna, coupled nitrification-denitrification dominated (Hellemann, unpublished data). Through their burrows and bioirrigation benthic macrofauna not only enhances solute fluxes but also increases the surface area of the oxic-anoxic interface in the sediments which triggers coupled nitrification-denitrification over the use of BBL-NO_3^- in both permeable and non-permeable sediment (Na et al., 2008; Stief, 2013).

In summary, NO_3^- from the BBL is not the main source for N-removal in permeable and non-permeable sediments of the Vistula estuary. The main substrate for denitrification is NO_3^- from nitrification in the oxic sediment layer. Thus, not being coupled to denitrification, BBL-nitrification is a major N-recycling process in the Bay of Gdansk.

3.3.5 Summary and conclusion

BBL-nitrification is not directly related to sediment properties and sedimentary NH_4^+ release. However, the large sedimentary NH_4^+ pools could serve as continuous source of substrate for BBL nitrification when other NH_4^+ sources are lacking. NO_3^- produced in the BBL likely remains in the water column, where it is subject to N-uptake or N-transport rather than N-removal by denitrification. This contrasts with the results of Korth et al. (2013), who suggested a close coupling of bottom water nitrification and sedimentary denitrification at stations located only a few hundred nautical miles further west and east of those in this study. By remaining in the water column, NO_3^- from the BBL could be subject to physical mixing and subsequent eastward transport parallel to the coast (Radtke et al., 2012). However, the direction of bottom water currents may be different or even opposite to those of surface water currents (Wild-Allen and Andrewartha, 2016). Thus, NO_3^- produced by nitrification in the BBL of the Bay of Gdansk might not be transported eastward immediately, but remains in the coastal area, where it can be regarded as a positive feedback loop for eutrophication as it adds more nitrogen to the Bay of Gdansk. Finally, the persistence of nitrified NO_3^- in the BBL, demonstrates the importance of investigating transport processes, especially those of bottom water currents, to fully understand N-turnover in open coastal zones and hence the coastal filter function.

3.4 Do distinct riverine N-loads lead to different coastal nitrification rates?

In this chapter, riverine N-loads and nitrification rates will be compared between the pristine Öre estuary and the eutrophied Vistula estuary and the role of nitrification in these distinct estuaries will be discussed.

3.4.1 River discharge, riverine N-loads and river plumes of the Öre River and Vistula River

River discharge and riverine N-loads in the Vistula River were roughly two orders of magnitude higher than in the Öre River (Table 8). In both rivers, discharge and DIN-loads were higher in spring than in summer, while the organic N-load in the Vistula River, but not in the Öre River was comparable (Table 8). Not only the magnitude of the N-loads differed, but also the relative portions of DIN, DON and PON to the total N-load were different, both between rivers and seasons (Figure 21). In the spring season, when the river discharge was high, the composition of the N-loads differed between sites. DON was the main N-species in the Öre River, followed by PON and the smallest fraction was DIN (Figure 21). In the Vistula River in spring, the opposite was the case, with DIN dominating, followed by equal portions of PON and DON (Figure 21). In the summer season, the proportions of the N-species were similar in the Öre River and the Vistula River with a dominance of organic nitrogen (Figure 21). In the Vistula estuary, there was no clear river plume existent during the summer cruise, but slightly higher silicate concentrations indicate a weak river plume signal at stations close to and west of the river mouth (Figure 21). In the Öre estuary, however, silicate concentrations of ≥ 50 µmol L^{-1} clearly showed the presence of river plume water in the inner part of the estuary in summer. In the spring season, a wide spread river plume was existent due to the high river discharge in the Vistula estuary, as shown by widely distributed silicate concentrations in the range of 30 - 200 µmol L^{-1}. In the Öre estuary in spring, the silicate concentrations and thus the river plume were similarly distributed as in summer (Figure 22). So, the river plumes in the Öre estuary did not show a clearly distinct situation between seasons, as it was the case in the Vistula estuary. At both sites, the river plume water was confined to the upper 5 m of the water column where it continuously mixed with the coastal surface water (Figure 22).

Table 8: Monthly river discharge and nitrogen loads of the Vistula River and the Öre River in the months of sampling, whereby April 2015 and March 2016 show typical spring season characteristics with high river discharge and high N-load and August 2015 and July 2014 show typical summer season characteristics with lower discharge and lower N-loads than in spring.

		river discharge	TN	DIN	DON	PON	DON+PON
		$m^3 s^{-1}$	$t\ month^{-1}$				
Öre River	April 2015	66	143	16	99	28	127
	August 2015	26	52	1	46	6	52
Vistula River	March 2016	1500	16172	14030	1217	926	2143
	July 2014	932	2621	91	n.a.	n.a.	2530

TN=total N, DIN=dissolved inorganic N, DON=dissolved organic N, PON=particulate organic N

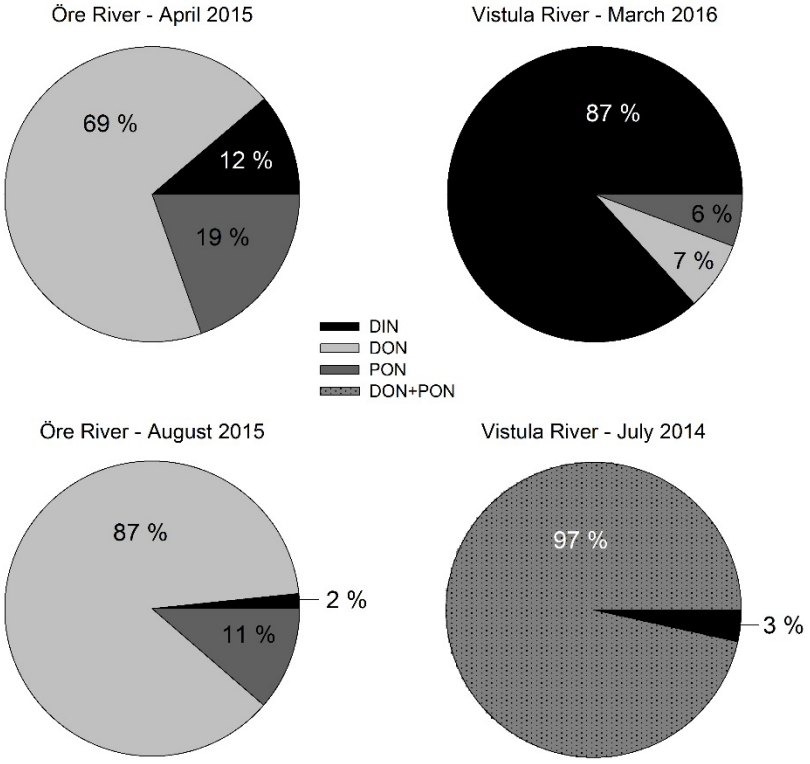

Figure 21: Relative portions of dissolved inorganic nitrogen (DIN), dissolved organic nitrogen (DON), and particulate organic nitrogen (PON) in the Öre River and Vistula River in summer and spring, respectively. Months of cruises/field campaigns are shown.

Along the salinity gradient, PON concentrations decreased rapidly below the mixing line at low salinity at both sites in spring (Figure 23). This indicates immediate loss of PON probably due to sedimentation. At higher salinity PON concentrations increased again, which indicates generation of PON through primary production. From the Vistula estuary in summer 2014, no mixing plot could be generated due to the lack of a riverine endmember, but since not only PON but also Chl.*a* concentrations were high, it is most likely, that primary production was occurring in the surface water. In the Öre estuary in summer, PON concentrations remained consistent along the salinity gradient.

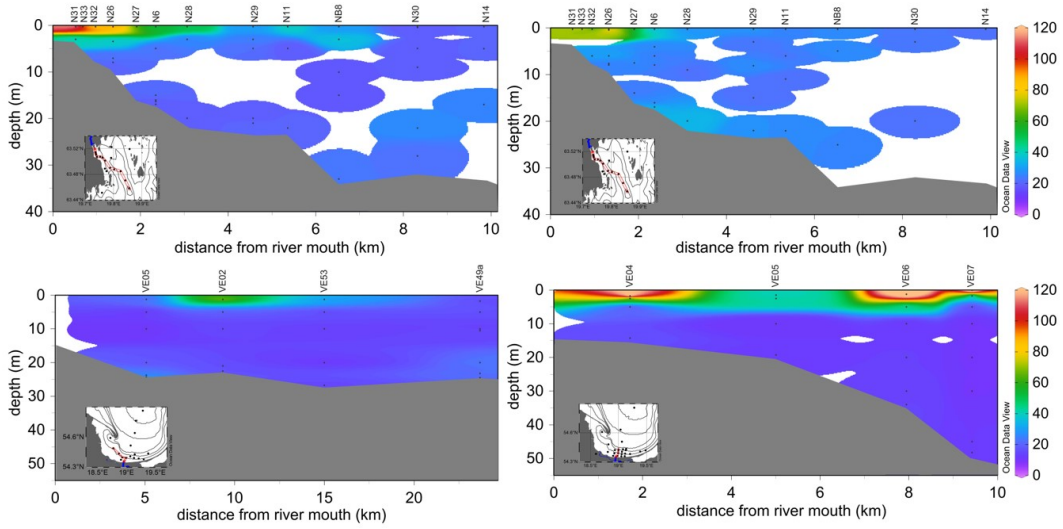

Figure 22: Transects along the river plume in the Öre estuary (upper panels) and the Vistula estuary (lower panels) in summer (left) and spring (left). High silicate concentrations in the surface water layer mark the river plume water.

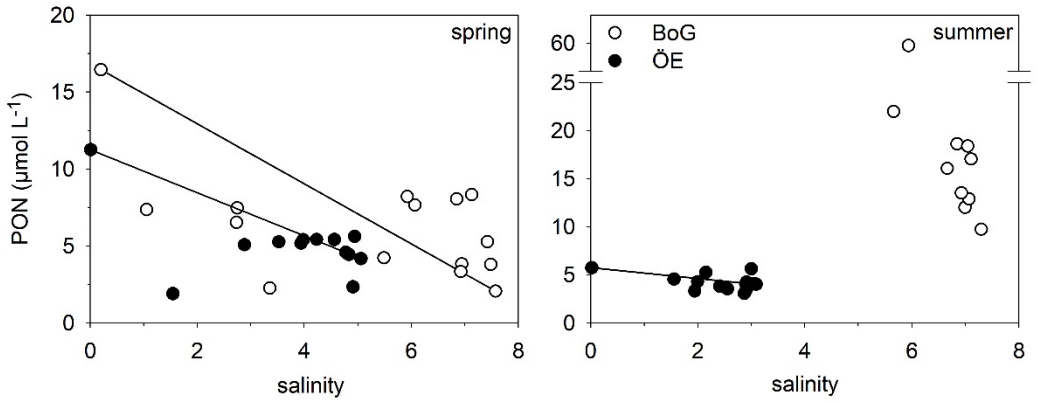

Figure 23: PON concentrations plotted over salinity in the Bay of Gdansk (BoG) and the Öre estuary (ÖE) in spring and summer.

3.4.2 Environmental variables and nitrification rates in Öre estuary and Vistula estuary

The most pronounced difference between the Öre estuary and the Vistula estuary was the distribution of salinity, which was higher in the latter (Figure 24). Also, NO_3^- and NH_4^+ concentrations were higher in the Vistula estuary in spring due to the high discharge of DIN by the Vistula River (Figure 24). Interestingly, DON concentrations were similar comparing the two sites, while NH_4^+ concentrations cover a wider range in the Vistula estuary. Temperature and PON reflected rather a seasonal difference than a difference between the sites, with higher temperatures and a higher variability of PON concentrations in summer (Figure 24). Since nitrification rates were mainly measured in the BBL, also environmental conditions in the BBL of the two sites were compared (Figure III in the appendix). They showed the same distributions in salinity, temperature, DON and PON as in the whole water column (Figure 24). Only NH_4^+ concentrations in the Vistula estuary and NO_3^- concentrations in the Öre estuary were significantly higher in the summer season compared to the respective other estuary. Nitrification rates were determined in the rivers, the surface water and in the BBL at both sites in spring whereas in summer, only rates from the BBL could be determined. A significant difference of nitrification rates was found between the Vistula River and the Öre River, with a much higher rate in the Vistula River (Table 9). But in the coastal waters, nitrification rates did not differ between the two estuaries (Figure 25). In the Öre estuary, slightly lower rates compared to the Vistula estuary were measured in spring. In the Vistula estuary, the variability of nitrification rates from 9 to 525 nmol L^{-1} d^{-1} (mean: 67 nmol L^{-1} d^{-1}) was greater than in the Öre estuary, where nitrification rates ranged from 14 – 98 nmol L^{-1} d^{-1} (mean: 40 nmol L^{-1} d^{-1}). The maximum nitrification rate with 525 nmol L^{-1} d^{-1} was 5 times higher than the maximum nitrification rate in the Öre estuary (98 nmol L^{-1} d^{-1}).

Table 9: Nitrification rates, substrate concentrations and NH_4^+ assimilation rates (AAR) in the Öre River and Vistula River.

cruise	nitrification rate (nmol L^{-1} d^{-1})	ammonium (µmol L^{-1})	DON (µmol L^{-1})	PON (µmol L^{-1})	AAR (nmol L^{-1} d^{-1})
Öre River April 2015	10 ± 1	0.68	39.95	11.24	1246
Vistula River March 2016	397 ± 22	8.82	21.62	16.45	1712

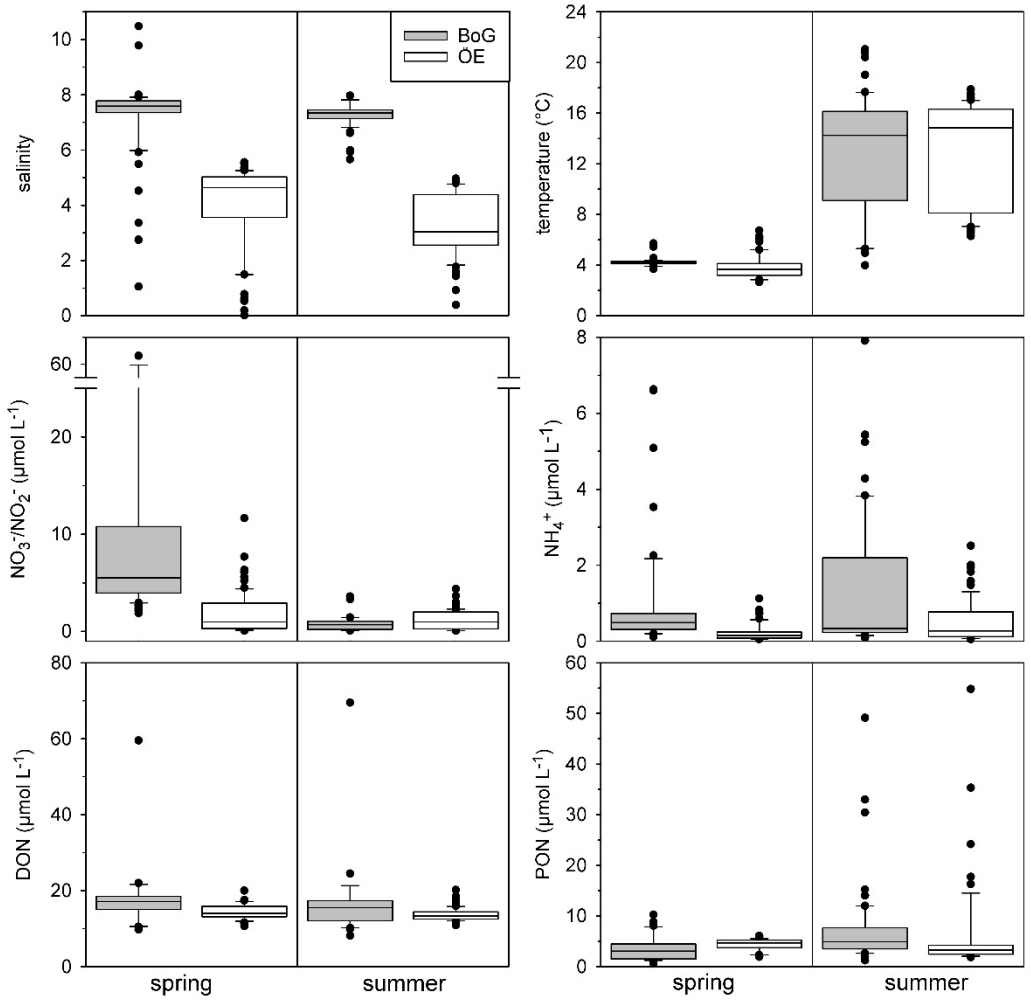

Figure 24: Distribution of environmental variables in the Vistula estuary (BoG) and the Öre estuary (ÖE) in spring and summer.

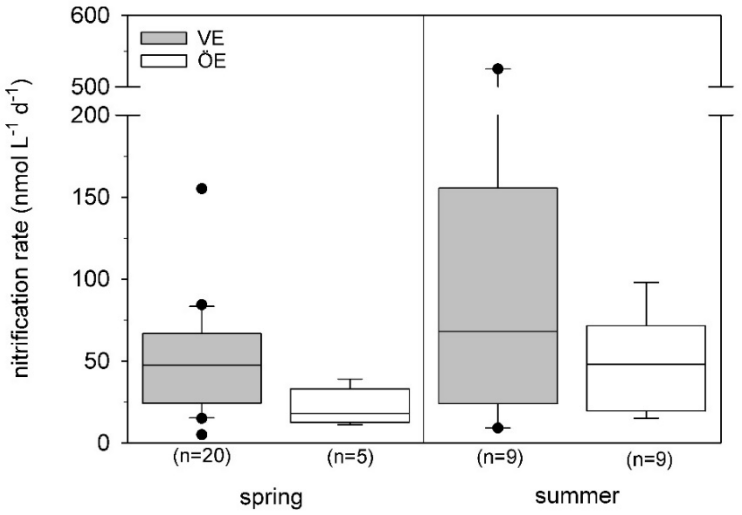

Figure 25: Nitrification rates in the Vistula estuary (BoG) and the Öre estuary (ÖE) in spring and summer.

3.4.3 Why are the nitrification rates similar at the two distinct coastal zones?

Several studies have shown that coastal or estuarine nitrification rates are positively related to the riverine N-load, especially to the NH_4^+ load (e.g. Brion et al., 2008; Iriarte et al., 1996; Dai et al., 2008). Therefore, I expected that nitrification rates would be higher in the Vistula estuary, where high riverine N-loads enter the bay (Table 8). Indeed, nitrification in the Vistula River was 40 times higher than in the Öre River (table 2). Usually highest nitrification rates of more than 3000 nmol L^{-1} d^{-1} are found in rivers with NH_4^+ concentrations of > 50 µmol L^{-1} (Table 10). But nitrification rates are highly variable and high rates also exist at low riverine NH_4^+ concentrations as found in the Vistula River (Table 10). So, nitrification rates in rivers do not necessarily reflect the ambient substrate concentration, although in my results it seemed to be the case. The much lower nitrification activity in the Öre River could be attributed to the high NH_4^+ assimilation rate of 1246 nmol L^{-1} d^{-1} which was two orders of magnitude higher than nitrification suggesting intense competition for the little available substrate NH_4^+. In the Vistula River on the contrary, NH_4^+ concentrations of 8 µmol L^{-1} allow high substrate availability for both processes and the NH_4^+ assimilation rate of 1712 nmol L^{-1} d^{-1} was only 4.5 times higher than the nitrification rate of 397 nmol L^{-1} d^{-1}. So, from the riverine perspective, there is the potential of higher nitrification rates in the Bay of Gdansk compared to the Öre estuary.

However, the nitrification rates in the two estuaries (Figure 25), surprisingly covered the same ranges at the two sites although the riverine N-load differs. The higher variability of nitrification rates and greater maximum nitrification rates in the Vistula estuary illustrates a higher potential of intense nitrification in this coastal zone compared to the Öre estuary. Rates from the Öre estuary are comparable to rates from the oligotrophic Lake Superior ranging from 18 – 51 nmol L^{-1} d^{-1} at similar environmental conditions (Small et al., 2013). It is rather surprising, that the majority of nitrification rates measured in the eutrophied Vistula estuary (20 out of 29 rates) is not higher than these oligotrophic nitrification rates while rates from other eutrophied systems exceed nitrification rates from the Vistula estuary by far (e.g. Andersson et al., 2006; Horrigan et al., 1990; Hsaio et al., 2014). The Rhône River estuary with an annual DIN-load of 77 kt yr^{-1} (Bianchi et al., 1999) can be well compared to the Vistula estuary with and annual DIN-load of ca. 64 kt yr^{-1} (recalculated from Pastuzak and Witek 2012, 2000-2016). However, nitrification rates in the nepheloid layer of the Rhône river estuary ranging between 288 – 1150 nmol L^{-1} d^{-1} (Bianchi et al., 1999) are much higher

than the BBL-nitrification in the Vistula estuary. So, on the one hand, there is the Öre estuary and the Bay of Gdansk differing in riverine N-loads, but having similar nitrification rates and on the other hand, there is the Rhône River estuary and the Bay of Gdansk, which are similar in riverine N-loads, but differ in their nitrification rates. Hence, nitrification in distinct coastal zones seems to be unaffected by the riverine N-load. Differences or similarities in nitrification rates in distinct coastal zones might reflect the influence of other factors than the trophic state or the riverine N-load. Those factors could be for example the shape of the coastal zone, physical conditions like wind induced mixing and thermohaline stratification, or the coupling of nitrification to substrates and other N-transformation processes (e.g. ammonification or NH_4^+ assimilation), and the nitrifier community composition or activity. The Vistula estuary is the coastal part of the Bay of Gdansk with a direct connection to the Baltic Proper while the Öre estuary is semi enclosed but also directly connected to the Bothnian Sea (Brydsten, 1992; Witek et al., 2003). Both estuaries are shallow with mean depths of 27 m and 25 m in the Vistula estuary and Öre estuary, respectively. Due to the shallow character, both estuaries are influenced by wind driven currents and mixing (Brydsten, 1992; Voss et al., 2005). Furthermore, both estuaries experience thermohaline stratification in summer, whereas in spring only the less dense river plume is separated from the remaining well mixed water column (Figure 22). Interestingly also the environmental conditions are rather similar in the two estuaries with only minor differences in temperature, NH_4^+, DON, and PON concentrations (Figure 24). Hence, although different in their shape, similar physical and environmental conditions might lead to the same range of measured nitrification rates.

Substrates for nitrification can be 1) NH_4^+ as the direct substrate for nitrification, and 2) DON and PON which supply NH_4^+ when degraded. Furthermore, nitrifiers are also capable of using urea, a dissolved organic matter compound (Alonso-Sàez et al., 2012). However, no correlation of nitrification rates was found with NH_4^+ or DON at both sites in both seasons. This implies that nitrification not only in the Vistula estuary (see chapter 3.2. and 3.3.) but also in the Öre estuary does not rely on ambient substrate concentrations. However, the distribution of NH_4^+ concentrations (Figure 24) and nitrification rates (Figure 25) follow the same pattern and when plotting the mean nitrification rates over the mean NH_4^+ concentrations there exists a positive trend between these two variables (Figure 26). Highest nitrification rates at highest NH_4^+ concentrations were found in the Vistula estuary in summer.

Table 10: NH_4^+ concentrations and nitrification rates of different Rivers as reported in the primary literature.

River	month	NH_4^+ (µmol L^{-1})	Nitrification (nmol L^{-1} d^{-1})	reference
Scheldt	April	ca. 155	3518	Andersson et al., 2006
Pearl River	March	341.9	2900	Dai et al., 2008
		377.8	10100	
Rhône River	May	9.8	2150	Feliatra and Bianchi, 1993
Sacramento River	February	16.2	100	Damashek et al., 2016
Chang Jiang	August	0.2	50	Hsaio et al., 2014
Vistula River	March	8.8	397	this study
Öre River	April	0.7	10	this study

So, although not directly correlated to ambient NH_4^+ concentrations, nitrification rates are likely higher at sites with higher NH_4^+ concentrations in the water. This reflects the general finding of Damashek et al. (2016), who reviewed studies about coastal nitrification, and found highest nitrification rates in coastal waters with highest NH_4^+ concentrations. Nevertheless, not NH_4^+ concentration alone, but rather a combination of physical and biogeochemical factors regulate nitrification (see section 3.2.). At both sites, PON concentrations seem to trigger nitrification rates in the BBL in summer (Figure 27, see chapter 3.2.), which may lead to the similar distribution of nitrification rates is that season. Furthermore, nitrification rates at both sites are not positively correlated to PON in spring, when high riverine PON-loads settle on the seafloor (Figure 27). So, the riverine PON which reaches the BBL in spring is not enhancing nitrification. Since the concentration is not an influencing factor nitrification in spring, the relationship of nitrification rates to organic matter quality, e.g. C:N and POC:Chl.*a* ratios, was analyzed. I expected higher nitrification rates at lower C:N and POC:Chl.*a* ratios, because this reflects "fresh" material. However, also here no correlations were found, neither in spring, nor in summer at both sites (PEARSON, $p > 0.05$). So, it seems that also the quality of POM does not influence nitrification rates. However, the lack of correlations in data from short cruises might not represent a complete picture on relationships between nitrification rates and environmental variables. Hellemann et al., (submitted) suggest from their results on the origin of POM and riverine NO_3^- loads, that nitrogen discharged in the spring flood is used in denitrification in summer in the Öre estuary. There is a time lag of 4 months in the relationship of POM and

denitrification. This could also be the case for nitrification. So, single cruises only represent a snapshot in time and studies over longer periods of time might give a better picture of the regulation of nitrification than short-term cruises do. The potential influence of other factors like frequent mixing and resuspension as a driver for nitrification has been discussed for the Vistula estuary (chapter 3.2.). This might also be the case in the Öre estuary, but the limited sample size of nitrification rates (n=5) does not allow a reasonable interpretation. Nevertheless, the same existence or lack of relationships between nitrification rates and substrates at the two investigated estuaries could be a reason for the same magnitude of nitrification rates.

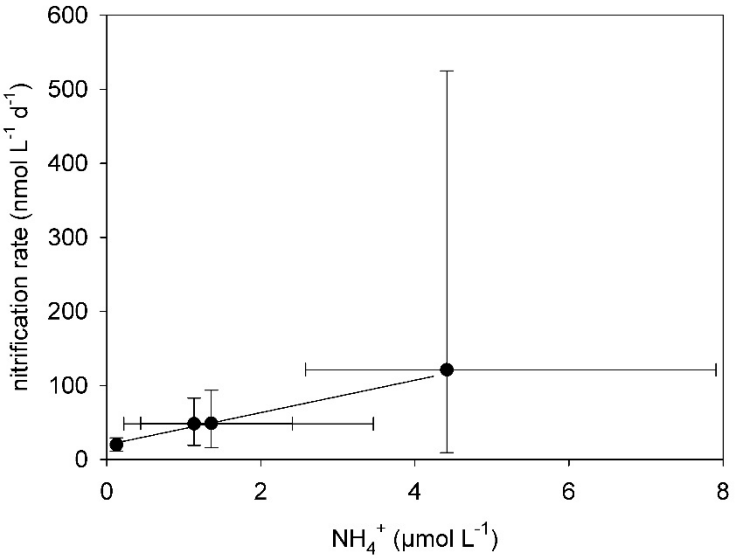

Figure 26:Mean nitrification rates plotted over mean NH_4^+ concentrations from the Vistula and Öre estuary in spring and summer. The whiskers represent the range from minimum to maximum value.

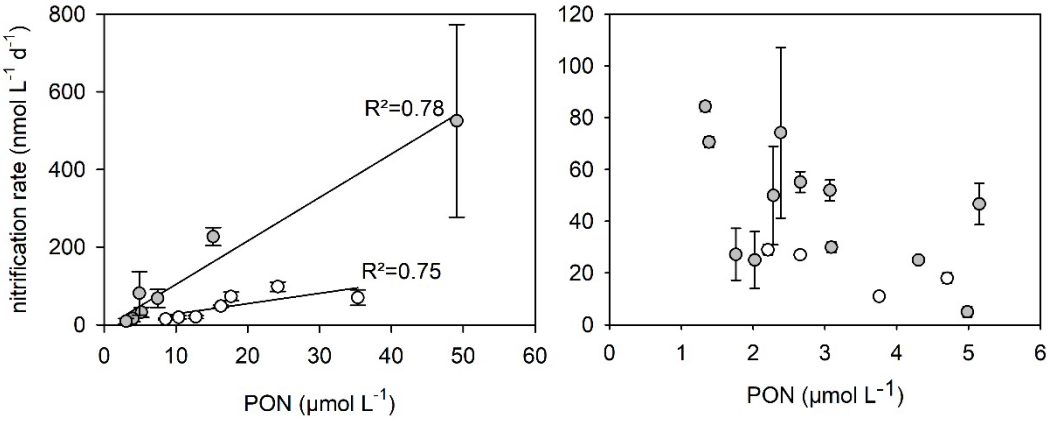

Figure 27: Relationship of nitrification rates to PON concentrations in the Vistula estuary (grey symbols) and the Öre estuary (white symbols) in summer (left) and spring (right).

Another similarity, which could be reflected in similar nitrification rates is the low contribution of nitrification to the total NH_{4+} consumption (sum of nitrification rates and NH_{4+} assimilation rates) summer with 2 % in the Vistula estuary and 26 % in the Öre estuary in summer. This means nitrifiers likely compete for NH_{4+} with assimilating microorganisms at both sites during the summer season. In spring, there is a difference between the sites with a much higher contribution of nitrification to total NH_4^+ consumption with 56 % in the Vistula estuary, while the contribution remains constant in the Öre estuary (21 % in spring). The overall high contribution of NH_4^+ assimilation in the Öre estuary reflects the net-heterotrophic state of this coastal zone (Sandberg et al., 2004). Stronger competition for NH_4^+ in the Öre estuary in spring might limit nitrification rates, which could mirror the slightly lower rates compared to the Vistula estuary in this season (Figure 25).

Results from community analysis regarding composition and activity of the AOA and AOB in the Bay of Gdansk (here winter 2015) and Öre estuary (April 2015) revealed different community compositions in the two rivers (Münster-Happel et al., in prep.). Most likely the freshwater nitrifiers in the Öre River are less active, since nitrification rates were lower (Table 9). But, in the coastal waters of the Vistula and Öre estuary, the community compositions were similar with the same most abundant archaeal and bacterial OTUs (operational taxonomic unit), respectively. Furthermore, in the AOA community, the same OTU was found to be most active in the BBL at both sites (Münster-Happel et al., unpublished). Hence, also the similar nitrifying community composition and activity, may be a reason for similar nitrification rates in the Öre estuary and the Bay of Gdansk, irrespective of the riverine N-load. Moreover, these results indicate, that the nitrification rates measured at the Öre estuary and the Bay of Gdansk represent typical estuarine water column nitrification rates in the coastal Baltic Sea.

3.4.4 The role of N-recycling in the Öre estuary and Vistula estuary

A difference between the Öre estuary and the Vistula estuary arose, when nitrogen budgets of the respective months of sampling were compared (Table 11). In spring, nitrification in the surface water and in the BBL only add a minor fraction of NO_3^- to the coastal system relative to the riverine DIN-load with 0.3 % in the Vistula estuary and less than 3.5 % in the Öre estuary. But in summer, N-recycling via nitrification is an important DIN source, since the riverine DIN-load is low (Table 11). In the Vistula

estuary, the riverine DIN-load and BBL-nitrification supply a similar amount of DIN to the system, while in the Öre estuary, BBL-nitrification is the dominating DIN source producing 3.5 times more DIN than discharged from the Öre River. So, although the nitrification rates are similar in both estuaries in summer, nitrification is a much more important DIN source in the Öre estuary than in the Vistula estuary. Humborg et al. (2003) described an import of DIN into pristine estuaries from the Bothnian Bay in summer. However, my results imply, that also nitrification within pristine estuaries, like the Öre estuary, can be an important DIN source in that season. Unfortunately, information of nitrification in the mid and surface water layer from the summer season are not yet available, but are crucial to better resolve the function of nitrification in the Öre estuary. Since this estuary underlies net heterotrophic conditions it is likely that organic matter degradation processes (ammonification) are dominant, as it was found during time periods of net heterotrophic states of the Scheldt estuary (Brion et al., 2008). This could enhance nitrification (Brion et al., 2008) and thus the important DIN source in the whole water column of an estuary.

It is furthermore important to note, that hardly any NO_3^- produced in the BBL is removed via sedimentary denitrification at both sites with less than 13 % of water-derived NO_3^- being denitrified (Hellemann et al., submitted; pers. comm. Dana Hellemann, Table 11). Hence, NO_3^- remains in the water column of the estuaries and may either enter a new N-cycle via uptake by primary producers or is subject to transport by lateral bottom water currents. Bottom water currents do not automatically export solutes from a coastal zone, but retain them via inward or recirculating flow (Wild-Allen and Andrewartha, 2016). So, recycled nitrogen can be retained in the coastal system to a large amount and thus contributes to the coastal filter function (Almroth-Rosell et al., 2016). The coastal filter function, i.e. N-recycling and N-removal, is regarded as a function of the water residence time within the coastal zone (Nixon et al., 1996; Humborg et al., 2003). A long residence time allows more nitrogen to be biogeochemically transformed, i.e. taken up, recycled or removed, resulting in a net removal of N (Voss et al., 2010). In estuaries and other coastal sites in the Baltic Sea, denitrification has been found to be low compared to the N-load, these coastal zones receive (Hellemann et al., submitted and cites therein). Also in the Vistula and Öre estuary, N-removal via denitrification is rather low, with less or equal turnover as nitrification in the BBL (Hellemann et al., submitted; Hellemann, unpublished data).

Hellemann et al. (submitted) thus suggest that nitrogen removal in Baltic coastal zones is less efficient than commonly thought.

Another N-recycling process is NH_4^+ assimilation whereby NH_4^+ is incorporated into biomass (PON). PON is a compound of particulate matter which can have much longer residence times than solutes. In the Öre estuary, the water residence time in April 2015 was estimated to be three weeks (Humborg et al., unpublished data), but particulate matter can remain in the system more than one year (Brydsten and Jansson, 1989). Thus, N bound to particles remains longer in the coastal zone and can be further sequestered via degradation, ammonification, nitrification and potentially removed by denitrification. In the Öre and Vistula estuary, N-recycling by NH_4^+ assimilation is always higher than by nitrification, except in the BBL in spring in the Vistula estuary (Table 11). Especially in the BBL, this process should not be underestimated regarding its role in N-recycling in coastal zones, since particle residence times can be long (Brydsten and Jansson, 1989). Finally, my results highlight the importance of BBL-nitrification as an additional DIN source, especially in pristine estuaries, and both, nitrification and NH_4^+ assimilation as contributors to N-retention in the Vistula and Öre estuary.

Table 11: N-budgets in t month^{-1} of the respective months of sampling comparing NO_3^- recycling via nitrification with the riverine DIN loads. "nitrification-dw" is the nitrification budget with subtracted water-derived denitrification, hence NO_3^- remaining in the water column. Numbers in parentheses represent the percentage of NO_3^- from nitrification on the riverine DIN-load. "n.a." denotes no available data.

		spring (t month^{-1})		**summer (t month^{-1})**	
		Vistula estuary	**Öre estuary**	**Vistula estuary**	**Öre estuary**
River	DIN-load	**14029**	**17**	91	**0.8**
surface	nitrification	**49** (0.3%)	**0.6** (3.5%)	n.a.	n.a.
	NH_4^+ ass.	**685**	**12.2**	n.a.	**16.3**
BBL	nitrification	**78** (0.6%)	**1.4** (8.2%)	**121** (133%)	**2.8** (350%)
	nitrification-dw	**75** (0.5%)	**1.4** (8.2%)	**116** (127%)	**2.5** (313%)
	NH_4^+ ass.	**60**	**6**	**539**	**12.3**

3.4.5 Summary and Conclusion

Since there is no difference in nitrification rates albeit distinct riverine N-loads in the Vistula and Öre estuary, other influencing factors might reflect the similar range of nitrification. Similar physical and environmental conditions, same relationships or lack of relationships with substrates, similar competition for NH_4^+, and the same nitrifier community composition and activity, are factors that can account for the non-different nitrification rates. The difference between the two sites evolves, when the role of nitrification is investigated. In the Öre estuary, nitrification is a very important DIN source compared to the riverine DIN-load, especially in summer. Furthermore, N-recycling via nitrification and NH_4^+ assimilation is strongly contributing to N-retention. Since, nitrogen removal is likely less efficient, the N-retention in Baltic coastal zones seems to rely on these recycling processes.

4. Final Conclusions and Perspectives

Rivers connect coastal ecosystems with the land on which the continuously growing human population (UN World Population Prospects) is extensively cultivating land by applying tremendous amounts of nitrogen fertilizers and producing waste waters (Gruber and Galloway, 2008). And, rivers are delivering these loads of anthropogenic nitrogen to the coastal system which perturbs the natural nitrogen cycle and leads to eutrophication (Smith et al., 1999). Finally, hypoxia and the loss of the coastal flora and fauna can turn coastal zones into a non-reversible state (Kemp et al., 2009). Therefore, it is crucial to expand our understanding about the fate of the anthropogenic nitrogen, i.e. about the nitrogen cycle and the dynamics in the coastal nitrogen turnover. The quantification of nitrogen transformation processes and the understanding of their linkages as well as the coastal filter function are hence the foci of the COCOA project, in which this thesis is integrated.

In the framework of this thesis, nitrification, a key nitrogen transformation process in coastal nitrogen turnover, was studied in two distinct coastal zones in the Baltic Sea: the Vistula estuary (Bay of Gdansk) and the Öre estuary. The results indicate that nitrification, although relatively low in turnover, has an important function in coastal nitrogen retention. Moreover, the results give new insights into potential regulation mechanisms and linkages to other nitrogen transformation processes in coastal zones. The river plume and the BBL are specific coastal environments that might be nitrification hotspots due to favourable conditions e.g. high substrate availability (Bianchi et al., 1999). However, no clear nitrification hotspots were not found in the Vistula estuary of the Bay of Gdansk. The Vistula river plume was not a hotspot, but a transition zone, with a shift in magnitude and regulation of nitrification rates at intermediate salinities. This indicates a shift in the nitrifier community composition and activity, which also has been stated for salinity gradients in the Chesapeake Bay (Bouskill et al., 2011) and the San Francisco Bay (Mosier and Francis, 2008). Yet, this is to my knowledge the first time that a shift in nitrification rates along a river plume salinity gradient was observed. Freshwater nitrifiers discharged into saline coastal waters are not only stressed by higher salinities (Damashek et al., 2016) but might also loose the competition for the substrate NH_4^+ with the enhanced phytoplankton and bacterial production (Ameryk et al., 2005, Wielgart-Rychert et al., 2013). In the Vistula estuary, particle associated nitrifiers might have become entrained with settling particles, as indicated by the exponential decrease of POM with increasing salinity. Intense organic matter degradation and subsequent

ammonification in organic particles may have triggered nitrification in the physically distinct BBL in summer. However, the BBL was only a hotspot relative to the overlying water within the summer season. In winter and spring, nitrification rates were similar throughout the water column at low ambient NH_4^+ and PON concentrations, indicating low substrate availability. I suggest that also other factors than the here studied environmental variables regulate nitrification in such a dynamic open bay. This suggestion is further supported by contradictory findings on relationships of nitrification rates with environmental variables like season (Andersson et al., 2006), salinity (Pakulski et al., 2000; Brion et al., 2008), temperature (Dai et al. 2008; Baer et al. 2014), NH_4^+ (Bianchi et al., 1999; Grundle and Juniper, 2011) or nitrifier abundance (Caffrey et al., 2007; Li et al., 2015). Firstly, the dynamic conditions itself, i.e. the hydrodynamic regime, may trigger nitrification by improving the accessibility of NH_4^+ especially to the mainly occuring particle associated nitrifiers (Ritzrau, 1996, Ritzrau et al., 1997). Secondly, nitrifiers may be able to adapt to low substrate availability by actively accumulating the substrate in the cell (Schmidt et al., 2004). Thirdly, nitrifiers might take advantage of the low ambient NH_4^+ assimilation rates which usually successfully compete for NH_4^+. Fourth, via resuspension active nitrifiers from the BBL (Münster-Happel et al., unpublished) or the sediment may be introduced to the water column by resuspension events, like a storm. Finally, a combination of all these mechanisms could contribute to the regulation of coastal water column nitrification, especially in dynamic open coastal bays. Nitrification rates in salinity gradients of river plumes have rarely been studied (Bianchi et al., 1999; Hsiao et al., 2014). Highly resolved sampling within river plume salinity gradients or lagrangian sampling following a parcel of river plume water over time in combination with measurements of nitrification rates as well as investigating the nitrifier community (composition, abundance, activity) would further shed light on the regulation and role of nitrification in river plumes. Furthermore, experiments addressing the four above proposed mechanisms of nitrification regulation are needed to support my suggestions.

A fifth mechanism regulating nitrification rates in the Vistula estuary, discussed in chapter 3.3., is NH_4^+ supply to BBL-nitrification via sedimentary NH_4^+ release. Surprisingly, I found no significant difference in sedimentary NH_4^+ release (diffusive and total NH_4^+ fluxes, Thoms et al., unpublished) and BBL-nitrification rates in and above different sediment types, respectively. Moreover, BBL-nitrification rates or BBL-NH_4^+ concentrations were not positively correlated to the NH_4^+ fluxes. Together with the lack

of increasing NH_4^+ concentrations towards the seafloor in winter and spring, it suggests strong mixing of BBL-water by the turbulent boundary layer flow (Dade et al., 2001). Still, the sedimentary NH_4^+ release was coupled to BBL-nitrification in winter and spring via refilling the ambient NH_4^+ pool in the BBL at slightly higher rate than NH_4^+ was consumed. NO_3^- from the BBL was hardly used by sedimentary denitrification in all sediment types (Dana Hellemann, unpublished data). This was surprising, in particular for permeable sediments, where NO_3^- from the sediment overlying water is assumed to be the dominant NO_3^- source for denitrification (Kessler et al., 2013). However, indications of high sedimentary nitrification activity by high pore water NO_3^- concentrations and sedimentary NO_3^- release (Thoms et al., unpublished) underscore the coupled nitrification-denitrification found in the permeable sediments of the Vistula estuary. Since the NO_3^- produced by BBL nitrification remains in the coastal ecosystem it is most likely transported by lateral bottom water currents or resuspended into the surface water and serving as nitrogen substrate for primary producers. Further investigations are needed to understand the fate of NO_3^- from the BBL. This will be realized for the Bay of Gdansk by combining results from a physical transport model (GETM) with biogeochemical data like concentrations of N-species and the N-turnover by nitrification (Bartl et al., in prep.).

Albeit the lower DON-dominated riverine nitrogen loads in the pristine Öre estuary, nitrification rates from this estuary in the northern Baltic Sea are similar to nitrification rates from the Vistula estuary, which receives two orders of magnitude more nitrogen (DIN-dominated). Among other findings, especially the similar physical and biogeochemical conditions and the same nitrifier community composition and activity (Münster-Happel et al., unpublished), are factors that may account for the non-different nitrification rates. However, nitrification in the Öre estuary serves as an important DIN source, especially in summer, when riverine DIN loads are low. That pristine estuaries in the northern Baltic Sea import DIN from in the Bothnian Bay has been shown by Humborg et al. (2003). The Öre estuary is located at the Kvarken Sea which connects Bothnian Bay and Bothnian Sea and would fall into the characterization of Humborg et al. (2003). However, the results in this thesis imply that pristine estuaries may also receive the missing DIN in summer via nitrification in the BBL which can reach the surface water through wind induced mixing. Rate measurements from the mid water column and the surface water are needed to strengthen the proposed function of BBL-nitrification in the whole water column of the heterotrophic Öre estuary.

Nitrogen retention is an important coastal filter function because it reduces the amount of nitrogen exported to the open sea thereby preventing the expansion of the eutrophication processes to open seas (Almroth-Rosell et al., 2016). Nitrogen retention can be defined as the net effect of permanent nitrogen removal and temporary nitrogen retention (Nixon, 1996). Nitrogen recycling processes, e.g. nitrification, can be regarded as temporary retention whereby nitrogen is recycled within the coastal system until eventually removed. Since nitrogen removal by denitrification is considered less efficient in Baltic coastal zones like the Vistula and Öre estuary (Hellemann et al., submitted and cites therein), nitrogen recycling might be more important for coastal nitrogen retention. Indeed, turnover of nitrogen via nitrification and also NH_4^+ assimilation rates exceed denitrification in both the Vistula and the Öre estuary as indicated by budget calculations of these processes for respective months of sampling. Short residence times of 2 and 3 weeks in the Vistula and Öre estuary, respectively, could result in significant export of nitrogen from the coastal systems. However, bottom waters and particles can have much longer residence times (Brydsten and Janssen, 1989) and nitrogen can be potentially retained longer in the Vistula (Witek et al., 2003) and Öre estuary. Hellemann et al., (submitted) suggest from their results on the origin of POM and riverine NO_3^- loads, that nitrogen discharged in the spring flood is denitrified in summer, which underlines the retention of nitrogen via recycling for at least 4 months in the Öre estuary. The understanding of the role of nitrification in in coastal nitrogen retention (chapter 3.4) is crucial since it is also a positive feedback regarding eutrophication by adding bioavailable nitrogen to the system. If nitrogen recycling outbalances nitrogen removal, irreversible eutrophication effects, e.g. seasonal hypoxia, could be the consequence. Nitrogen removal efficiency can by reduced not only by increasing nitrogen concentrations over phosphorus (Mulholland et al., 2008), but also by extensive dredging and sediment removal in estuaries (Dähnke et al., 2008). Through the latter, the Elbe estuary is assumed to have lost its denitrification capacity, since the estuary changed from being a nitrogen sink to being a nitrogen source to the adjacent coastal North Sea (Dähnke et al., 2008).

N-recycling becomes also a focus in coastal modelling studies, e.g. by Almroth-Rosell et al. (2016) in the Stockholm archipelago. However, model results showed a minor effect of temporary nitrogen retention probably due to the long residence time of water in the Stockholm archipelago which allows effective nitrogen removal. Furthermore, nitrification was implemented in the model as temperature and oxygen dependend recycling process and only occurring in the water column. Both settings most likely do

not represent natural conditions as suggested by results from this thesis. Other regulation mechanisms than temperature and oxygen have an impact on nitrification (chapter 3.2 and 3.3), and also sedimentary nitrification exists (chapter 3.3) in Baltic coastal zones. Nevertheless, the implementation of nitrogen recycling processes in coastal biogeochemical models is a major step forward and should be further developed to better understand coastal filter functions. Therefore, quantification and understanding of nitrogen recycling processes like nitrification, ammonification (Brion et al., 2008), assimilation and DNRA (Bonaglia et al., 2017) are necessary for the implementation into models. There exist only few studies that not only studied one nitrogen transformation process, but quantified a set of nitrogen processes and combined the results to the nitrogen retention capacity (e.g. Brion et al., 2008). Such studies are however crucial for our understanding of coastal nitrogen cycling and the coastal filter function. Within the COCOA project, Dana Hellemann, Franziska Thoms and I are aiming to expand the understanding of nitrogen cycling in the Öre estuary and Vistula estuary by combining results of denitrification rates, nitrification rates and benthic nitrogen fluxes from the five field campaigns (manuscript in preparation). Future studies should also focus on measurements over longer periods of time, since results from cruises as it is the case in this thesis, are only "snapshots" in time. Also experiments, e.g. under in situ conditions may help to understand the complex regulation of processes in coastal zones. Further a combination of these results with coastal transportation models (Bartl et al., in prep.) or biogeochemical models (Almroth-Rosell et al., 2016) will help to resolve the change of the filter capacity in coastal zones.

5. References

Almroth-Rosell, E., Edman, M., Eilola, K., Meier, H.E.M., Sahlberg, J., 2016. Modelling nutrient retention in the coastal zone of an eutrophic sea. Biogeosciences 13, 5753–5769. doi:10.5194/bg-13-5753-2016

Alongi, D.M., 1998. Coastal ecosystem processes, Marine science series. CRC Press, Boca Raton.

Alonso-Sáez, L., Waller, A.S., Mende, D.R., Bakker, K., Farnelid, H., Yager, P.L., Lovejoy, C., Tremblay, J.-É., Potvin, M., Heinrich, F., Estrada, M., Riemann, L., Bork, P., Pedrós-Alió, C., Bertilsson, S., 2012. Role for urea in nitrification by polar marine Archaea. Proc. Natl. Acad. Sci. U. S. A. 109, 17989–94. doi:10.1073/pnas.1201914109

Ameryk, A., Podgorska, B., Witek, Z., 2005. The dependence between bacterial production and environmental conditions in the Gulf of Gdańsk. Oceanologia 47, 27–45.

Andersson, M., Brion, N., Middelburg, J., Middelburg, J.J., 2006. Comparison of nitrifier activity versus growth in the Scheldt estuary—a turbid, tidal estuary in northern Europe. Aquat. Microb. Ecol. 42, 149–158. doi:10.3354/ame042149

Baer, S.E., Connelly, T.L., Sipler, R.E., Yager, P.L., Bronk, D.A., 2014. Effect of temperature on rates of ammonium uptake and nitrification in the western coastal Arctic during winter, spring, and summer. Global Biogeochem. Cycles 28, 1455–1466. doi:10.1002/2013GB004765

Beman, J.M., Popp, B.N., Francis, C.A., 2008. Molecular and biogeochemical evidence for ammonia oxidation by marine Crenarchaeota in the Gulf of California. ISME J. 2, 429–441. doi:10.1038/ismej.2007.118

Bianchi, M., Feliatra, Lefevre, D., 1999. Regulation of nitrification in the land-ocean contact area of the Rhone River plume (NW Mediterranean). Aquat. Microb. Ecol. 18, 301–312. doi:10.3354/ame018301

Bonaglia, S., Deutsch, B., Bartoli, M., Marchant, H.K., Brüchert, V., 2014. Seasonal oxygen, nitrogen and phosphorus benthic cycling along an impacted Baltic Sea estuary: regulation and spatial patterns. Biogeochemistry 119, 139–160. doi:10.1007/s10533-014-9953-6

Bonaglia, S., Hylén, A., Rattray, J.E., Kononets, M.Y., Ekeroth, N., Roos, P., Thamdrup, B., Brüchert, V., Hall, P.O.J., 2017. The fate of fixed nitrogen in marine sediments with low organic loading: an in situ study. Biogeosciences 14, 285–300. doi:10.5194/bg-14-285-2017

Bouskill, N.J., Eveillard, D., Chien, D., Jayakumar, A., Ward, B.B., 2012. Environmental factors determining ammonia-oxidizing organism distribution and diversity in marine environments. Environ. Microbiol. 14, 714–729. doi:10.1111/j.1462-2920.2011.02623.x

Brion, N., Andersson, M.G.I., Elskens, M., 2008. Nitrogen cycling, retention and export in a eutrophic temperate macrotidal estuary. Mar. Ecol. Prog. Ser. 357, 87–99. doi:10.3354/meps07249

Bristow, L.A., Sarode, N., Cartee, J., Caro-Quintero, A., Thamdrup, B., Stewart, F.J., 2015. Biogeochemical and metagenomic analysis of nitrite accumulation in the Gulf of Mexico hypoxic zone. Limnol. Oceanogr. 60, 1733–1750. doi:10.1002/lno.10130

Bronk, D.A., Killberg-Thoreson, L., Sipler, R.E., Mulholland, M.R., Roberts, Q.N., Bernhardt, P.W., Garrett, M., O'Neil, J.M., Heil, C.A., 2014. Nitrogen uptake and regeneration (ammonium regeneration, nitrification and photoproduction) in waters of the West Florida Shelf prone to blooms of Karenia brevis. Harmful Algae 38, 50–62. doi:10.1016/j.hal.2014.04.007

Brydsten, L., 1992. Wave-induced sediment resuspension in the ?re estuary, northern Sweden, in: Sediment/Water Interactions. Springer Netherlands, Dordrecht, pp. 71–83. doi:10.1007/978-94-011-2783-7_6

Brydsten, L., Jansson, M., 1989. Studies of estuarine sediment dynamics using 137Cs from the

Tjernobyl accident as a tracer. Estuar. Coast. Shelf Sci. 28, 249–259. doi:10.1016/0272-7714(89)90016-4

Burdige, D.J., 2006. Geochemistry of marine sediments. Princeton University Press.

Caffrey, J.M., Bano, N., Kalanetra, K., Hollibaugh, J.T., 2007. Ammonia oxidation and ammonia-oxidizing bacteria and archaea from estuaries with differing histories of hypoxia. ISME J. 1, 660–662. doi:10.1038/ismej.2007.79

Carini, S.A., McCarthy, M.J., Gardner, W.S., 2010. An isotope dilution method to measure nitrification rates in the northern Gulf of Mexico and other eutrophic waters 30, 1795–1801.

Casciotti, K.L., Sigman, D.M., Hastings, M.G., Böhlke, J.K., Hilkert, A., 2002. Measurement of the Oxygen Isotopic Composition of Nitrate in Seawater and Freshwater Using the Denitrifier Method. Anal. Chem. 74, 4905–4912. doi:10.1021/AC020113W

Cloern, J., 2001. Our evolving conceptual model of the coastal eutrophication problem. Mar. Ecol. Prog. Ser. 210, 223–253. doi:10.3354/meps210223

Conley, D.J., 1997. Riverine contribution of biogenic silica to the oceanic silica budget. Limnol. Oceanogr. 42, 774–777. doi:10.4319/lo.1997.42.4.0774

Conley, D.J., Carstensen, J., Aigars, J., Axe, P., Bonsdorff, E., Eremina, T., Haahti, B.-M., Humborg, C., Jonsson, P., Kotta, J., Lännegren, C., Larsson, U., Maximov, A., Medina, M.R., Lysiak-Pastuszak, E., Remeikaité-Nikiené, N., Walve, J., Wilhelms, S., Zillén, L., 2011. Hypoxia is increasing in the coastal zone of the Baltic Sea. Environ. Sci. Technol. 45, 6777–83. doi:10.1021/es201212r

Cyberska, B., Krzyminski, W., 1988. Extension of the Vistula River water in the Gulf of Gdansk, in: Proceedings of the16th Conference of the Baltic Oceanographers. Institute of Marine Research Kiel, Kiel, pp. 290–304.

Dade, W.B., Hogg, A.J., Boudreau, B.P., 2001. Physics of flow above the sediment-water interface.

Dähnke, K.; Bahlmann, E.; Emeis, K., 2008. A nitrate sink in estuaries? An assessment by means of stable nitrate isotopes in the Elbe estuary. [WWW Document]. Limnol. Ocean. URL http://aslo.net/lo/toc/vol_53/issue_4/1504.pdf (accessed 3.3.14).

Dähnke, K., Emeis, K., Johannsen, A., Nagel, B., 2010. Stable isotope composition and turnover of nitrate in the German Bight. Mar. Ecol. Prog. Ser. 408, 7–18. doi:10.3354/meps08558

Dai, M., Wang, L., Guo, X., Zhai, W., Li, Q., He, B., Kao, S.-J., 2008. Nitrification and inorganic nitrogen distribution in a large perturbed river/estuarine system: the Pearl River Estuary, China. Biogeosciences 5, 1227–1244. doi:10.5194/bg-5-1227-2008

Daims, H., Lebedeva, E. V., Pjevac, P., Han, P., Herbold, C., Albertsen, M., Jehmlich, N., Palatinszky, M., Vierheilig, J., Bulaev, A., Kirkegaard, R.H., Bergen, M. von, Rattei, T., Bendinger, B., Nielsen, P.H., Wagner, M., 2015. Complete nitrification by Nitrospira bacteria. Nature 528, 504. doi:10.1038/nature16461

Dalsgaard, T., Thamdrup, B., Canfield, D.E., 2005. Anaerobic ammonium oxidation (anammox) in the marine environment. Res. Microbiol. 156, 457–464. doi:10.1016/j.resmic.2005.01.011

Damashek, J., Casciotti, K.L., Francis, C.A., 2016. Variable Nitrification Rates Across Environmental Gradients in Turbid, Nutrient-Rich Estuary Waters of San Francisco Bay. Estuaries and Coasts 39, 1050–1071. doi:10.1007/s12237-016-0071-7

Davis, J., Benner, R., 2005. Seasonal trends in the abundance, composition and bioavailability of particulate and dissolved organic matter in the Chukchi/Beaufort Seas and western Canada Basin. Deep Sea Res. Part II Top. Stud. Oceanogr. 52, 3396–3410. doi:10.1016/j.dsr2.2005.09.006

Devol, A.H., 2015. Denitrification, Anammox, and N 2 Production in Marine Sediments. Ann. Rev. Mar. Sci. 7, 403–423. doi:10.1146/annurev-marine-010213-135040

Diaz, R.J., Rosenberg, R., 2008. Spreading dead zones and consequences for marine ecosystems. Science 321, 926–9. doi:10.1126/science.1156401

Dugdale, R.C., Wilkerson, F.P., 1986. The use of 15N to measure nitrogen uptake in eutrophic oceans; experimental considerations. Limnol. Oceanogr. 31, 673–689. doi:10.4319/lo.1986.31.4.0673

Ehrenhauss, S., Witte, U., Janssen, F., Huettel, M., 2004. Decomposition of diatoms and nutrient dynamics in permeable North Sea sediments. Cont. Shelf Res. 24, 721–737. doi:http://dx.doi.org/10.1016/j.csr.2004.01.002

Emeis, K., Christiansen, C., Edelvang, K., Jähmlich, S., Kozuch, J., Laima, M., Leipe, T., Löffler, A., Lund-Hansen, L.C., Miltner, A., Pazdro, K., Pempkowiak, J., Pollehne, F., Shimmield, T., Voss, M., Witt, G., 2002. Material transport from the near shore to the basinal environment in the southern Baltic Sea: II: Synthesis of data on origin and properties of material. J. Mar. Syst. 35, 151–168. doi:http://dx.doi.org/10.1016/S0924-7963(02)00127-6

Enoksson, V., 1986. Nitrification rates in the baltic sea: comparison of three isotope techniques. Appl. Environ. Microbiol. 51, 244–50.

Feliatra, F., Bianchi, M., 1993. Rates of nitrification and carbon uptake in the Rhone River plume (northwestern Mediterranean Sea). Microb. Ecol. 26, 21–28. doi:10.1007/BF00166026

Floderus, S., Jähmlich, S., Ekebom, J., Saarso, M., 1999. Particle flux and properties affecting the fate of bacterial productivity in the benthic boundary layer at a mud-bottom site in South-Central Gulf of Riga. J. Mar. Syst. 23, 233–250. doi:10.1016/S0924-7963(99)00060-3

Forsgren, G., Jansson, M., 1992. The turnover of river-transported iron, phosphorus and organic carbon in the ?re estuary, northern Sweden. Hydrobiologia 235–236, 585–596. doi:10.1007/BF00026246

Forster, S., Bobertz, B., Bohling, B., 2003. Permeability of Sands in the Coastal Areas of the Southern Baltic Sea: Mapping a Grain-size Related Sediment Property. Aquat. Geochemistry 9, 171–190. doi:10.1023/B:AQUA.0000022953.52275.8b

Francis, C.A., Roberts, K.J., Beman, J.M., Santoro, A.E., Oakley, B.B., 2005. Ubiquity and diversity of ammonia-oxidizing archaea in water columns and sediments of the ocean 102, 14683–14688.

Galloway, J.N., Townsend, A.R., Erisman, J.W., Bekunda, M., Cai, Z., Freney, J.R., Martinelli, L.A., Seitzinger, S.P., Sutton, M.A., 2008. Transformation of the Nitrogen Cycle: Recent Trends, Questions, and Potential Solutions. Science (80-.). 320, 889–892. doi:10.1126/science.1136674

Granger, J., Sigman, D.M., 2009. Removal of nitrite with sulfamic acid for nitrate N and O isotope analysis with the denitrifier method. Rapid Commun. Mass Spectrom. 23, 3753–3762. doi:10.1002/rcm.4307

Grant, W.D., Madsen, O.S., 1986. The Continental-Shelf Bottom Boundary Layer. Annu. Rev. Fluid Mech. 18, 265–305. doi:10.1146/annurev.fl.18.010186.001405

Grasshoff, K., Kremling, K., Ehrhardt, M., 1999. Methods of Seawater Analysis, 3rd ed. Wiley-VCH, Weinheim.

Gruber, N., Galloway, J.N., 2008. An Earth-system perspective of the global nitrogen cycle. Nature 451, 293–296.

Grundle, D.S., Juniper, S.K., 2011. Nitrification from the lower euphotic zone to the sub-oxic waters of a highly productive British Columbia fjord. Mar. Chem. 126, 173–181.

doi:10.1016/j.marchem.2011.06.001

Hagopian, D.S., Riley, J.G., 1998. A closer look at the bacteriology of nitrification. Aquac. Eng. 18, 223–244. doi:10.1016/S0144-8609(98)00032-6

Hansen, H.P., Koroleff, F., 1983. Determination of nutrients, in: Methods of Seawater Analysis. Wiley-VCH Verlag GmbH, Weinheim, Germany, pp. 159–228. doi:10.1002/9783527613984.ch10

Heiss, E.M., Fulweiler, R.W., 2016. Coastal water column ammonium and nitrite oxidation are decoupled in summer. Estuar. Coast. Shelf Sci. 178, 110–119. doi:10.1016/j.ecss.2016.06.002

Helcom, 2009. Eutrophication in the Baltic Sea. An integrated thematic assessment of the effects of nutrient enrichment in the Baltic Sea region. Balt. Sea Environ. Proc. No. 115B.

Hietanen, S., Jantti, H., Buizert, C., Jurgens, K., Labrenz, M., Voss, M., Kuparinen, J., 2012. Hypoxia and nitrogen processing in the Baltic Sea water column. Limnol. Oceanogr. 57, 325–337. doi:10.4319/lo.2012.57.1.0325

Holtappels, M., Kuypers, M.M.M., Schlueter, M., Bruchert, V., 2011. Measurement and interpretation of solute concentration gradients in the benthic boundary layer. Limnol. Oceanogr. 9, 1–13. doi:10.4319/lom.2011.9.1

Horak, R.E.A., Qin, W., Schauer, A.J., Armbrust, E.V., Ingalls, A.E., Moffett, J.W., Stahl, D.A., Devol, A.H., 2013. Ammonia oxidation kinetics and temperature sensitivity of a natural marine community dominated by Archaea. ISME J. 7, 2023–2033. doi:10.1038/ismej.2013.75

Horrigan, S.G., Montoya, J.P., Nevins, J.L., McCarthy, J.J., Ducklow, H., Goericke, R., Malone, T., 1990. Nitrogenous nutrient transformations in the spring and fall in the Chesapeake Bay. Estuar. Coast. Shelf Sci. 30, 369–391. doi:10.1016/0272-7714(90)90004-B

Howarth, R., Chan, F., Conley, D.J., Garnier, J., Doney, S.C., Marino, R., Billen, G., 2011. Coupled biogeochemical cycles: eutrophication and hypoxia in temperate estuaries and coastal marine ecosystems. Front. Ecol. Environ. 9, 18–26. doi:10.1890/100008

Howarth, R.W., Marino, R., 2006. Nitrogen as the limiting nutrient for eutrophication in coastal marine ecosystems: Evolving views over three decades. Limnol. Oceanogr. 51, 364–376. doi:10.4319/lo.2006.51.1_part_2.0364

Hsiao, S.S.Y., Hsu, T.C., Liu, J. w., 2014. Nitrification and its oxygen consumption along the turbid Chang Jiang River plume. Biogeosciences 11, 2083–2098. doi:10.5194/bg-11-2083-2014

Huettel, M., Berg, P., Kostka, J.E., 2014. Benthic Exchange and Biogeochemical Cycling in Permeable Sediments. Ann. Rev. Mar. Sci. 6, 23–51. doi:10.1146/annurev-marine-051413-012706

Huettel, M., Røy, H., Precht, E., Ehrenhauss, S., 2003. Hydrodynamical impact on biogeochemical processes in aquatic sediments. Hydrobiologia 494, 231–236.

Huettel, M., Rusch, A., 2000. Transport and degradation of phytoplankton in permeable sediment. Limnol. Oceanogr. 45, 534–549.

Huettel, M., Ziebis, W., Forster, S., 1996. Flow-induced uptake of particulate matter in permeable sediments. Limnol. Oceanogr. 41, 309–322.

Huettel, M., Ziebis, W., Forster, S., Luther, G.W., 1998. Advective transport affecting metal and nutrient distributions and interfacial fluxes in permeable sediments. Geochim. Cosmochim. Acta 62, 613–631. doi:10.1016/s0016-7037(97)00371-2

Humborg, C., Danielsson, Å., Sjöberg, B., Green, M., 2003. Nutrient land–sea fluxes in oligothrophic and pristine estuaries of the Gulf of Bothnia, Baltic Sea. Estuar. Coast. Shelf

Sci. 56, 781–793. doi:10.1016/S0272-7714(02)00290-1

Hunter, W.R., Veuger, B., Witte, U., 2012. Macrofauna regulate heterotrophic bacterial carbon and nitrogen incorporation in low-oxygen sediments. Int. Soc. Microb. Ecol. 6, 2140–2151.

Iriarte, A., de la Sota, A., Orive, E., 1997. Seasonal variation of nitrification along a salinity gradient in an urban estuary. Hydrobiologia 362, 115–126. doi:10.1023/A:1003130516899

Jähmlich, S., Lund-Hansen, L.C., Leipe, T., 2002. Enhanced settling velocities and vertical transport of particulate matter by aggregation in the benthic boundary layer. Danish J. Geogr. 102, 37–49.

Jähmlich, S., Thomsen, L., Graf, G., 1999. Factors controlling aggregate formation in the benthic boundary layer of the Mecklenburg Bight (western Baltic Sea). J. Sea Res. 41, 245–254. doi:10.1016/S1385-1101(99)00010-6

Jäntti, H., Hietanen, S., 2012. The Effects of Hypoxia on Sediment Nitrogen Cycling in the Baltic Sea. AMBIO A J. Hum. Environ. 41, 161–169.

Jickells, T.D., Andrews, J.E., Parkes, D.J., Suratman, S., Aziz, A.A., Hee, Y.Y., 2014. Nutrient transport through estuaries: The importance of the estuarine geography. Estuar. Coast. Shelf Sci. 150, 215–229. doi:10.1016/j.ecss.2014.03.014

Johan Rockstrom, 2009. Safe Operating Space for Humanity. Nature 461, 472–476. doi:10.1038/461472a

Joye, S.B., Anderson, I.C., 2008. Nitrogen Cycling in Coastal Sediments, in: Nitrogen in the Marine Environment. Elsevier, pp. 867–915. doi:10.1016/B978-0-12-372522-6.00019-0

Karl, D.M., Knauer, G.A., Martin, J.H., Ward, B.B., 1984. Bacterial chemolithotrophy in the ocean is associated with sinking particles. Nature 309, 54–56. doi:10.1038/309054a0

Kemp, W.M., Testa, J.M., Conley, D.J., Gilbert, D., Hagy, J.D., 2009. Temporal responses of coastal hypoxia to nutrient loading and physical controls. Biogeosciences 6, 2985–3008. doi:10.5194/bg-6-2985-2009

Kessler, A.J., Glud, R.N., Cardenas, M.B., Cook, P.L.M., 2013. Transport zonation limits coupled nitrification-denitrification in permeable sediments. Environ. Sci. Technol. 47, 13404–11. doi:10.1021/es403318x

Koops, H.-P., Purkhold, U., Pommerening-R?ser, A., Timmermann, G., Wagner, M., 2006. The Lithoautotrophic Ammonia-Oxidizing Bacteria, in: The Prokaryotes. Springer New York, New York, NY, pp. 778–811. doi:10.1007/0-387-30745-1_36

Koops, H.P., Pommerening-Röser, A., 2001. Distribution and ecophysiology of the nitrifying bacteria emphasizing cultured species. FEMS Microbiol. Ecol. doi:10.1016/S0168-6496(01)00137-4

Korth, F., Fry, B., Liskow, I., Voss, M., 2013. Nitrogen turnover during the spring outflows of the nitrate-rich Curonian and Szczecin lagoons using dual nitrate isotopes. Mar. Chem. 154, 1–11. doi:10.1016/j.marchem.2013.04.012

Lääne, A., Kraav, E., Titova, G., 2005. Global international waters assessment : regional assessment 17, Baltic Sea, in: GIWA Regional Assessment 17. University of Kalmar on behalf of United Nations Environment Programme, Kalmar, Sweden, pp. 1–69.

Lappe, C., Umlauf, L., 2016. Efficient boundary mixing due to near-inertial waves in a non-tidal basin: Observations from the Baltic Sea. J. Geophys. Res. Ocean. 121, 8287–8304. doi:10.1002/2016JC011985

Lehtovirta-Morley, L.E., Sayavedra-Soto, L.A., Gallois, N., Schouten, S., Stein, L.Y., Prosser, J.I., Nicol, G.W., 2016. Identifying Potential Mechanisms Enabling Acidophily in the Ammonia-

Oxidizing Archaeon ?Candidatus Nitrosotalea devanaterra? Appl. Environ. Microbiol. 82, 2608–2619. doi:10.1128/AEM.04031-15

Li, J., Nedwell, D.B., Beddow, J., Dumbrell, A.J., McKew, B.A., Thorpe, E.L., Whitby, C., 2015. amoA Gene abundances and nitrification potential rates suggest that benthic ammonia-oxidizing bacteria and not Archaea dominate N cycling in the Colne Estuary, United Kingdom. Appl. Environ. Microbiol. 81, 159–65. doi:10.1128/AEM.02654-14

Lipsewers, Y.A., Bale, N.J., Hopmans, E.C., Schouten, S., Sinninghe Damsté, J.S., Villanueva, L., 2014. Seasonality and depth distribution of the abundance and activity of ammonia oxidizing microorganisms in marine coastal sediments (North Sea). Front. Microbiol. 5, 472. doi:10.3389/fmicb.2014.00472

Lonborg, C., Davidson, K., Álvarez-Salgado, X.A., Miller, A.E.J., 2009. Bioavailability and bacterial degradation rates of dissolved organic matter in a temperate coastal area during an annual cycle. Mar. Chem. 113, 219–226. doi:10.1016/j.marchem.2009.02.003

Lunau, M., Voss, M., Erickson, M., Dziallas, C., Casciotti, K., Ducklow, H., 2013. Excess nitrate loads to coastal waters reduces nitrate removal efficiency: mechanism and implications for coastal eutrophication. Environ. Microbiol. 15, 1492–1504. doi:10.1111/j.1462-2920.2012.02773.x

Magalhães, C., Machado, A., Bordalo, A., 2009. Temporal variability in the abundance of ammonia- oxidizing bacteria vs. archaea in sandy sediments of the Douro River estuary, Portugal. Aquat. Microb. Ecol. 56, 13–23. doi:10.3354/ame01313

Malmgren, L., Brydsten, L., 1992. Sedimentation of river-transported particles in the Öre estuary, northern Sweden. Hydrobiologia 235–236, 59–69. doi:10.1007/BF00026200

Mann, K., Lazier, J., 2006. Dynamics of Marine Ecosystems: Biological-Physical Interactions in the Oceans. Wiley.

Martens-Habbena, W., Berube, P.M., Urakawa, H., de la Torre, J.R., Stahl, D.A., 2009. Ammonia oxidation kinetics determine niche separation of nitrifying Archaea and Bacteria. Nature 461, 976–979. doi:10.1038/nature08465

Middelburg, J., Nieuwenhuize, J., 2001. Nitrogen isotope tracing of dissolved inorganic nitrogen behaviour in tidal estuaries. Estuar. Coast. Shelf Sci. 53, 385–391.

Middelburg, J.J., Levin, L.A., 2009. Coastal hypoxia and sediment biogeochemistry. Biogeosciences 6, 1273–1293. doi:10.5194/bg-6-1273-2009

Mohrholz, V., Naumann, M., Nausch, G., Krüger, S., Gräwe, U., 2015. Fresh oxygen for the Baltic Sea - An exceptional saline inflow after a decade of stagnation. J. Mar. Syst. 148, 152–166. doi:10.1016/j.jmarsys.2015.03.005

Mosier, A.C., Francis, C.A., 2008. Relative abundance and diversity of ammonia-oxidizing archaea and bacteria in the San Francisco Bay estuary. Environ. Microbiol. 10, 3002–3016. doi:10.1111/j.1462-2920.2008.01764.x

Mulholland, P.J., Helton, A.M., Poole, G.C., 2008. Stream denitrification across biomes and its response to anthropogenic nitrate loading. Nat. Lett. 452.

Na, T., Gribsholt, B., Galaktionov, O.S., Lee, T., Meysman, F.J.R., 2008. Influence of advective bio-irrigation on carbon and nitrogen cycling in sandy sediments. J. Mar. Res. 66, 691–722. doi:10.1357/002224008787536826

Newell, S.E., Babbin, A.R., Jayakumar, A., Ward, B.B., 2011. Ammonia oxidation rates and nitrification in the Arabian Sea. Global Biogeochem. Cycles 25, n/a-n/a. doi:10.1029/2010GB003940

Nixon, S.W., 1995. Coastal marine eutrophication: A definition, social causes, and future

concerns. Ophelia 41, 199–219. doi:10.1080/00785236.1995.10422044

Nixon, S.W., Ammerman, J.W., Atkinson, L.P., Berounsky, V.M., Billen, G., Boicourt, W.C., Boynton, W.R., Church, T.M., Ditoro, D.M., Elmgren, R., Garber, J.H., Giblin, A.E., Jahnke, R.A., Owens, N.J.P., Pilson, M.E.Q., Seitzinger, S.P., 1996. The fate of nitrogen and phosphorus at the land-sea margin of the North Atlantic Ocean, in: Nitrogen Cycling in the North Atlantic Ocean and Its Watersheds. Springer Netherlands, Dordrecht, pp. 141–180. doi:10.1007/978-94-009-1776-7_4

Offre, P., Kerou, M., Spang, A., Schleper, C., 2014. Variability of the transporter gene complement in ammonia-oxidizing archaea. Trends Microbiol. 22, 665–675. doi:10.1016/j.tim.2014.07.007

Paerl, H.W., 2009. Controlling eutrophication along the freshwater-Marine continuum: Dual nutrient (N and P) reductions are essential. Estuaries and Coasts 32, 593–601. doi:10.1007/s12237-009-9158-8

Paerl, H.W., Piehler, M.F., 2008. Nitrogen and Marine Eutrophication, in: Nitrogen in the Marine Environment. Elsevier, pp. 529–567. doi:10.1016/B978-0-12-372522-6.00011-6

Pakulski, J.D., Benner, R., Whitledge, T., Amon, R., Eadie, B., Cifuentes, L., Ammerman, J., Stockwell, D., 2000. Microbial Metabolism and Nutrient Cycling in the Mississippi and Atchafalaya River Plumes. Estuar. Coast. Shelf Sci. 50, 173–184. doi:10.1006/ecss.1999.0561

Pastuszak, M., Witek, Z., 2012. Discharges of water and nutrients by the Vistula and Oder rivers draining Polish territory, in: Pastuszak, M., Igras, J. (Eds.), Temporal and Spatial Differences in Emission of Nitrogen and Phosphorus from Polish Territory to the Baltic Sea. National Marine Fisheries Research Institute, Institute of Soil Science and Plant Cultivation, Fertilizer Research Institute, Gdynia, pp. 309–346.

Peng, X., Fuchsman, C.A., Jayakumar, A., Warner, M.J., Devol, A.H., Ward, B.B., 2016. Revisiting nitrification in the Eastern Tropical South Pacific: A focus on controls. J. Geophys. Res. Ocean. 121, 1667–1684. doi:10.1002/2015JC011455

Phillips, C.J., Smith, Z., Embley, T.M., Prosser, J.I., 1999. Phylogenetic differences between particle-associated and planktonic ammonia-oxidizing bacteria of the beta subdivision of the class Proteobacteria in the Northwestern Mediterranean Sea. Appl. Environ. Microbiol. 65, 779–86.

Ploug, H., Bergkvist, J., 2015. Oxygen diffusion limitation and ammonium production within sinking diatom aggregates under hypoxic and anoxic conditions. Mar. Chem. 176, 142–149. doi:10.1016/j.marchem.2015.08.012

Pritchard, 1967. What is an estuary: physical viewpoint. Estuaries. Am. Assoc. Adv. Sci. Publ. 83.

Qin, W., Amin, S.A., Martens-Habbena, W., Walker, C.B., Urakawa, H., Devol, A.H., Ingalls, A.E., Moffett, J.W., Armbrust, E. V., Stahl, D.A., 2014. Marine ammonia-oxidizing archaeal isolates display obligate mixotrophy and wide ecotypic variation. Proc. Natl. Acad. Sci. 111, 12504–12509. doi:10.1073/pnas.1324115111

Radtke, H., Neumann, T., Voss, M., Fennel, W., 2012. Modeling pathways of riverine nitrogen and phosphorus in the Baltic Sea. J. Geophys. Res. Ocean. 117, n/a-n/a. doi:10.1029/2012JC008119

Rao, A.M.F., McCarthy, M.J., Gardner, W.S., Jahnke, R.A., 2008. Respiration and denitrification in permeable continental shelf deposits on the South Atlantic Bight: N2:Ar and isotope pairing measurements in sediment column experiments. Cont. Shelf Res. 28, 602–613. doi:10.1016/j.csr.2007.11.007

Reimers, C.E., Stecher, H.A., Taghon, G.L., Fuller, C.M., Huettel, M., Rusch, A., Ryckelynck, N., Wild, C., 2004. In situ measurements of advective solute transport in permeable shelf sands.

Cont. Shelf Res. 24, 183–201. doi:10.1016/j.csr.2003.10.005

Richards, K.J., 1990. Physical Processes in the Benthic Boundary Layer. Philos. Trans. R. Soc. London A Math. Phys. Eng. Sci. 331.

Richardson, K., Jørgensen, B.B., 2013. Eutrophication: Definition, History and Effects, in: Eutrophication in Coastal Marine Ecosystems. American Geophysical Union, pp. 1–19. doi:10.1029/CE052p0001

Ritzrau, W., 1996. Microbial activity in the benthic boundary layer: Small-scale distribution and its relationship to the hydrodynamic regime. J. Sea Res. 36, 171–180. doi:10.1016/S1385-1101(96)90787-X

Ritzrau, W., Thomsen, L., Lara, R., Graf, G., 1997. Enhanced microbial utilisation of dissolved amino acids indicates rapid modification of organic matter in the benthic boundary layer. Mar. Ecol. Prog. Ser. 156, 43–50. doi:10.3354/meps156043

Rysgaard, S., Risgaard-Petersen, N., Niels Peter, S., Kim, J., Lars Peter, N., 1994. Oxygen regulation of nitrification and denitrification in sediments. Limnol. Oceanogr. 39, 1643–1652. doi:10.4319/lo.1994.39.7.1643

Sandberg, J., Andersson, A., Johansson, S., Wikner, J., 2004. Pelagic food web structure and carbon budget in the northern Baltic Sea: potential importance of terrigenous carbon. Mar. Ecol. Prog. Ser. 268, 13–29. doi:10.3354/meps268013

Santoro, A.E., Casciotti, K.L., 2011. Enrichment and characterization of ammonia-oxidizing archaea from the open ocean: phylogeny, physiology and stable isotope fractionation. ISME J. 5, 1796–1808. doi:10.1038/ismej.2011.58

Schmidt, I., Look, C., Bock, E., Jetten, M.S.M., n.d. Ammonium and hydroxylamine uptake and accumulation in Nitrosomonas. doi:10.1099/mic.0.26719-0

Seitzinger, S., 2008. Out of reach. Nature 452, 162–163.

Seitzinger, S.P., Mayorga, E., Bouwman, A.F., Kroeze, C., Beusen, A.H.W., Billen, G., Van Drecht, G., Dumont, E., Fekete, B.M., Garnier, J., Harrison, J.A., 2010. Global river nutrient export: A scenario analysis of past and future trends. Global Biogeochem. Cycles 24, n/a-n/a. doi:10.1029/2009GB003587

Sharples, J., Middelburg, J.J., Fennel, K., Jickells, T.D., 2017. What proportion of riverine nutrients reaches the open ocean? Global Biogeochem. Cycles 31, 39–58. doi:10.1002/2016GB005483

Sigman, D.M., Casciotti, K.L., Andreani, M., Barford, C., Galanter, M., Böhlke, J.K., 2001. A Bacterial Method for the Nitrogen Isotopic Analysis of Nitrate in Seawater and Freshwater. Anal. Chem. 73, 4145–4153. doi:10.1021/ac010088e

Simpson, J.H., 1997. Physical processes in the ROFI regime. J. Mar. Syst. 12, 3–15. doi:10.1016/S0924-7963(96)00085-1

Small, G.E., Bullerjahn, G.S., Sterner, R.W., 2013. Rates and controls of nitrification in a large oligotrophic lake. Limnol. Oceanogr. 58, 276–286.

Smith, J.M., Chavez, F.P., Francis, C.A., 2014. Ammonium Uptake by Phytoplankton Regulates Nitrification in the Sunlit Ocean. PLoS One 9, e108173. doi:10.1371/journal.pone.0108173

Smith, V.H., Tilman, G.D., Nekola, J.C., 1999. Eutrophication: impacts of excess nutrient inputs on freshwater, marine, and terrestrial ecosystems. Environ. Pollut. 100, 179–196. doi:10.1016/S0269-7491(99)00091-3

Soetaert, K., Middelburg, J.J., Heip, C., Meire, P., Van Damme, S., Maris, T., 2006. Long-term change in dissolved inorganic nutrients in the heterotrophic Scheldt estuary (Belgium, The

Netherlands). Limnol. Oceanogr. 51, 409–423.

Statham, P.J., 2012. Nutrients in estuaries--an overview and the potential impacts of climate change. Sci. Total Environ. 434, 213–27. doi:10.1016/j.scitotenv.2011.09.088

Stehr, G., Böttcher, B., Dittberner, P., Rath, G., Koops, H.-P., 1995. The ammonia-oxidizing nitrifying population of the River Elbe estuary. FEMS Microbiol. Ecol. 17, 177–186. doi:10.1111/j.1574-6941.1995.tb00141.x

Stief, P., 2013. Stimulation of microbial nitrogen cycling in aquatic ecosystems by benthic macrofauna: mechanisms and environmental implications. Biogeosciences 10, 7829–7846. doi:10.5194/bg-10-7829-2013

Thorpe, S.A., 2005. The turbulent ocean. Cambridge University Press.

Tolar, B.B., King, G.M., Hollibaugh, J.T., 2013. An Analysis of Thaumarchaeota Populations from the Northern Gulf of Mexico. Front. Microbiol. 4, 72. doi:10.3389/fmicb.2013.00072

Turnewitsch, R., Graf, G., 2003. Variability of particulate seawater properties related to bottom mixed layer-associated internal waves in shallow water on a time scale of hours. Limnol. Oceanogr. 48, 1254–1264. doi:10.4319/lo.2003.48.3.1254

Umlauf, L., Burchard, H., 2011. Diapycnal Transport and Mixing Efficiency in Stratified Boundary Layers near Sloping Topography. J. Phys. Oceanogr. 41, 329–345. doi:10.1175/2010JPO4438.1

van Kessel, M.A.H.J., Speth, D.R., Albertsen, M., Nielsen, P.H., Op den Camp, H.J.M., Kartal, B., Jetten, M.S.M., L?cker, S., 2015. Complete nitrification by a single microorganism. Nature 528, 555–9. doi:10.1038/nature16459

Van Raaphorst, W., Kloosterhuis, H.T., Berghuis, E.M., Gieles, A.J.M., Malschaert, J.F.P., Van Noort, G.J., 1992. Nitrogen cycling in two types of sediments of the Southern North sea (Frisian front, broad fourteens): field data and mesocosm results. Netherlands J. Sea Res. 28, 293–316. doi:10.1016/0077-7579(92)90033-B

Veuger, B., Pitcher, A., Schouten, S., Sinninghe Damsté, J.S., Middelburg, J.J., 2013. Nitrification and growth of autotrophic nitrifying bacteria and Thaumarchaeota in the coastal North Sea. Biogeosciences 10, 1775–1785. doi:10.5194/bg-10-1775-2013

Vitousek, P.M., Aber, J.D., Howarth, R.W., Likens, G.E., Matson, P.A., Schindler, D.W., Schlesinger, W.H., Tilman, D.G., 1997. Technical Report: Human Alteration of the Global Nitrogen Cycle: Sources and Consequences. Ecol. Appl. 7, 737. doi:10.2307/2269431

Voss, M., Deutsch, B., Liskow, I., 2010. Nitrogen retention in the Szczecin Lagoon, Baltic Sea. Isotopes Environ. Health Stud. 46, 355–369.

Voss, M., Emeis, K.-C., Hille, S., Neumann, T., Dippner, J.W., 2005a. Nitrogen cycle of the Baltic Sea from an isotopic perspective. Global Biogeochem. Cycles 19, GB3001. doi:10.1029/2004GB002338

Voss, M., Liskow, I., Pastuszak, M., Rüβ, D., Schulte, U., Dippner, J.W., 2005b. Riverine discharge into a coastal bay: A stable isotope study in the Gulf of Gdańsk, Baltic Sea. J. Mar. Syst. 57, 127–145. doi:http://dx.doi.org/10.1016/j.jmarsys.2005.04.002

Ward, B., 2005. Temporal variability in nitrification rates and related biogeochemical factors in Monterey Bay, California, USA. Mar. Ecol. Prog. Ser. 292, 97–109. doi:10.3354/meps292097

Ward, B.B., 2011. Measurement and Distribution of Nitrification Rates in the Oceans, in: Methods in Enzymology. pp. 307–323. doi:10.1016/B978-0-12-381294-0.00013-4

Ward, B.B., 2008. Nitrification in Marine Systems, in: Capone, D.G., Bronk, D.A., Mulholland, M.R.,

Carpenter, E.J. (Eds.), Nitrogen in the Marine Environment. Elsevier, pp. 199–261. doi:10.1016/B978-0-12-372522-6.00005-0

Ward, B.B., Talbot, M.C., Perry, M.J., 1984. Contributions of phytoplankton and nitrifying bacteria to ammonium and nitrite dynamics in coastal waters. Cont. Shelf Res. 3, 383–398. doi:10.1016/0278-4343(84)90018-9

Wasmund, N., Topp, I., Schorires, D., 2006. Optimising the storage and extraction of chlorophyll samples. Oceanologia 48, 125–144.

Weidinger, K., NeuhÃ¤user, B., Gilch, S., Ludewig, U., Meyer, O., Schmidt, I., 2007. Functional and physiological evidence for a Rhesus-type ammonia transporter in *Nitrosomonas europaea*. FEMS Microbiol. Lett. 273, 260–267. doi:10.1111/j.1574-6968.2007.00805.x

Wielgat-Rychert, M., Ameryk, A., Jarosiewicz, A., Kownacka, J., Rychert, K., Szymanek, L., Zalewski, M., Agatova, A., Lapina, N., Torgunova, N., 2013. Impact of the inflow of Vistula river waters on the pelagic zone in the Gulf of Gdańsk. Oceanologia 55, 859–886. doi:10.5697/oc.55-4.859

Wikner, J., Andersson, A., 2012. Increased freshwater discharge shifts the trophic balance in the coastal zone of the northern Baltic Sea. Glob. Chang. Biol. 18, 2509–2519. doi:10.1111/j.1365-2486.2012.02718.x

Wild-Allen, K., Andrewartha, J., 2016. Connectivity between estuaries influences nutrient transport, cycling and water quality. Mar. Chem. 185, 12–26. doi:10.1016/j.marchem.2016.05.011

Witek, Z., Humborg, C., Savchuk, O., Grelowski, A., Łysiak-Pastuszak, E., 2003. Nitrogen and phosphorus budgets of the Gulf of Gdańsk (Baltic Sea). Estuar. Coast. Shelf Sci. 57, 239–248. doi:10.1016/S0272-7714(02)00348-7

Wolanski, E., 2007. Estuarine Ecohydrology. Elsevier.

Wuchter, C., Abbas, B., Coolen, M.J.L., Herfort, L., van Bleijswijk, J., Timmers, P., Strous, M., Teira, E., Herndl, G.J., Middelburg, J.J., Schouten, S., Sinninghe Damsté, J.S., 2006. Archaeal nitrification in the ocean. Proc. Natl. Acad. Sci. U. S. A. 103, 12317–22. doi:10.1073/pnas.0600756103

List of figures

List of tables

Acknowledgements

I have 15 special thanks to give which are all equally important to me:

Thanks to Maren Voss for the good supervision during my PhD time, and the great support and confidence in my scientific career! She always had the right advice at the right time, which was a great help for me. I also want to thank her for the opportunity to participate in the COCOA project with all the great COCOA scientists. I enjoy it so much.

Thanks to my thesis committee, Stefan Forster, Joanna Norkko and Lars Umlauf. The few, but intense meetings helped a lot in the progress of my PhD-thesis.

Thanks to Iris, for the guidance in the lab and the teaching of methods. I gained a tremendous amount of experience through Iris, not only in the lab, but also in the preparation of cruises and on these cruises. I could continue writing about all the cool stuff she trained me in, but that would explode the acknowledgement text. So, Iris, thank you so much! "I love my work!"

Thanks to the working group "Marine nitrogen cycle" at the IOW for the always good working atmosphere, the intense, fruitful and funny discussions about our beloved nitrogen, and the nice coffee breaks of course. You are a great work-family!

Thanks to Nicola and Iris for all the good times in our cozy office 100. Thanks for letting me put up all the station or sediment maps, profiles and mind maps on the walls. Coming to our office feels a bit like coming home, because I know you are there and I can share all my thoughts or doubts with you.

Thanks to Dana for the literally cool times in the climate rooms during our cruises and field samplings with all the nice music and science or non-science chats. It wouldn´t have been the same without you! I am so looking forward to work on our joint manuscript!

Thanks to Franzi, first of all for letting me use her extremely valuable flux data, but also for the great teamwork and the great brainstorming and discussions about coastal N cycling. Your view on not only nitrogen processes but also on being a PhD-student comes from a different angle than mine, and that always broadens my horizon. Thank you for that!

Thanks to Daniel Conley and Johan Wikner for the organization of the Öre estuary field campaigns. Thank you, Daniel, for the delicious COCOA-cocktails you mixed for us in August 2015.

Thanks to Aisha for being the helping hand in sampling and especially filtering the water samples for hours (!) during the Öre estuary field campaigns. I would not have all these great data without her help.

Thanks to the crews of the R/V Elisabeth Mann-Borgese and the R/V Alkor as well as to the technical staff at UMF who all were a great support in sampling.

Thanks to Kirstin Schulz and Lars Umlauf for teaching me in the basic physics in the bottom boundary layers and the interesting discussions linking BBL-physics and biogeochemistry.

Thanks to Robert Mars for the time and help regarding all my CTD-related questions. I learned a lot!

Thanks to my family and friends for all the love, support and necessary distractions during the three years of my PhD!

Thanks to my boyfriend Hannes for all his love, patience and support, especially during times of doubt and stress. Thank you also for the great questions you always have about nitrogen cycling, when I practice my presentations with you. They always help to specify my conclusions or rethink about the results.

Thanks to myself, too. One thanks oneself way to seldom, so thanks to myself for the strength and persistence to keep on doing the marine science which I love.

Appendix

Materials and methods on environmental data in the sediment

Sampling and basic sediment properties

At each station where nitrification rates in the BBL were determined, sediment cores (n=5 - 6) were sampled with a Mutlicorer (MUC) or a HAPS-corer (KC Denmark) for determination of the the basic sediment properties: grain size, water content, porosity and loss on ignition (LOI). The HAPS-corer was used if sediments were very coarse and sampling with the MUC was not possible. Three sediment cores were sliced and samples were frozen immediately at -20 °C without any preservation treatment. In the upper 3 cm the sediment was sliced in 0.5-cm-intervals followed by 1-cm-intervals down to 10 cm and 2-cm-intervals from 10 to 20 cm sediment depth. At the IOW, each sediment slice was homogenized and subsamples were used for the different analyses.

All sediment data were kindly provided by Franziska Thoms and will be presented in her PhD thesis as well. The Methods are therefore only briefly described. The grain size analysis was conducted with the laser-granolumeter Cilas 1180. The sediment type designations are based on the median grain size determined by the instrument. The water content (in %ww) was determined by the weight difference of wet weight (ww) and dry weight (dw). The dry weight was measured after freeze-drying the sediment samples for 2.5 days to constant weight.

$$water\ content = \frac{(ww-dw)*100}{ww} \quad (1)$$

The porosity is known as the ratio of the volume of pore space (which is equal to the volume of the water in a sediment sample) to the total volume of a sediment sample. It was calculated according to Burdige (2006):

$$\phi = \frac{\frac{(m_w)}{\rho_w}}{\frac{\frac{m_w}{\rho_w}+(m_d-(S\times m_w))}{\rho_s}} \quad (2)$$

with m_w and m_d as the mass water and dried sediment, resepectively, ρ_w and ρ_s being the density of the ambient seawater and the sediment ($\rho = 2.65$ g cm^{-3}) and S being the salinity. To determine LOI, which is a measure for the organic content of the sediment, a sediment subsample was burned in a muffle furnace at 550 °C for five hours. The LOI (in %dw) was calculated as follows:

$$LOI = \frac{(dw-dw_{550})}{dw} * 100 \quad (3)$$

with dw_{550} being the dry weight after combustion at 550 °C. Roughly 40 % of the LOI correspond to the organic C content of the sediment in the Baltic Sea, which makes LOI a good qualitative measure of sediment organic content. Data on surface sediment permeability (m^2) were kindly provided by Dana Hellemann (University of Helsinki, collaboration within COCOA, Hellemann et al., submitted). PON and POC concentrations of the sediment were measured with the element analyser (Thermo Flash 2000). Each subsample was dried for 2 – 4 days at 50 °C and then homogenized with mortar and pestle. Subsamples of muddy (5 mg) and sandy (up to 100 mg) sediments were pelletized in silver capsules and then analysed with the element analyser. For the determination of the POC content, samples had to be acidified (2N HCl) prior to measurement to remove inorganic carbon.

Pore water and nutrient fluxes

Pore water samples were mostly extracted by Franziska Thoms via rhizons (Seeberg-Elverfeldt et al., 2005) from MUC-cores (n=2, d=10cm) through 2 alternating lines of drilled holes, each 2 cm apart. With the alternating arrangement of holes, sampling of pore water in 1-cm intervals was possible. When sediment cores were taken with the HAPS-corer (d = 20 cm), the sediment was subsampled with a MUC-liner for pore water analysis. The rhizons (Rhizosphere) had a 5-cm membrane with pore sizes of 0.12-0.18 µm. Before use, the rhizons were prerinsed with MilliQ water and kept in MilliQ for at least 15 minutes prior to sampling. After discarding the first millilitre of pore water, up to 4 ml of sample was extracted with a 6-ml plastic syringe from the core at different sediment depths at varying intervals: 1-cm intervals in the top 5 cm, 2-cm intervals from 7 to 11 cm, and individual samples at 15 and 20 cm depths. Occasionally, the sampling depths had to be adjusted in order to accommodate shorter cores. In all cores, pore water samples were extracted from top to bottom and immediately frozen at -20 °C. Only the samples from the cruise AL449 in February 2015 were measured on board. From the other two cruises, nutrients were analysed by Christian Burmeister at the IOW with the continuous segmented flow analyser (QuAAtro, Seal Analytical, see section 2.2.1).

From the pore water profiles of NH_4^+ and NO_3^- concentrations, depth-integrated concentration pools were calculated for the surface sediment layer (1-3cm depth) and the deeper sediment layer (3-11cm depth). Additionally, diffusive NH_4^+ fluxes were calculated for stations with muddy sediments with no inhabiting macrofauna, i.e. where diffusive fluxes are the dominant transport processes. Those stations were VE38, VE39

and TF0233 along the transect to the Gdansk deep (offshore stations). Diffusive fluxes (in µmol m^{-2} d^{-1}) were calculated according to Fick´s first law:

$$J = -\phi D_s \left(\frac{\delta c}{\delta z}\right) \quad (4)$$

with ϕ being the porosity, D_s being the sedimentary diffusion coefficient, δc and δz being the difference in concentration and sediment depth (i.e. the concentration gradient and steady state conditions, which are assumed to exist here). The sedimentary diffusion coefficient D_s is calculated as:

$$D_s = \frac{D_0}{\theta^2} \quad (5)$$

with D_0 as the molecular diffusion coefficient and θ^2 as the tortuosity. The values for D_0 of NH_4^+ were used from Schulz and Zabel (2006). The tortuosity in turn was calculated after Boudreau (1997):

$$\theta^2 = 1 - \ln(\phi^2). \quad (6)$$

The NH_4^+ flux was calculated from the concentration gradient in the upper sediment layer (1 – 4 cm) where the gradient is stronger. The NH_4^+ from this layer will be directly transported to the overlying BBL water and is therefore important when studying the connection between BBL and sediment. Total benthic nutrient fluxes across the sediment water interface were determined by Franziska Thoms using the Automated Mini Chamber Lander System from Unisense (Thoms et al., in preparation; Thoms PhD-thesis).

Figure I: BBL thickness in the Öre estuary

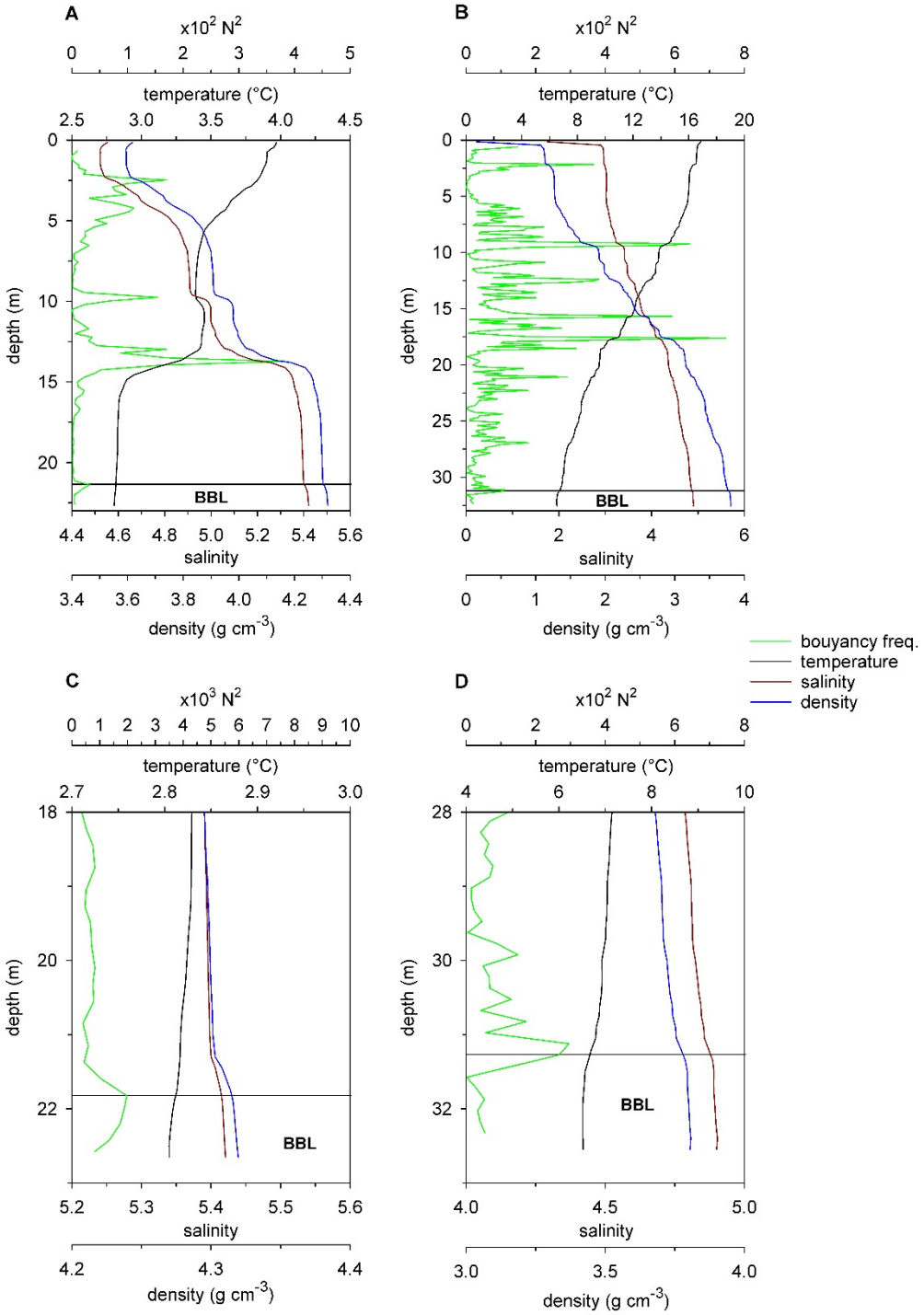

Figure I: Depth profiles of temperature, salinity, density, and buoyancy frequency N^2 in the Öre estuary: A) station N11 in April 2015 and B) station NB8 in August 2015. Panels C and D are close-ups at lower depth. The upper boundary of the BBL was identified by the peak in N^2 and the beginning of invariable distribution of temperature, salinity and density. Please note the different scaling of the variables. Distinct water layers are marked by the horizontal black line.

Figure II: Deep water layer in the offshore Bay of Gdansk

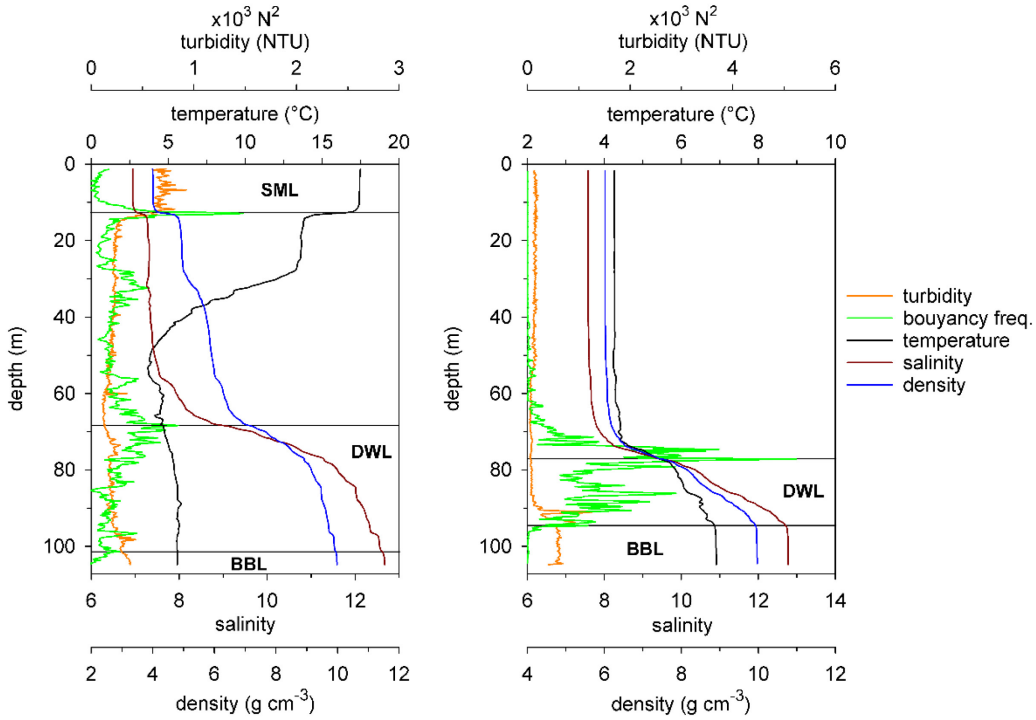

Figure II: Depth profiles of temperature, salinity, density, buoyancy frequency N^2, and turbidity in the offshore area of the Bay of Gdansk in summer (left) and spring (right). The upper boundary of the DWL was identified by the peak in N^2 at the depth of the pycnocline.

Table I: Tracer signal mainly in NO_2^-

Table I: The isotopic composition of nitrification samples at the end of the incubation when NO_2^- was kept ($\delta^{15}N\text{-}NO_3^- + NO_2^-$) or removed ($\delta^{15}N\text{-}NO_3^- - NO_2^-$).

Date (UTC)	Station	depth [m]	$\delta^{15}N\text{-}NO_3^-$ $+NO_2^-$	$\delta^{15}N\text{-}NO_3^-$ $-NO_2^-$
29.02.2016	VE07	45	47.08	11.22
29.02.2016	VE07	51	30.91	14.97
02.03.2016	VE06	30	180.81	10.73
02.03.2016	VE06	35	77.76	9.08
07.03.2016	VE05	20	87.74	12.39
07.03.2016	VE05	23	33.82	9.63

Figure III: Phytoplankton composition in the Vistula estuary

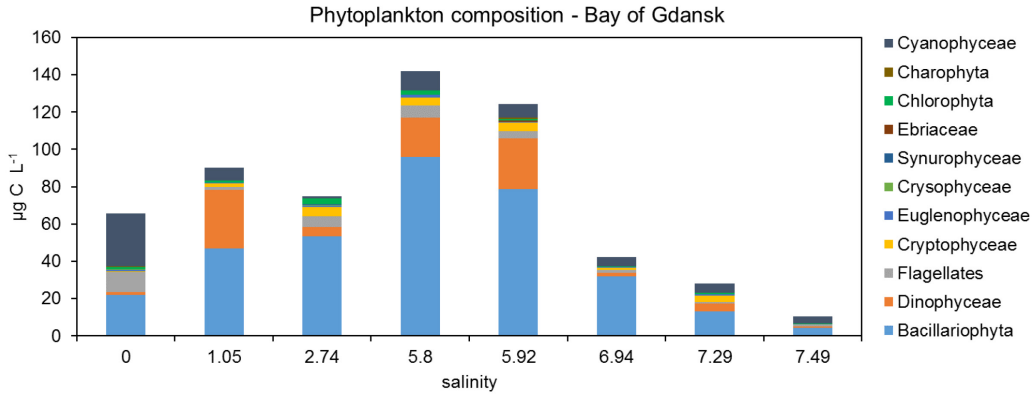

Figure III: Phytoplankton composition of the Vistula estuary plotted over the salinity of the respective station. Salinity 0 represents the Vistula River. Samples were collected during the cruise in spring 2016.

Methods discussion – BBL profiles

Samples from the BBL-profile taken with the modified chamber lander always had NO_3^- concentrations being 0.5 – 2 µmol L^{-1} higher than water samples from the overlying BBL water above (i.e. deepest CTD cast). A similar pattern was found for the SiO_2 concentrations at VE05 and VE13, and for the NO_2^- concentrations at VE10 (data not shown). However, PO_4^{3-} and NH_4^+ profiles did not show this pattern and remained overall low without any gradient. All samples were measured with the same methods (see section 2.2.1) why we can exclude this as potential source of error. The shift towards slightly higher concentrations in the BBL samples could be due to the sampling procedure. There was a delay time between deployment of the device and sampling of the water, to avoid sampling BBL water which was affected from the resuspension effect of the deployment (Holtappelts et al., 2011). During this delay time, the frame of the chamber lander might have deflected bottom water currents artificially, leading to more turbulence, which in turn might have resulted in some advective pore outflow. If this would have happened, all nutrient concentrations, especially NH_4^+ and PO_4^{3-} should be slightly increased. Another possibility is a NO_3^- contamination of the filters which were used to filtrate the samples. The filters were always rinsed with 5 ml sample water prior to sampling. If there was a NO_3^- contamination, this still does not explain the same pattern found in SiO_2 and NO_2^-. Excluding these potential sources of variation, the slight increase in NO_3^- concentration within the last meter above the sediment surface might be a true finding.

Sediment characteristics in the Bay of Gdansk

Five sediment types were found in the Bay of Gdansk (table) based on the median grain size from the surface sediment layer (0 – 1 cm). The sediment was moderately to well sorted to a sediment depth of 20 cm which shows that the determined sediment types are not constrained to the first centimeter of the sediment (Thoms et al., unpublished). Muddy sediments (silt and coarse silt) are mainly located in the offshore area of the Bay of Gdansk below 50 m depth whereas sandy sediments (fine, medium, coarse sands) are dominant in the Vistula estuary (figure). Water content, porosity and LOI are lower at the sandy coastal stations than at the muddy offshore stations (Thoms et al., unpublished). Patches of silty sediments exist in the Vistula estuary very close to the river mouth (stations VE03, deep sediment of VE04). A mixed sediment type of sand and silt is found at intermediate stations at approximately 50 m water depth (VE07 and VE23) reflecting the transition from Vistula estuary to the offshore area.

Table II: Sediment types classification in the Bay of Gdansk based on grain size.

sediment type	grain size (µm)
medium silt	16-25
coarse silt	30-75
fine sand	163-198
medium sand	208-441
coarse sand	953

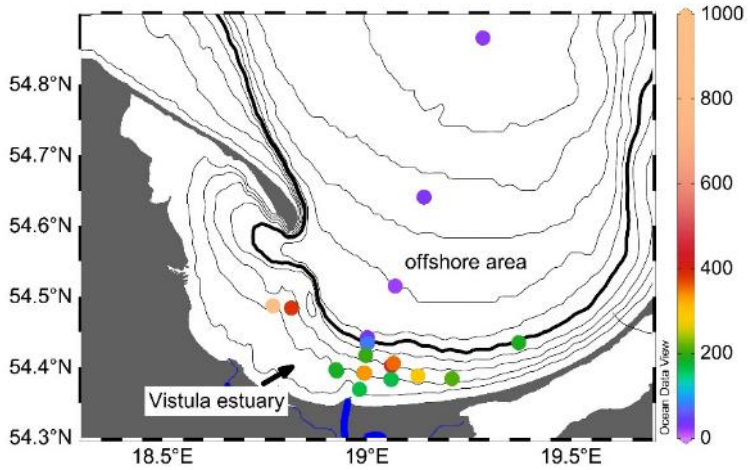

Figure IV: Grain size distribution in the Bay of Gdansk with fine to medium sands in the Vistula estuary (< 50 m depth) and silts in the offshore area (> 50 m depth). The 50m depth isoline is marked in bold.

Table III: Sample sizes

Table I: Sample sizes of sediment properties, NH_4^+ flux and nitrification rates from the sediment types based on permeability and absence/presence of macrofauna.

	grain size	wc (%ww)	perm. (m^2)	LOI (%dw)	PON (%dw)	surf. NO_3^- (µmol L^{-1})
N-M	3	4	0	5	3	5
N+M	5	6	3	6	1	6
P+M	9	11	11	11	5	10

	surf.NH_4^+ pool (µmol L^{-1})	deep NH_4^+ pool (µmol L^{-1})	NH_4^+ flux (µmol m^{-2} d^{-1})	nitrification rate (nmol L^{-1} d^{-1})
N-M	5	5	5	5
N+M	1	4	1	6
P+M	4	0	4	11

Figure V: Environmental variables in the BBL of the Öre estuary

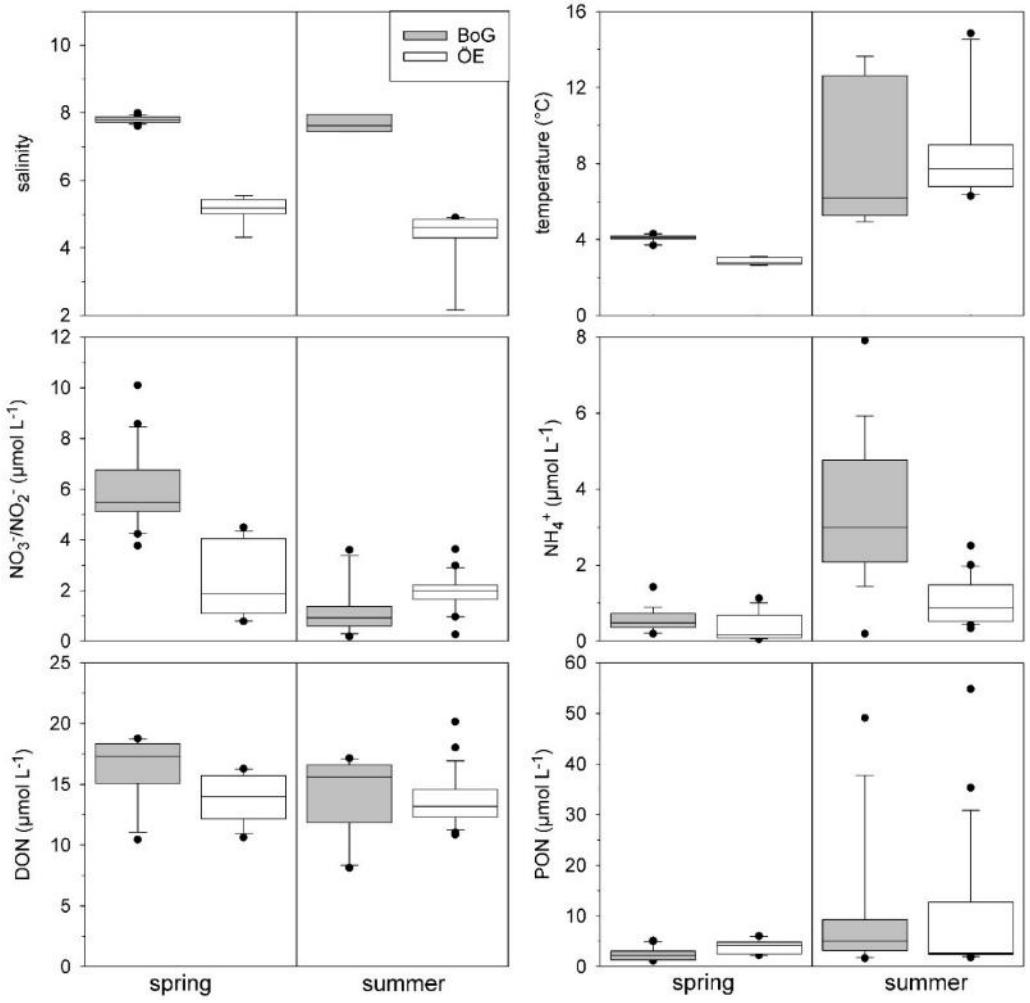

Figure V: Distribution of environmental variables in the BBL of the Vistula estuary (BoG) and the Öre estuary (ÖE) in spring and summer.

Declaration

Hiermit versichere ich, dass ich die vorliegende Arbeit selbstständig angefertigt und ohne fremde Hilfe verfasst habe, keine außer den von mir angegebenen Hilfsmitteln und Quellen dazu verwendet habe und die den benutzten Werken inhaltlich und wörtlich entnommenen Stellen als solche kenntlich gemacht habe.

Rostock, den 28.06.2017